Investigation of the Effect of Blade Sweep
on Rotor Vibratory Loads

AD-A135 603

F. J. Tarzanin, Jr.
R. R. Vlaminck

DTIC FILE COPY

NASA

DTIC
CTE
DEC 1 2 1983

A

N84-18196

83 12 09 160

Investigation of the Effect of Blade Sweep
on Rotor Vibratory Loads

F. J. Tarzanin, Jr.
R. R. Vlaminck
Boeing Vertol Company
Philadelphia, Pennsylvania

1. Report No. NASA CR-166526	2. Government Accession No. AD.A135603	3. Recipient's Catalog No.
4. Title and Subtitle INVESTIGATION OF THE EFFECT OF BLADE SWEEP ON ROTOR VIBRATORY LOADS		5. Report Date October, 1983
		6. Performing Organization Code
7. Author(s) F. J. Tarzanin, Jr. and R. R. Vlaminck		8. Performing Organization Report No.
		10. Work Unit No. K1585
9. Performing Organization Name and Address Boeing Vertol Company Boeing Center P. O. Box 16858 Philadelphia, PA 19142		11. Contract or Grant No. NAS2-11151
		13. Type of Report and Period Covered Contractor Report
12. Sponsoring Agency Name and Address Aeromechanics Laboratory U.S. Army Research and Technology Laboratories Moffett Field, CA 94035		
		14. Sponsoring Agency Code

15. Supplementary Notes

Point of Contact: Technical Monitor, Donald L. Kunz, MS 215-1
Ames Research Center, Moffett Field, CA 94035
(415) 965-5891 or FTS 448-5891

16. Abstract

The effect of helicopter rotor blade planform sweep on rotor vibratory hub, blade, and control system loads has been analytically investigated. The importance of sweep angle, sweep initiation radius, flap bending stiffness and torsion bending stiffness is discussed. The mechanism by which sweep influences the vibratory hub loads is investigated.

17. Key Words (Suggested by Author(s)) Helicopter vibration Rotor Loads Planform sweep Hub loads Helicopter Rotor		18. Distribution Statement Unclassified – Unlimited	
19. Security Classif. (of this report) Unclassified	20. Security Classif. (of this page) Unclassified	21. No. of Pages 131	22. Price*

*For sale by the National Technical Information Service, Springfield, Virginia 22161

ABSTRACT

The effect of blade sweep on rotor vibratory hub, blade, and
control system loads has been analytically investigated. The
importance of sweep angle, sweep initiation radius, flap bend-
ing stiffness, and torsion bending stiffness is discussed along
with the mechanism that produces the hub load reduction.

SUMMARY

The effect of blade sweep on vibratory hub, blade, and control system loads has been analytically investigated using the Boeing Vertol C-60 aeroelastic computer program. A four bladed reference rotor was selected for this study that demonstrated a reduction in vertical hub load due to outboard blade aft sweep.

For the reference rotor the following significant results were obtained.

o   Sweep significantly reduced the 4/rev vertical, inplane, and hub moments over the entire range of airspeeds investigated. This was 120 knots (62 m/s) to 220 knots (113 m/s). Rotor horsepower, alternating flap bending moments, and control system loads were also reduced by blade sweep.

The table below shows the percentage reduction from the unswept blade values of these loads for two favorable sweep configurations, 10 degrees (.1745 rad) and 20 degrees (.3490 rad) sweep at .87 radius. These data are for the 150 knot (77.2 m/s) reference flight condition.

PARAMETER	PERCENT REDUCTION 10 DEG (.1745 RAD) SWEEP .87R	PERCENT REDUCTION 20 DEG (.3490 RAD) SWEEP .87R
4/rev vert. hub load	36.5	60.0
4/rev lat. hub load	15.9	30.2
4/rev long. hub load	48.8	64.2
4/rev roll hub moment	31.3	41.0
4/rev pitch hub moment	.29	22.7
Alternating pitch link load	45.0	36.4
Maximum alternating flap bending moment	20.4	19.4
Rotor horsepower	7.2	7.1

o Flap and torsion stiffness variations showed that specific blade frequency placement and flexible flap/pitch coupling are not necessary (in this case) to obtain hub load reductions with sweep. Blade torsional stiffness does, however, play a significant role in the sweep effectiveness.

o Analysis of independent mass and aerodynamic chordwise distribution showed that mass forward of the elastic axis and aerodynamic center aft of the elastic axis reduced the vertical 4/rev hub loads.

o Rotor blade sweep and chordwise CG/AC distributions influence elastic blade twist. The study results show that when the 4/rev blade elastic tip pitch angle is reduced with

either sweep or CG/AC chordwise distribution the 4/rev vertical hub load is also reduced.

In addition, it was discovered that sweep was not beneficial for all rotor blades. Four other blade designs were investigated which showed a hub load increase for aft blade sweep. Further investigation is needed to understand the reasons for this behavior.

The concepts developed during the analysis of the reference rotor were applied to a blade which produced an increase in vertical vibratory hub load when swept. By adjusting the blade torsional stiffness and tip region physical properties, a reduction in vertical hub load was obtained with sweep.

TABLE OF CONTENTS

LIST OF ILLUSTRATIONS

INTRODUCTION

As helicopters achieve higher and higher airspeeds, the fundamental differences between the advancing and retreating blade environment and the high advancing tip Mach Number combine to increase helicopter rotor loads. The resulting large blade and control loads can usually be compensated for by increasing component strength, at the expense of weight and increased cost. Generally, the most difficult load increase to counter is the vibratory hub load.

Vibratory hub loads cause fuselage vibration which could result in:

- Fatigue failures of aircraft components (increasing maintenance costs, reducing operational availability, and aborting missions).
- Pilot fatigue (reducing endurance and effectiveness).
- Passenger discomfort (reducing commercial acceptance).

There are two general approaches to reducing aircraft vibration:

- The first approach is to reduce the helicopter response to the vibratory hub loads. This approach includes isolation, absorbers and detuning the fuselage response.

- The second approach is to reduce the prime vibration source; the vibratory hub loads. This approach includes improved rotor design, rotor absorbers and higher harmonic control.

The advent of new materials and construction techniques now allow the potential to define new rotor blades that are designed with inherently low vibratory hub loads. One blade design approach is the use of sweep on the outboard section of the rotor blade. Published (References A through H) and unpublished analytical studies have shown that significant hub load reductions are possible. However, load reductions did not occur for all rotors. In some instances aft sweep reduced loads, sometimes forward sweep reduced loads and sometimes the results showed little change.

This report documents an analytical study that was performed primarily to systematically obtain an understanding of the fundamental mechanism for the hub load reduction, so that a blade with low hub loads can be defined.

Since the effect of sweep appears to vary from blade to blade, the first task is to define a baseline blade that demonstrates significant vibratory hub load reductions due to aft blade sweep. (Aft blade sweep was selected since aerodynamic benefits could be provided as well). Once a baseline blade has been selected that shows significant aft sweep benefits, further investigation into why the load reduction occurs can be performed.

The importance of sweep angle, sweep initiation radius, blade natural frequency, flap bending stiffness, torsional bending stiffness, aerodynamic center and chordwise center of gravity is discussed. This investigation was performed primarily on vertical vibratory hub loads. However, limited results of the effect of sweep on inplane hub loads, hub moments, control system load, blade flap bending moments and rotor power requirements is also presented.

DISCUSSION

1. BLADE SELECTION

In order to select the baseline rotor for this study several conventionally articulated rotor blade designs were analyzed to determine their vibratory hub load sensitivity to sweep. These blades included the following:

o   CH47C blade -- which represents a typical current technology design

o   Four Conceptual blades - All four blades have identical planforms, and differ only in their physical properties. These blades are designed as designs A through D.

The four conceptual blades were selected since they represent a set of blades having identical geometry, with different physical properties. Therefore, analyzing these four blades allows the effects of large physical property changes (including different frequency changes) to be evaluated.

These blades were selected so that insights into the effects of sweep on hub loads can be inferred from the results, to help define the direction for further investigation. If all the

design A through D blades showed similar sensitivity to sweep it could be concluded that the specific physical properties were relatively unimportant and that the baseline planform and airfoils were significant. If the sweep sensitivity varied significantly from blade to blade then physical properties would be the significant factors.

Vibratory hub loads were calculated using the Boeing Vertol C60 aeroelastic computer analysis. A description of this computer program and the rotor trim used for these studies is presented in Appendixes A and B respectively. Appendix C gives a description of the design A rotor and the definition of blade sweep angle.

Vibratory hub loads calculations were performed at a 150 knot (77.2 m/s) reference flight condition and sweep initiation radii of .83R, .87R and .91R. The nominal rotor speed was 270 rpm for design A, B, C and D rotors and 235 RPM for the CH-47C rotor.

Analysis of designs B, D, and the CH-47C blades showed that 4/rev vertical hub loads actually increased when these blades were swept aft. (See Figures 1.-1 through 1.-4.) (Forward sweep did reduce these hub loads, but this phenomenon was not investigated further). Design C demonstrated a slight decrease in hub load with sweep. Design A, however, showed a large reduction in 4/rev vertical hub load with sweep and was selected as the baseline rotor for this study.

Coupled flap/pitch natural frequencies in air without damping for these blades are presented below in the table.

BLADE NATURAL FREQUENCIES

IN AIR WITHOUT DAMPING

BLADE MODE	DESIGN A	DESIGN B	DESIGN C	DESIGN D	METAL CH-47C
1st Torsion	4.22/rev	3.63/rev	5.00/rev	4.26/rev	5.35/rev
1st Flap	1.11/rev	1.22/rev	1.15/rev	1.15/rev	1.08/rev
2nd Flap	2.63/rev	2.81/rev	2.70/rev	2.70/rev	2.59/rev
3rd Flap	5.66/rev	4.67/rev	4.63/rev	4.81/rev	4.65/rev

These frequency data showed the following:

o   Designs A and D have almost identical 1st torsion frequencies that are close to 4/rev.

o   Design B and the CH-47C metal blades have 1st torsion frequencies below and above 4/rev respectively.

o   Designs C and D have identical 2nd flap frequencies.

As shown, designs A through D have very different frequency placement, especially the torsional frequency which varies from 3.63Ω to 5.00Ω. It was anticipated that if these blades showed different sensitivities to blade sweep it would be the result of specific torsion and/or flap frequency placement (i.e.: torsion frequency above or below 4/rev, or 2nd/3rd flap frequency near

or close to 4/rev or some relation between flap and torsion frequencies). If frequency placement were important, specific groups of blades, with similar frequency placements would show similar trends with blade sweep. However, a review of the variation of 4/rev vertical hub load with blade sweep for designs A through D indicates that a unique torsion and/or flap frequency relationship may not be a strong contributing factor in the hub load reduction mechanism. This tentative conclusion is based on the observation that designs A and D have similar frequency placement relative to 4/rev for the first torsion and second flap modes, but very different behavior with respect to 4/rev vertical hub load changes due to blade sweep. This tentative conclusion is investigated further in sections 4 and 5.

2.   EFFECT OF BLADE SWEEP

2.1   VERTICAL HUB LOADS

The primary purpose of this phase of the study was to determine.
the effect of sweep on vertical 4/rev hub loads at the 150 knot
(77.2 m/s) reference flight condition for the baseline design A
blade.   Sweep parameters investigated included the initiation
radius and sweep angle.   Initiation radii studied were .83R,
.87R and .91R, with sweep angles up to 34 degrees (.5933 rad).
The baseline values of blade flap and torsion stiffness were
used.   The control system pitch stiffness was 600,000 in. lb./
rad. (6788 N m/rad).

The effect of sweep angle and initiation radius on 4/rev vertical
hub load is presented in Figure 2.1-1.   These data show that the
largest vertical hub load reduction was obtained with a 30 degree
(.5235 rad) sweep angle at an initiation radius of .87R.   With
this blade configuration the 4/rev vertical vibratory hub load
is decreased from 1300 lb. (5782 N) to 280 lb. (1245 N), a re-
duction of 79% (to 21% of the baseline value).   For all sweep
initiation radii studied on the Design A blade, aft sweep re-
duced the 4/rev vertical hub load until the program convergence
began to deteriorate.   Hub loads for sweep angles larger than
those shown in Figure 2.1-1 were generally larger and had a
large variation, indicating a nonconverged solution.   (Note: a
converged solution is defined as having an angle of attack

change of less than .1 degree (.00175 rad) for the last two rotor revolutions at blade azimuth positions of 0, 90 (1.571 rad), 180 (3.141 rad), and 270 (4.712 rad) degrees).

2.2 VERTICAL ROOT SHEAR HARMONICS

Harmonics of vertical root shear for the baseline unswept and 20 degree (.349 rad) sweep at .87R configurations at the reference flight condition are presented in Figure 2.2-1. These data show that the 2nd thru 5th harmonics of vertical root shear are reduced by sweep. The 6th thru 10th harmonics, however, are increased by sweep.

2.3 FLAP BENDING MOMENT HARMONICS

Harmonics of flap bending moment at .165R for the baseline unswept and 20 degree (.349 rad) sweep at .87R configurations at the reference flight condition are presented in Figure 2.3-1. These data show that the 1st thru 5th harmonics of flap bending moment are reduced by sweep. The 6th thru 10th harmonics, however, are increased by sweep.

2.4 PITCH LINK LOAD WAVEFORMS

Figure 2.4-1 presents pitch link load waveforms for the baseline unswept and 20 degrees (.349 rad) sweep at .87R configurations

E/566   19

at the reference flight condition. These data clearly show that aft sweep reduces the nose down pitching moment on the advancing blade.

2.5 CHORD BENDING MOMENT HARMONICS

Harmonics of chord bending moment at .51R for the baseline unswept and 20 degrees (.349 rad) sweep at .87R configurations at the reference flight condition are presented in Figure 2.5-1. All harmonics of· chord bending except the 7th and 10th are significantly reduced by blade sweep.

3. EFFECT OF AIRSPEED

3.1 VERTICAL HUB LOADS

Section 2 of this report showed that at 150 knots (77.2 m/s), 30 degrees (.5235 rad) of sweep with an initiation radius of .87R produced the largest vertical vibratory hub load reduction. To determine the optimum sweep angle, analyses were conducted from 120 knots (61.7 m/s) to 220 knots (113 m/s) at sweep angles of 10 degrees (.1745 rad), 20 degrees (.349 rad), and 30 degrees (.5236 rad). The initiation radius was .87R. These data, presented in Figure 3.1-1 show several important conclusions:

o The 30 degree (.5236 rad) swept blade diverges for airspeeds above 180 knots (92.6 m/s).

o Sweep reduces the vibratory vertical loads over the entire range of airspeeds investigated (except for the diverged region).

o There is not an optimum sweep angle for all airspeeds.

Between 120 knots (61.7 m/s) and 180 knots (92.6 m/s) the blades with 30 degrees (.5236 rad) sweep at .87R produce the lowest 4/rev vertical hub loads. Between 120 knots (61.7 m/s) and 192 knots (98.8 m/s) the blades with 20 degrees (.349 rad) sweep at .87R produce lower vibratory loads than the 10 degree (.1745

rad) configuration. With 10 degrees (.1745 rad) of sweep at
.87R there is a large decrease in hub load with airspeed above
192 knots (98.8 m/s). At 220 knots (133 m/s) the baseline rotor
develops 1750 lb. (7784 N) vibratory load while the rotor with
10 degrees (.1745 rad) sweep develops only 160 lb. (712 N) of
4/rev vertical load. This is a reduction of 91% to only 9% of
the baseline value!

3.2 INPLANE HUB LOADS

Longitudinal and lateral vibratory hub loads were computed as a
function of airspeed and blade sweep angle at .87R and are pre-
sented in Figures 3.2-1 and 3.2-2 respectively. These data show
that 4/rev longitudinal hub loads are reduced by blade sweep over
the entire range of airspeeds investigated. The lowest loads
were developed by the 30 degree (.5236 rad) swept blades. This
configuration, however, diverges above 180 knots (92.6 m/s). At
220 knots (113 m/s) the 20 degree (.349 rad) swept blades reduce
the longitudinal hub load from 1930 lb. (8585 N) to 1090 lb.
(4848 N). This is a reduction of 44% (to 56% of the baseline value

The 4/rev lateral hub loads are lower on the baseline blade for
the 10 degrees (.1745 rad) and 20 degrees (.349 rad) sweep configura-
tions over the entire range of airspeeds investigated. The 30
degree (.5236 rad) swept blades produce higher lateral hub loads
than the baseline blade between 144 knots (74.1 m/s) and 175 knots
(90.0 m/s). At 220 knots (113 m/s) the lateral hub load was

reduced from 2210 lb. (9830 N) to 1780 lb. (7917 N), a 19% re-
duction (to 81% of the baseline value).

3.3 HUB MOMENTS

Figures 3.3-1 and 3.3-2 show hub roll and pitch moments respec-
tively as a function of airspeed and blade sweep angle at .87R.
Both vibratory hub moment components are reduced by blade sweep
above 148 knots (76.2 m/s). Below 148 knots (76.2 m/s) there is
a slight increase in pitch moment for the 30 deg (.5236 rad) blade
Above 180 knots (92.6 m/s) the blades with 20 degrees (.349 rad)
sweep produce the lowest roll and pitch moments. At 220 knots
(113 m/s) the 20 degree (.349 rad) swept blades reduce the roll
moment from 49000 in. lb. (5536 Nm) to 32000 in. lb. (3615 Nm),
a reduction of 35% (to 65% of the baseline value). At this air-
speed the pitch moments are reduced from 43000 in. lb. (4858 Nm)
to 36500 in. lb. (4124 Nm), a reduction of 15% (to 85% of the base-
line value).

For an articulated rotor the 4/rev hub moments are produced by
3/rev and 5/rev vertical shears. Therefore, if the 4/rev hub
moments are reduced, the 3/rev and 5/rev vertical shear at the
flap pin is reduced. Figure 3.3-3 presents 3/rev vertical shear
at the flap pin for the baseline, 10 degrees (.1745 rad), 20
degrees (.349 rad), and 30 degrees (.5236 rad) sweep .87R con-
figurations. As expected, these data show a trend similar to
the fixed system 4/rev hub moments. The 5/rev vertical shears

at the flap pin are less than 10% of the 3/rev shears and are not shown, however they also show a reduction due to blade aft sweep.

3.4 ROTOR HORSEPOWER

Blade sweep produced significant reductions in required rotor horsepower, especially at the higher airspeeds. Figure 3.4-1 shows at 220 knots (113 m/s) power required was reduced 9.2 percent from 4900 HP (3,653,734 Nm/s) to 4450 HP (3,318,187 Nm/s) for both the 10 degree (.1745 rad) and 20 degree (.349 rad) sweep at .87R configurations. It is interesting that there is very little difference between the 10 degree (.1745 rad) sweep and 20 degree (.349 rad) swept blade results. Between 120 knots (61.76 m/s) and 180 knots (92.6 m/s) the 10 degree (.1745 rad) and 20 degree (.349 rad) swept blades produce larger re-ductions in required rotor horsepower than the 30 degrees (.5236 rad) configuration.

3.5 FLAP BENDING MOMENTS

Maximum alternating flap bending moments, shown in Figure 3.5-1, were significantly reduced by the 10 degree (.1745 rad) and 20 degree (.349 rad) swept at .87R blades over the entire range of airspeeds investigated. Between 135 knots (69.4 m/s) and 160 knots (82.3 m/s) the 30 degree (.5236 rad) sweep .87R configura-tion increased the alternating flap bending moments. At the

higher airspeeds sweep does not produce as large a percentage reduction in moment. At 220 knots (113.2 m/s) the 20 degree (.349 rad) swept blades reduce the maximum alternating flap bending moments from 51000 in. lb. (5762 Nm) to 48500 in. lb. (5479 Nm) (a 4.9% reduction). At 200 knots (102.9 m/s) this sweep configuration reduces the moment from 44500 in. lb. (5028 Nm) to 31000 in. lb. (3502 Nm). This is a 30% reduction (to 70% of the baseline value).

Four per rev flap bending moments versus blade nondimensional radius at the 150 knot (77.2 m/s) reference flight condition for the unswept, 20 degree (.349 rad), and 30 degree (.5235 rad) sweep at .87R configurations are presented in Figure 3.5-2. These data show that sweep significantly reduces the 4/rev flap bending moments along the entire blade span. The maximum 4/rev moment, which occurs at .16R, is reduced from 3850 in. lb. (434.9 Nm) on the unswept blade to 800 in. lb. (90 Nm) on the 30 degree (.5235 rad) sweep .87R configuration. This is a reduction of 79% (to 21% of the unswept value).

3.6 CONTROL SYSTEM LOADS

Alternating pitch link loads, shown in Figure 3.6-1, were also reduced by the 10 degree (.1745 rad) and 20 degree (.349 rad) sweep configurations over the entire range of airspeeds investigated. Above 162 knots (83 m/s) the largest load reductions were achieved with 20 degrees (.349 rad) of sweep. At 220 knots

(113 m/s) this configuration reduced the load from 2950 lb. (13122 N) to 2100 lb. (9341 N), a 29% reduction (to 71% of the baseline value). The 30 degree (.5236 rad) swept blades increased the alternating pitch link loads between 120 knots (61.8 m/s) and 175 knots (90.1 m/s).

4. BLADE FREQUENCIES

The prime objective of this contract is to systematically obtain
an understanding of the fundamental mechanism for the hub load
reduction. One of the possible hub load reduction scenario re-
quires model cancellation of vertical shear at the rotor hub. A
further subset of this scenario requires that specific torsion
and/or flap frequency placement is needed to obtain the modal
root shear cancellation. The results of section 1 tentatively
implied that unswept frequency placement was not a critical com-
ponent of the hub load reduction mechanism.

It is clear that blade planform sweep will cause a change in blade
frequency. It is possible that sweep induced frequency changes
cause specific frequency relationships that result in the 4/rev
vertical hub load reduction. However, simply calculating the
blade frequency in a vacuum may be very misleading. One of the
effects of blade sweep is to couple flap displacement into pitch
displacement. The significance of this coupling is much more
apparent when aerodynamic effects are considered in addition to
inertial effects. Therefore, to seriously investigate the effect
of planform sweep on blade frequency both vacuum and in air fre-
quencies should be calculated. The next question is, should the
frequency be calculated in the classical sense with only real
terms (i.e. no air damping) or is the sweep induced flap/pitch
coupling significantly influenced by the aerodynamic flap and
pitch damping. The only way to fairly evaluate the role of sweep

induced blade frequency on the vibratory hub loads is to calcul-
ate the frequency for three sets of conditions: 1) in a vacuum,
2) in air with no damping and 3) in air with aerodynamic damping.

For the three conditions defined above, blade coupled flap/pitch
frequencies were computed with the nominal control system pitch
stiffness of 600,000 in-lb/rad (67,788 nm/rad). The air without
damping analysis includes linear aerodynamic terms that are func-
tions of the blade flap and pitch displacements and accelerations.
With damping the linear aerodynamic loads due to blade flap and
pitch velocities are also included.

A summary of the calculated coupled flap/pitch natural frequencies
at the nominal rotor speed for the design A blade at zero degrees,
10 degrees (.1745 rad), 20 degrees (.349 rad), 30 degrees (.5235
rad), and 40 degrees (.698 rad) sweep configurations with the
sweep initiation radius at .87R are presented in Figure 4.-1.

Blade frequency spectra are presented in Figures 4.-2 through
4.-4 and show the following significant conclusions:

(a) In a vacuum the blade torsion frequency changed significant-
     ly with sweep angle. As expected, it was reduced as the
     sweep angle increased (from 4.34Ω for no sweep to 3.49Ω for
     40 degrees of sweep). Outboard of the sweep initiation
     radius the mass offset from the blade's unswept elastic
     axis is increased thereby increasing the effective pitch
     inertia. (See Figure 4-2.)

(b) In air without damping, the 2nd flap and first torsion modes coalesce above the nominal rotor speed. As the torsion frequency decreases the coalescence point moves towards the nominal rotor speed, and above 30 degrees sweep the coalescence point is below the nominal rotor speed.

This coalescence results from strong sweep induced flap/pitch coupling. Blade sweep allows airloads generated by flap deflection to change blade pitch, resulting in large airload changes. These airload changes results in an effective flap spring that is strong enough to increase the blade flap frequency. The net effect of the inphase aerodynamic loads on the blade natural frequency is to reduce the torsion mode and increase the second flap mode. (See Figure 4-3.)

(c) When airforces with damping are included in the natural frequency analysis, results similar to airloads with no damping are observed, except the second flap and first torsion modes do not coalesce. Instead, as the second flap frequency increases the first torsion frequency decreases, the modes repel each other and become highly coupled, until eventually the torsion mode becomes a flap mode and the flap mode becomes a torsion mode. This behavior is typical of a flap/torsion mode for a typical rotor blade with flap/pitch coupling in a vacuum.

These frequency results show no obvious frequency placement that
is causing the aft sweep induced 4/rev vertical hub load reduc-
tion. However, these results do not mean that modal cancellation
is not the mechanism for the hub load reduction, it only means
that simple or obvious frequency placements (like a frequency
approaching 4/rev, a flap/pitch coelescence at 4/rev etc.) will
not explain the vertical hub load reduction. If the reduction
mechanism involves frequency placement (as opposed to a natural
aeroelastic feedback mechanism) it is much more subtle than
originally expected.

There is the possibility that these natural frequency results
could provide some insight into the instability observed for over-
swept blades.

Natural frequencies in air with damping at 270 rpm for the 40
degree (.698 rad) .87R swept blades, which diverged for the for-
ward flight analyses, and the 30 degree (.5236 rad) .87R swept
blades, are presented below in the table.

BLADE MODE	40 DEGREES (.698 RAD) SWEEP .87R	30 DEGREES (.5236 RAD) SWEEP .87R
1st Flap	1.05	1.02
2nd Flap	2.65	2.55
3rd Flap	5.95	5.90
Torsion	3.35	3.45

These data show that there is not a significant difference in
frequencies between these two configurations and confirm there
is not a unique frequency relationship for the 40 degree (.698
rad) .87R configuration that would cause the divergence. Forced

response calculations with a unit force at the blade tip in air with damping showed large root shears at 1/rev and 2.5/rev (see Section 6.1). It is possible that a large subharmonic at 2.5/rev is causing the poor analysis convergence for sweep above 30 degrees (.5235 rad).

Another possibility is that forward speed causes significant changes in aerodynamic damping as a function of blade azimuth position. It should be noted that the above natural frequency analysis assumes aerodynamic loads for a hovering rotor. When the rotor is flying at a reasonable forward speed the air damping and air spring vary with the blade azimuth position. The natural frequency in air <u>without</u> damping shows a coalesence of the flap and torsion frequencies for sweep angles above 30 degrees. If part of the blade azimuth position has low aerodynamic damping this may explain the poor analysis convergence for sweep angles above 30 degrees when at high airspeeds.

In simple terms, the aerodynamic lift can be written as

$$L = KV^2 \left(\theta + \frac{\dot{z}}{V}\right)$$

where $KV^2\theta$ represents the lift due to pitch
and $KV\dot{z}$ represents the lift due to flap

Introducing outboard sweep into the blade forces a kinematic coupling between inboard and outboard flap and pitch. For aft sweep inboard blade flap causes some outboard blade pitch, the resulting outboard pitch causes increased lift resulting in more inboard flap and changes in inboard pitch. Clearly, the blade sweep establishes a relationship between flap and pitch. As shown from the above equation, as the airspeed increases, for the same proportion of flap and pitch motion the relative lift due to pitch becomes proportionally larger than the relative lift due to flap velocity. Therefore, the flap damping with respect to the pitch induced lift becomes smaller and the blade frequencies may approach the "in air without damping" frequencies for a portion of the rotor disc.

Clearly, these ideas regarding the poor analysis convergence (and sometimes divergence) are only conjecture, and further investigation is necessary to prove or disapprove these theories.

Further investigation into the effects of blade frequency on the load reduction mechanism is included in Section 5.

5. EFFECT OF BLADE STIFFNESS

The effect of airspeed, sweep angle, and sweep initiation radius on the vibratory loads produced by the design A blade were discussed in previous sections. These analyses were conducted with the nominal values of flap bending and torsion bending stiffness. This section of the report documents the effect of varying flap and torsion stiffness on the blade natural frequencies and vertical vibratory hub loads. Torsion stiffness variations were mad by changing the blade torsion stiffness and the control system pitch stiffness. The values of torsion and flap stiffnesses investigated covered a wide range of flap/torsion frequency relationships. The table below shows the frequency range of blade flexible flap and torsion modes investigated.

MODE	FREQUENCY RANGE PER REV
2nd Flap	2.5 to infinity
3rd Flap	5.4 to infinity
4th Flap	8.1 to infinity
Torsion	3.9 to infinity

5.1 FLAP STIFFNESS VARIATIONS

5.1.1 BLADE FLAP FREQUENCIES

Blade natural frequencies were computed in a vacuum as a function of flap stiffness factor at the nominal value of torsional stiffness. This factor scales the blade flap bending stiffness from the center of rotation to the tip. These data, presented in

Figure 5.1.1-1 show that the 2nd flap frequency increases slightly even up to a flap stiffness factor of two. The 3rd and 4th flap frequencies, however, increase significantly. Doubling the flap stiffness increases the 3rd flap frequency from 5.7/rev to 6.75/ rev.

5.1.2 VERTICAL HUB LOADS

Four per rev vertical hub load as a function of blade sweep angle at .87R initiation radius were computed for flap stiffness factors of .75, 1.0, 1.5, 2.0, and infinity. The results of this study are presented in Figures 5.1.2-1 and 5.1.2-1A, and show several important results.

o Increasing the flap stiffness of the unswept blade reduces the 4/rev vertical hub load. Doubling the flap stiffness reduces this load from 1295 lb. (5760 N) to 1200 lb. (5338 N), a 7.3 percent decrease. Reducing the flap stiffness by 25% increases the 4/rev vertical hub load to 1723 lb. (7663 N), a 33% increase.

o The percentage reduction of the 4/rev vertical hub load with sweep is reduced as the flap stiffness is increased.

o Similar reduction trends with sweep occur over the entire range of flap stiffness factors.

o Sweep reduces the 4/rev vertical hub load even when the flap
   stiffness is infinite. This is a very significant finding
   and shows that elastic flap deflection and/or elastic flap/
   pitch coupling are not significantly involved in this hub
   load reduction mechanism. It also shows that a unique flap/
   torsion frequency relationship or a specific flap frequency
   is not necessary to obtain the hub load reduction.

5.2 TORSION STIFFNESS VARIATIONS

5.2.1 BLADE FREQUENCIES

Blade torsion frequencies were computed in a vacuum at the nomi-
nal value of control system stiffness as a function of the tor-
sional stiffness factor. This factor scales the blade torsion
bending stiffness from the center of rotation to the tip. Figure
5.2.1-1 shows that the baseline blade's torsion frequency is in-
creased from 4.3/rev to 6.7/rev when this factor is four. This
range of stiffness places the torsion mode well below and above
the third flap mode natural frequency. In addition, as part of
the torsional stiffness variation the torsional stiffness factor
was increased to infinity, and the only elastic pitch resulted
from control system deflection. Finally, to obtain an infinite
torsional stiffness and have no elastic pitch both the torsional
stiffness factor and the control system stiffness was increased
to infinity. The impact of these torsional stiffness changes
on the 4/rev vertical hub loads are discussed in the next section.

5.2.2 VERTICAL HUB LOAD

Figure 5.2.2.-1 presents 4/rev vertical shaking force vs. blade
sweep angle at .87R initiation radius computed for torsion stiff-
ness factors of .6, 1.0, 1.5, 2.0, 4.0, and infinity, and with
an infinite control system stiffness with an infinite GJ factor.
Several important conclusions can be drawn from the figure.

o Increasing the torsion stiffness of the unswept blade re-
  duces the 4/rev vertical hub load. Doubling the torsion
  stiffness reduces this load from 1295 lb. (5760 N) to 729
  lb. (3203 N), a 44 percent reduction. However, an infinitely
  stiff torsional system (i.e. no elastic pitch) does not re-
  sult in the lowest 4/rev vertical hub load. (See Figure
  5.2.2-1A.)

o The effectiveness of sweep is reduced as the torsion stiff-
  ness is increased. Above a torsion stiffness factor of
  approximately two, sweep increases the 4/rev vertical hub
  load. Therefore, a certain minimal torsional flexibility
  is required for sweep to be effective in reducing the verti-
  cal hub loads. (See Figure 5.2.2-1A.)

o Relative placement of the torsion and flap mode frequencies
  is not a factor in the hub load reduction mechanism.

Additional computer studies were performed to determine the effect of torsional stiffness inboard and outboard of the sweep initiation radius. The results of this investigation are presented in Figure 5.2.2-2 and clearly show that the blade torsion stiffness outboard of the sweep initiation radius does not significantly affect the load reduction trend. The critical torsional stiffness must occur inboard of the sweep initiation point.

6. HUB LOAD REDUCTION MECHANISM

Computer studies were initiated to gain detailed information on the hub load reduction mechanism. These analyses included the following:

o Forced response calculations were made with a variable frequency unit force at the blade tip. This defined the basic response characteristics of the baseline and swept blades. The objective of these calculations was to use the sweep-induced changes in the blade response to help identify the load reduction mechanism.

o Vibratory hub loads were computed simulating independent mass and aerodynamic sweep. This was done to decouple the aerodynamic and inertial effects of blade sweep.

o Blade twist and spanwise inertial and thrust loading was examined for the baseline and swept blades to show what blade response characteristics changed when the hub loads were reduced.

o Tip planform shape was studied to determine.the effect of swept aerodynamic blade area on vibratory hub loads. This was done to investigate changing the relative magnitude of the aerodynamic force to the inertial force in the swept portion of the blade.

6.1 UNIT LOAD FORCED RESPONSE

Figures 6.1-1 presents blade vertical root shear amplitude and
phase versus a 10 lb tip force excitation frequency for the base-
line unswept blade in a vacuum without damping. Large responses
occur at each of the flap mode natural frequencies. There is
very little flap/pitch coupling because the blade masses are near
the elastic axis. The root shear response from the torsion mode
is, therefore, very small. Figure 6.1-2 shows how the response
changes when air is included in the analysis but no damping.
There are small changes in the natural frequencies and the
response due to the aerodynamic $\Omega\beta$ pseudo non-circulatory pitch
rate term at .75 chord is now evident near the blade torsion
natural frequency. When aerodynamic damping is included (see
Figure 6.1-3) the blade frequencies change, the peak response at
resonance is reduced, and the response due to the airloads at .75
chord is eliminated.

Figures 6.1-4 through 6.1-6 present the results of 10 lb tip
forced response calculation with the blade swept 20 degrees (.349
rad) at .87R. In a vacuum without damping the response at the
torsion mode frequency is now evident because of the strong iner-
tial flap/pitch coupling induced by sweep. With sweep the masses
outboard of the sweep initiation radius are offset from the blade's
unswept elastic axis and pitch axis, increasing the effective
pitch inertia. In air with damping sweep amplifies the response
from the 1st flap mode, but attenuates the response from the 2nd

and 3rd flap modes. (Note the near zero vertical root shear for the response at 2.75/rev for both the in air with damping and the in air without damping responses).

A summary plot of vertical root shear versus tip force excitation frequency is shown in Figure 6.1-7 for the baseline blade, 10 degrees (.1745 rad), 20 degrees (.349 rad), 30 degrees (.5235 rad), and 40 degrees (.698 rad) sweep at .87R sweep initation radii. These results show that sweep reduces 2/rev, 3/rev, 5/rev, 6/rev etc. vertical root shear, but does not significantly reduce vertical root shear at the 4/rev frequency. This does not agree with the results of the forward flight loads analyses which showed large reduction in the 4/rev hub load at all airspeeds with 10 degrees (.1745 rad) and 20 degrees (.349 rad) sweep.

The tip force analysis does show a very large increase in 1/rev and 2.5/rev vertical root shear as the blade sweep is increased from 30 to 40 degrees. This corresponds to the coelescence of the torsion and flap modes at a rotor speed below the normal operating speed, and is probably responsible for the poor program convergence for sweep angles above 30 degrees.

It is clear that forcing at the blade tip does not illustrate all the effects observed in the forward flight loads analysis. It is probably necessary to force the blade at various spanwise locations to fully observe the 4/rev hub load change. If forcing

along the blade span does show the 4/rev vertical root shear re-
duction, this method could become a powerful tool for evaluating
different blade designs.

6.2 SPANWISE LOADING DISTRIBUTIONS

.

Spanwise distribution of 4/rev vertical inertial force and thrust
are presented in Figures 6.2-1 and 6.2-2 for the baseline unswept
and 20 degree (.3490 rad) swept at .87R blades at the reference
flight condition. The data is presented as 4ψ cosine and sine
components, with ψ (the blade azimuth angle) equal to zero when
the blade is trailed down wind. As expected, inertial and aero-
dynamic forces are out of phase and of approximately equal mag-
nitude. The relatively large inertial forces inboard of the
cutout at .21 radius result primarily from vertical acceleration
of the relatively heavy articulation hardware. As shown, there
are larger inertia and aerodynamic forces in the region of the
blade tip for the 20 degrees swept blade as compared to the
straight blade. Similar results were obtained for the 10 degree
(.1745 rad), and 30 degree (.5236 rad) sweep configurations but
are not presented here. Figure 6.2-2A shows the distribution
of lumped masses in the blade design A analytical model.

Figure 6.2-3 presents the 4/rev incremental vertical shear dis-
tribution along the blade for the unswept, 5 degree (.0873 rad),
20 degree (.349 rad), and 30 degree (.5236 rad) sweep at .87R

configurations. (The shear increment is the net shear that results from the difference between the airloads and the inertia loads). These data show several significant results:

o The relatively large shears at .13R, .45R and .87R are produced by vertical acceleration of the articulation hardware, the flap tuning weight, and the tip weight.

o Incremental shears are significantly lower on most of the swept blades. (There is a relatively large incremental shear at about .8R for the 30 degree swept blade).

For an articulated rotor the 4/rev vertical hub loads are produced by the 4/rev vertical root shears. Therefore, if the 4/rev vertical hub loads are reduced, the 4/rev vertical root shears are reduced. The root shear is the spanwise integral of the incremental shear. Figure 6.2-4 presents the 4/rev vertical shear summation (the integrated vertical shear along the blade) for the unswept, 5 degrees (.0873 rad), 20 degrees (.349 rad), and 30 degrees (.5236 rad) sweep at .87R configurations. These data clearly show the reduction in root shear as the sweep angle is increased.

The above figures show that the shear is reduced all along the blade and so is the flap bending moment (See Figure 3.5-2). However, this data does not show why the reduction occurs. Examining the blade deflections may provide that insight.

Four/rev vertical acceleration vs. nondimensional blade radius is presented in Figure 6.2-5 for the baseline unswept, 10 degree (.1745 rad) .87R, and 20 degree (.349 rad) .87R sweep configurations at the reference flight conditions. These data show that vertical accelerations inboard of the sweep initiation radius are significantly reduced by blade sweep and the accelerations outboard of the blade sweep are significantly increased. Figure 6.2-6 presents the spanwise distribution of 4/rev elastic pitch angle (relative to the disc plane) for these configurations and shows a 180° change in phase angle due to increasing sweep angle.

The elastic pitch angle phase change is the most significant fact observed from this investigation. Figure 6.2-7 presents the elastic twist, pitch angle, and angle of attack for the baseline unswept and 20 degrees (.349 rad) .87R sweep configurations. These data clearly show that sweep reduces the higher harmonics of elastic twist between the tip and cutout. Higher harmonics of blade pitch angle at the tip are also reduced by sweep. The tip angle of attack is reduced by sweep on the advancing blade, but is increased by sweep on the retreating blade. At the 150 knot (77.2 m/s) reference flight condition the 4/rev root pitch angle is reduced from .1412 degrees (.00246 rad) on the baseline unswept blade to .05129 degrees (.000895 rad) on the 20 degree (.349 rad) sweep at .87R configuration.

6.3 SIMULATED SWEEP

The results presented in the previous section showed that the
major difference between the swept and unswept blade response
was the elastic twist of the blade and the resulting change in
angle-of-attack of the tip region. To understand the mechanism
that causes the elastic twist, the separate pitching moment com-
ponents caused by blade sweep are examined using the technique
of blade sweep simulation.

Physical blade sweep causes the local inertia reference (the cg),
aerodynamic reference (the 1/4 chord) and elastic reference (the
shear center) to sweep as a portion of the blade is swept. The
rotor loads program, C-60, (See Appendix A) representation of
blade sweep causes the simultaneous sweep of all three references
(inertial, aerodynamic and elastic). To help understand the
effects of sweep, the effects of individually changing the iner-
tial and aerodynamic references due to sweep will be investigated.
This can be done by using a straight blade, with no elastic refer-
ence sweep, and then simulating the inertial and aerodynamic sweep
effects by changing the cg reference and the 1/4 chord reference.
Figure 6.3-1 compares the full sweep results with the simulated
sweep for the 150 knot (77.2 m/s) flight condition with 5 degrees
(.0873 rad) sweep initiated at the spanwise position of .87R.
As shown, there is good agreement of the calculated 4/rev verti-
cal hub load between the actual swept blade and the simulated
swept blade for a small sweep angle.

It will be shown below that the simulated sweep approximation is valid only for <u>small sweep angles</u> and/or sweep over a <u>very small portion</u> of the rotor blade. For a sweep initiation radius of .87R, 5 degrees of simulated sweep is the approximate limit before significant distortions result relative to actual sweep.

As shown in Figure 6.3-1, the 4/rev vertical hub load is reduced 13.4 percent for the actual swept blade and 18.4 percent for the simulated 5 degree (.0873 rad) sweep configuration. This confirms that simulated sweep is a viable tool to study independent aerodynamic and mass sweep effects. It should be noted that the simulated sweep configuration produces larger inertial and aerodynamic moments about the unswept elastic axis for the swept portion of the blade. This can best be shown by examining the blade outboard elastic twist between the sweep initiation point and the tip, and inboard elastic twist between the sweep initiation point and the root cutout. These data are presented in Figures 6.3-2 and 6.3-3 and show the following:

o Elastic twist inboard of the sweep initiation radius is comparable for the actual and simulated sweep configurations. Both of these configurations have significantly lower elastic twist than the baseline unswept blade.

o As expected, the simulated sweep configuration has significantly larger twist outboard of .87R due to the mass and aero forces being offset from the unswept elastic axis.

o Elastic twist outboard of the sweep initiation radius at
   .87R is comparable for the unswept and swept blades. There-
   fore, sweep does not significantly change the elastic twist
   of the swept portion of the blade.

Simulation of independent forward and aft mass and aerodynamic
sweep was analyzed for the 150 knot (77.2 m/s) flight condition
and showed the key relationships of aerodynamic center and mass
C.G. locations.

Figures 6.3-4 and 6.3-5 present the several significant results
obtained from these studies:

o Aft aerodynamic sweep reduces the vertical 4/rev hub load
   by 47.9 percent, but aft mass sweep increases this load by
   42.6 percent.

o Forward mass sweep decreases the 4/rev vertical hub load by
   34.1 percent.

o Translating the mass of the swept blade forward to the
   unswept blades' pitch axis produced a 43.9 percent reduc-
   tion of the 4/rev vertical load. This is much larger than
   the reduction achieved with the actual 5 degrees (.0873 rad)
   of sweep.

o   Translating the aerodynamic bays of the swept blade forward
    to the unswept blades pitch axis resulted in a 28.6 percent
    increase in load.

These test cases showed that 4/rev vertical hub loads were re-
·duced by forward mass sweep and aft aerodynamic sweep. This
configuration was analyzed and produced the largest reduction in
load, a 55.4 percent decrease from the baseline case.

In Section 6.2 it was shown that when sweep reduced the 4/rev
hub loads, the pitch angle on the advancing blade was more nose
up and the higher harmonic component of the pitch angle was re-
duced. To determine if the simulated sweep gives the same results,
·tip pitch angle was examined for the simulated sweep results.

Figure 6.3-6 presents the tip pitch angle vs. azimuth position
for the baseline unswept blade, 5 degrees (.0873 rad) forward,
and 5 degrees (.0873 rad) aft simulated mass sweep configurations.
These data show that the increase in 4/rev vertical hub load is
accompanied by a significant increase in vibratory pitch angle.
The forward mass sweep has reduced vertical loa s, reduced
vibratory pitch angle, and the pitch angle on the advancing blade
is more nose up.

Similar results were found for the simulated aerodynamic sweep
studies. Figure 6.3-7 shows that forward aerodynamic sweep
produced significant increases in both 4/rev vertical hub load,

vibratory pitch angle and a more nose down pitch angle on the advancing blade. Aft aerodynamic sweep produced significant reductions in the hub load, reduced higher harmonic content of the pitch angle, and the advancing blade pitch angle is more nose up.

These results have demonstrated that reducing blade vibratory pitch with sweep reduces the 4/rev vertical hub load. This is one of the most significant results of the sweep investigation.

The blade sweep investigated during this study, involved sweeping the inertia, aerodynamic and elastic references together. Therefore, for aft sweep to reduce the 4/rev vertical hub load, the simulated sweep results imply that the beneficial effect of aft aerodynamic sweep is larger than the detrimental effect of aft mass sweep. If this is true, it is the tip aerodynamic and mass properties that cause the beneficial effects of sweep. This also explains the observation that aft sweep does not reduce the vertical hub shear for all blades. If the tip properties are such that the detrimental effects of aft mass sweep are larger than the beneficial effects of aft aerodynamic sweep, then aft sweep would make the loads worse and perhaps forward sweep would reduce the loads. This hypothesis will be investigated further in the following sections.

6.4 TIP SHAPE

In the previous section the hypothesis that the aerodynamic and
inertia properties of the swept region determines the behavior
of the blade as sweep was introduced. It was also concluded t'·at
aft aerodynamic sweep was beneficial and aft inertia sweep was
detrimental. If this hypothesis is true, then increasing the
aerodynamic surface of the swept portion of the blade should in-
crease the effectiveness of aft sweep for reducing 4/rev vertical
shear. To substantiate this hypothesis, analyses were conducted
to determine if a square tip, which has more aerodynamic surface
area (then the reference blades 3 to 1 tip taper), demonstrated
a larger reduction in hub load with sweep. The results of this
study are presented in Figure 6.4-1 and show that the unswept
square tip blade develops higher vibratory vertical force than
the 3 to 1 tapered tip blade. The 4/rev vertical hub load for
the unswept blade is increased from 1300 lb. (5782 N) to 1400
lb. (6227 N), an 8.1% increase. As expected, the square tip
blade has a larger rate of decrease in hub load with sweep than
the tapered tip blade up to approximately 14 degrees (.2443 rad).
At angles larger than 14 degrees (.2443 rad) the square tip
convergence begins to deteriorate and the vertical 4/rev load
increases with sweep. The 14 degrees (.2443 rad) sweep at .87R
square tip configuration reduces the 4/rev vertical hub load
from 1400 lb. (6227 N) to 390 lb. (1735 N), a 72% reduction (to
28% of the unswept value). The tapered tip blade with 30 degrees

(.5236 rad) sweep at .87R produces 280 lb. (1245 N) of 4/rev
vertical hub load, slightly lower than the optimum square tip
configuration of 14 degrees (.2443 rad) sweep.

These results substantiate the hypothesis, since the effective-
ness of sweep (i.e,; the change of 4/rev vertical shear/sweep
angle) was increased by increasing the aerodynamic area. How-
ever, the increased aerodynamic area also caused the sweep in-
duced convergence deterioration to begin at 14 degrees instead
of 30 degrees. If this convergence deterioration can be under-
stood and the resulting hub load increase controlled, then
significantly larger reductions in hub loads may be possible.

7. ANALYSIS OF OTHER BLADES

In Section 1 it was stated that aft sweep increased the 4/rev vertical hub load on several of the blades analyzed. These blades had different physical properties including airfoils, tip shape, torsional stiffness, flap stiffness, pitch axis location, mass distribution, chord size, radius, and rotor speed.

In Section 6 it was hypothesized that the physical properties of the swept portion of the blade determines the effectiveness of blade sweep for reducing the 4/rev vertical hub load. If this hypothesis is true, changing the physical properties of the swept portion of the blade could dramatically change the blade behavior with aft sweep. Therefore, a blade that exhibits increasing 4/rev vertical hub loads as a result of aft blade sweep could be transformed into a blade that exhibits decreasing 4/rev vertical hub loads as a result of aft blade sweep. This section will check this hypothesis by determining if the behavior of the CH-47C metal blade due to aft sweep can be modified by replacing the swept portion of the blade with the Design A properties.

First, let's examine the behavior of the CH-47C metal blade. When aft sweep is introduced at the 150 knot (77.2 m/s) flight condition, the 4/rev vertical hub loads increase. For the straight blade the vertical hub load is 1500 lbs. (6672 N),

with 10 degrees (1745 rad) of aft sweep the load increases to
2500 lbs. (11120 N). Additional studies were conducted to de-
termine if the load increase with sweep on the CH-47C metal
blade was unique to the 150 knot (77.2 m/s) flight condition.
Figure 7.1 shows that between 120 knots (61.7 m/s) and 220
knots (113 m/s) the baseline blade develops significantly
lower 4/rev vertical hub loads than the blade with 10 degrees
(.1745 rad) sweep at .87R. Loads computed with 20 degrees
(.349 rad) of sweep at .87R were very large and the analysis
had poor convergence.

One of the differences between the CH-47C and the Design A
blade is the airfoils. Blade Design A has advanced VR15 and
VR12 airfoils, the CH-47C has the 23010 airfoil. When the
CH-47C with 10 degrees (.1745 rad) sweep at .87R was analyzed
using VR15 and VR12 airfoils at the 150 knot (77.2 m/s) refer-
ence flight condition the 4/rev vertical hub load was reduced
by 1.6% and confirmed that airfoil characteristics are not a
significant factor in the hub load reduction mechanism in this
case.

The next step was to determine if changing the physical prop-
erties of the swept portion of the CH-47C blade would change
the effect of aft sweep. Replacing selected blade properties
on the CH-47C outboard of the sweep initiation point with those
from blade Design A produced a reduction in hub load with blade
sweep. For no sweep, the modified CH-47C 4/rev vertical hub

load was 1800 lbs. (8006 N), and for 10 degrees (.1745 rad) of
aft sweep the load was reduced to 1450 lbs. (6450 N). The modi-
fied properties are: 1) distance from pitch axis to mass C.G.,
2) distance from mid-chord to pitch axis, 3) mass, 4) pitch
inertia about the pitch axis. Comparison plots of these para-
meters for the CH-47C metal and design A blades are presented
in Figure 7.2 to 7.4. The CH-47C metal blade, which has a 1.6
percent larger chord and square tip, has significantly more
mass and higher pitch inertia outboard of the sweep initiation
radius. More important, the mass C.G. locations are aft of the
pitch axis. This was previously shown to cause increased 4/rev
vertical hub loads.

Clearly, changing the physical properties in the swept portion
of the blade changed the CH-47C behavior for aft sweep. How-
ever, the vertical hub load reduction was small. In Section
5.2.2, it was discovered that torsional stiffness plays a role
in the ability of aft sweep to reduce hub loads. Above a cer-
tain torsional stiffness the blade has very little sensitivity
to sweep. Clearly a certain minimal torsional stiffness is
needed to allow the necessary elastic twist to occur. Compar-
ing the torsional stiffness of the two blades shows that the
CH-47C metal blade has three times the stiffness of the De-
sign A blade. Therefore, a combination of Design A tip prop-
erties and .5 torsion stiffness factor was evaluated. This
configuration increased the unswept blade's vibratory vertical
hub load by 55 percent; but with blade sweep a significant re-

duction in 4/rev vertical hub load was achieved. For zero sweep the 4/rev vertical hub load was 2375 lbs. (10564 N), for 10 degrees (.1745 rad) of the aft sweep the load was reduced to 1080 lbs. (4804 N). These results are summarized in Figure 7-5.

Reviewing Figure 5.2.2-2 shows that minimal torsional flexibility of the swept portion of the blade is not required, in fact high torsional stiffness in this region may be beneficial. Based upon the information we now have, a simplistic explanation of the sweep induced vertical hub load reduction mechanism can be formulated.

The current understanding of the hub load reduction mechanism is summarized below and in Figure 7-6.

1. Certain physical properties (aero center and chordwise center of gravity and possibly total mass, pitch inertia, and shear center) are required in the swept portion of the blade to generate the required aerodynamic/inertial force.

2. A minimal torsional flexibility is required in the unswept portion of the blade to obtain the necessary elastic twist (the torsional stiffness can probably be distributed between blade and control system stiffness).

3. The torsional stiffness in the swept portion of the blade has little influence, and a high stiffness may be beneficial.

4. The flap stiffness has little influence.

For the hub load reduction to occur, the net aero/inertial force generated on the swept portion of the blade uses the large sweep induced moment arms to twist the unswept portion of the blade (and of course changing the pitch angle of the swept region). If the phase and amplitude of the sweep induced elastic twist reduces the tip down twist of the advancing blade and reduces the higher harmonic twist introduced from other sources, the 4/rev vertical hub load is reduced.

8. CONCLUSIONS

Analytical studies have shown that blade sweep can significantly reduce vibratory hub and control system loads. Several blades analyzed, however, demonstrated an increase in loads when the blade was swept. Torsional flexibility was shown to be a necessary requirement to insure that sweep produces the desired loads reduction. A reference rotor with sweep was analyzed to determine the effect of airspeed, flap stiffness, torsion stiffness and physical properties of the swept portion of the blade. The following significant conclusions were drawn from these investigations.

o Vertical and inplane vibratory hub loads, control system loads, flap bending moments and rotor horsepower were reduced at all airspeeds analyzed due to aft sweep of the Design A blade.

o There is not an optimum sweep angle for all airspeeds. For the reference rotor, vertical 4/rev hub loads are lower with ·10 degrees (.349 rad) sweep than with 10 degrees (.1745) between 120 knots (61.7 m/s) and 192 knots (98.8 m/s). Above 192 knots (98.8 m/s), however, the 10 degree (.1745 rad) sweep configuration develops significantly lower vertical hub loads.

o Specific blade frequency placement and flexible flap/ pitch coupling are not necessary to obtain hub load reduction with sweep. Blade torsional stiffness does, however, play a significant roll in the sweep effectiveness.

o Analysis of independent mass and aerodynamic chordwise distribution showed that mass forward of the elastic axis and aerodynamic center aft of the elastic axis reduced the vertical 4/rev hub loads.

o The 4/rev vertical hub load reduction mechanism requires carefully selected physical properties of the swept portion of the blade and sufficient torsional flexibility of the unswept portion of the blade (to allow the necessary elastic twist to occur). This understanding was verified by modifying a blade that exhibited increased hub loads due to aft sweep until the modified blade showed decreased hub loads with aft sweep.

o The fundamental physical property requirements of the swept portion of the blade have not been fully defined and understood.

o Improving the blade stability margin may allow even further hub load reductions, but the instability mechanism has not been investigated.

9.   RECOMMENDATIONS

The following recommendations are provided to indicate additional
work that should be performed to better understand the effect of
sweep on vibratory hub loads so that the fundamental mechanism
can be best implemented in a blade design with low hub loads.

1.   Understand which tip parameters are important to obtain
      the hub load reduction with sweep. This can be done
      by systematically varying the tip physical properties
      one at a time and in combination over a significant
      range and observing the resulting hub loads. Calculate
      the pitching moment generated by motion and airloads
      by the swept portion of the blade on the unswept por-
      tion of the blade for each of the parameter changes.
      If necessary, use the simulated sweep method to de-
      couple some of the effects to obtain further insight.
      The simulated sweep approach can be used for larger
      sweep angles if the blade section outboard of the sweep
      initiation point is infinitely stiff in torsion.

2.   Complete the understanding of the influence of flap
      stiffness and torsional stiffness on the sweep induced
      hub load reduction. The flap stiffness investigation
      can be expanded by extending the flap stiffness study
      to include hingeless rotors. This could be accom-
      plished by progressively stiffening the flap hinge

spring. The torsional stiffness investigation can be
expanded by determining if torsional requirements are
defined by stiffness or torsional frequency and deter-
mine if torsional frequency can be used to determine
specific harmonics for vertical hub load reduction. It
can also be determined if torsional flexibility require-
ments can be obtained by modifying the control system
stiffness instead of the blade GJ.

3. Determine if the unit force analysis method can be used
to predict the effects of sweep on vibratory hub loads
for all harmonics and airloading conditions. If this
approach is successful, optimization routines can be
used to define the lowest hub load configuration in-
dependent of specific trim flight conditions. This
approach can be evaluated by varying the unit force
along the blade span for the baseline unswept and two
swept configurations to determine if unit forcing is a
viable tool for evaluating sweep. If this evaluation
is positive, airload spanwise spectra representing a
wide range of flight conditions can be used in conjunc-
tion with the unit force response at each spanwise
position to quickly evaluate and optimize blade designs
for all flight conditions.

4. Investigate the hub load reduction mechanism on a blade
with the same planform but different baseline physical

properties. Select a blade that indicates hub load
reduction potential due to forward blade sweep. Find
the sweep initiation radius and forward sweep angle
that provides the largest hub load reduction. Deter-
mine if forward sweep provides greater hub load reduc-
tion than aft sweep, or if the stability margin is im-
proved. Compare tip parameter and overall blade para-
meter differences and similarities to help clarify the
hub load reduction mechanism. Determine if it is pos-
sible to modify the critical physical properties (as
determined above) to cause the vibratory hub loads to
reduce with aft sweep instead of forward sweep.

5.   Investigate the unit force hub load notch illustrated
      in figures 6.1-5,6 and 7 at a frequency of 3.75   for
      a blade with 20 degrees of aft sweep. This can be done
      by determining blade parameter changes (or a change in
      rotor rpm) that will move the hub load notch to 4/rev
      or any other integer multiple of rotor speed. Then
      analyze this modified rotor configuration using the
      C-60 rotor analysis program to calculate the hub loads
      at the notch integer/rev frequency for various flight
      conditions. If very low vertical hub loads are de-
      fined for the integer/rev frequency, define a plan for
      further investigation.

6. Understand the source of the rotor instability. Use simulated sweep at large sweep angles to systematically investigate the effects of each blade parameter on the sweep induced instability. To prevent excessive elastic pitch outboard of the sweep initiation radius for the simulated sweep (as shown in figure 6.3-2) perform this investigation with an infinite torsional stiffness outboard of the sweep initiation radius. Once the instability is understood, define modifications to the blade properties as required to improve stability without reducing the effectiveness of sweep for reducing vibratory hub loads. Determine if increasing the blade stability margin will allow larger sweep angles and even lower hub loads.

7. Based on the understanding of the sweep induced hub load reduction and rotor instability mechanisms, develop design criteria for swept blades with low vibratory hub loads. Apply the criteria to either (or both) an existing blade or a generic baseline blade having uniform mass and stiffness properties, to determine if vibratory hub loads are significantly reduced from the baseline.

8. Define a low vibratory hub load blade using the design criteria developed above. Include all aspects of blade design (blade loads, control loads, performance etc.)

and include all components of blade loads in a trade study (not just vertical loads). If appropriate consider using optimization techniques to obtain the blade design.

9.   Wind tunnel test swept and unswept versions of the low vibration blade design from above. Include a control blade in the testing that represents a dynamic/mach scaled version of an existing rotor blade to provide a link to current technology blades.

10. APPENDICES

APPENDIX A

AEROELASTIC ROTOR ANALYSIS PROGRAM

Boeing Vertol has developed an aeroelastic rotor loads analysis,
the C-60 Program (References I, J, and K), which calculates:

o   blade loads and motions for steady-state flight conditions

o   control-system forces

o   steady and vibratory hub loads

o   rotor performance

o   rotor trim

for articulated, teetering, and hingeless rotors with from two
to nine blades. The blades may be of arbitrary planform, twist,
and radial variation in airfoil section. This analysis is limited
to steady-state flight at constant rotor-tip speeds.

The analysis considers coupled flapwise and torsion deflections
and uncoupled chordwise deflections of the rotor blades. The
blade dynamics are represented by 25 lumped masses interconnected

in series by elastic elements. The dynamic parameters include variations of planform sweep, shear center, vertical neutral axis, chordwise center of gravity, and pitch axis. The solution is obtained using the associated-matrix method to equate the tip-boundary conditions to the root-boundary conditions. The solution is expanded in a Fourier series and the coefficients are obtained by inverting the matrix equation that relates the tip- and root-boundary conditions.

Airload calculations include airfoil-section geometry, compressibility, stall, three-dimensional flow, unsteady aerodynamics with center of pressure shift, and nonuniform downwash. Static airfoil tables are used to account for compressibility, static stall, and airfoil shape. The unsteady aerodynamic loads are calculated by modifying the static loading resulting from the airfoil tables to include Theordorsen's shed-wake function, dynamic stall effects based on oscillating-airfoil data, and yawed flow across the blade.

The nonuniform downwash calculations are based on a tip and root vortex trailed from each blade. Through an iterative technique, each trailed vortex is made compatible with the calculated blade-lift distribution; the lift distribution is compatible with the nonuniform downwash field. The vortex wake is assumed to be rigid and to drift relative to the hub with a constant resultant velocity composed of thrust-induced uniform downwash and the speed of the aircraft. The analysis is capable of recalculating

the nonuniform downwash field during any stage of the analysis
to account for the redistribution of airloads resulting from
elastic blade deflections.

The solution for the nonlinear aerodynamic loads and the coupled
flap and pitch blade response is performed in series. Up to 20
iterations between the airloads and blade response are used
to obtain the final solution. An iterative solution is used to
account for the nonlinear coupling between the blade deflections
and airloads that result from stall and compressibility. A sum-
mary of the analytical features is provided in Figure A-1.

APPENDIX B

ROTOR FLIGHT CONDITIONS

Sweep analyses were conducted at the flight condition described
below in the Table.

Airspeed = 150 kt. (77.2 m/s)

Rotor speed = 270 RPM

Air density = .002378 lb. sec^2/ft^4 (.125 kg sec^2/m^4)

Thrust = 16463 lb. (73227 N)

Lateral cyclic = -2.9 deg. (-.0506 rad)

Longitudinal cyclic = -7.0 deg. (-.1222 rad)

Collective = 13.9 deg. (.2426 rad)

Propulsive force = 1396 lb. (6209 N)

Non-dimensional thrust = .0776 C_T/σ

Non-dimensional propulsive force = .0789 C_x/σ

Advance ratio = .356

For airspeed sweeps the rotor controls were fixed and the propul-
sive force scaled by the square of the airspeed. This minimized
the parametric changes which could mask the effect of sweep at
other airspeeds.

APPENDIX C

DESCRIPTION OF REFERENCE ROTOR

The reference 4-bladed rotor selected (referred to as Design A) is fully articulated, has a tapered planform, advanced airfoils, a 24.85 ft. radius, and operates at a nominal rotor speed of 270 RPM. The blade chord and pitch arm are 22 inches and 8.5 inches respectively. The blade physical properties are summarized in Figure C-1. A plan view is presented in Figure C-2 which shows the baseline unswept and swept blades. The sweep angle is defined as the angle between the elastic axes of the straight and swept blade sections.

11. REFERENCES

A) Rotor Blade Tip Shape Effects on Performance and Control Loads From Full-Scale Wind Tunnel Testing, Robert H. Stroub, John F. Rabbott, Jr., Charles F. Niebanch. Journal of the American Helicopter Society, October, 1979.

B) Dynamic Analysis of Constant-Lift and Free-Tip Rotors, Inderjit Chopra. Journal of the American Helicopter Society, January 1983.

C) Experimental Effect of Tip Shape on Rotor Blade and Control Loads, J.P. Rabbott, Jr., USAAVRADCOM and C.F. Niebanch, Sikorsky Aircraft Division. American Helicopter Society Annual Forum Publication, 1978.

D) General Purpose Research Rotor, R. Jones, H.E. Howes, Kaman Aerospace Corp., L. Hoslins, NASA Ames Research Center. American Helicopter Society Annual Forum Publication 1981.

E) Wind Tunnel Evaluation of Aeroelastically Conformable Rotors. R.H. Blackwell, Sikorsky Aircraft Div., W.T. Yeager, USA RTL Structures Lab, P.H. Mirich, USA RTL Applied Technology Lab.

F)   Controllable Twist Rotor, Performance and Blade Dynamics,
     A.Z. Lemnios, A.F. Smith, Kaman Aerospace Corp., W.E.
     Nettles, USAAMRDL, Eustis Directorate. American Heli-
     copter Society Annual Forum Publication 1972.

G)   Wind Tunnel Evaluation of Aeroelastically Conformable
     Rotors, R.H. Blackwell, R.J. Murrill, W.T. Yeager, Jr.,
     P.H. Mirich. Journal of The American Helicopter Society,
     April 1981.

H)   The Aeroelastically Conformable Rotor Concept, R.H.
     Blackwell and D.J. Merkley. Journal of The American
     Helicopter Society, July 1979.

I)   Prediction of Control Loads Due to Blade Stall,
     F.J. Tarzanin, Jr. 27th Annual National V/STOL
     Forum of the American Helicopter Society, Preprint
     No. 513, May 1971.

J)   V/STOL Dynamics and Aeroelastic Rotor-Airframe
     Technology, Volume II, Description and Correlation
     of New Methodologies, Alexander, H., Amos, A.,
     Tarzanin, F., Taylor R., AFFDL-TR-72-40, May 1972.

K)   Current Loads Technology for Helicopter Rotors,
     R. Gabel. ALARD April 1973.
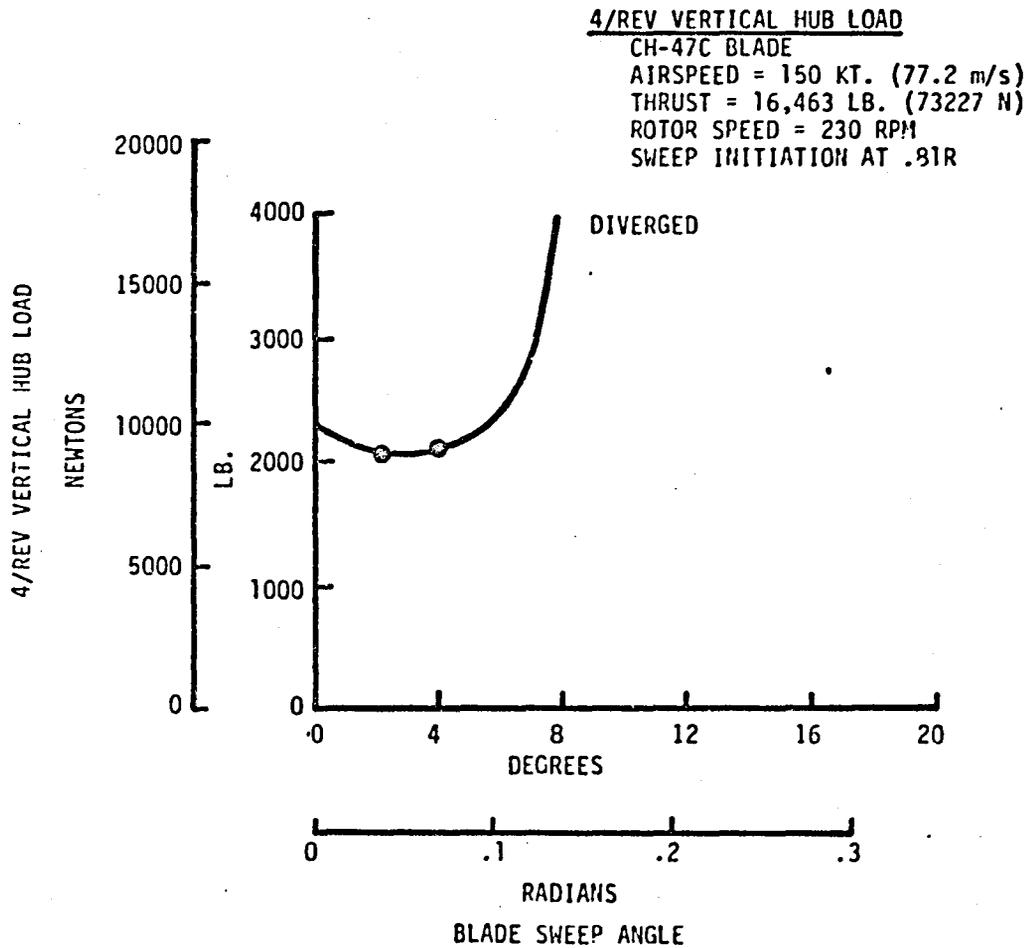
FIGURE 1.-1 4/REV VERTICAL HUB LOAD VS. BLADE SWEEP ANGLE, CH-47C BLADE
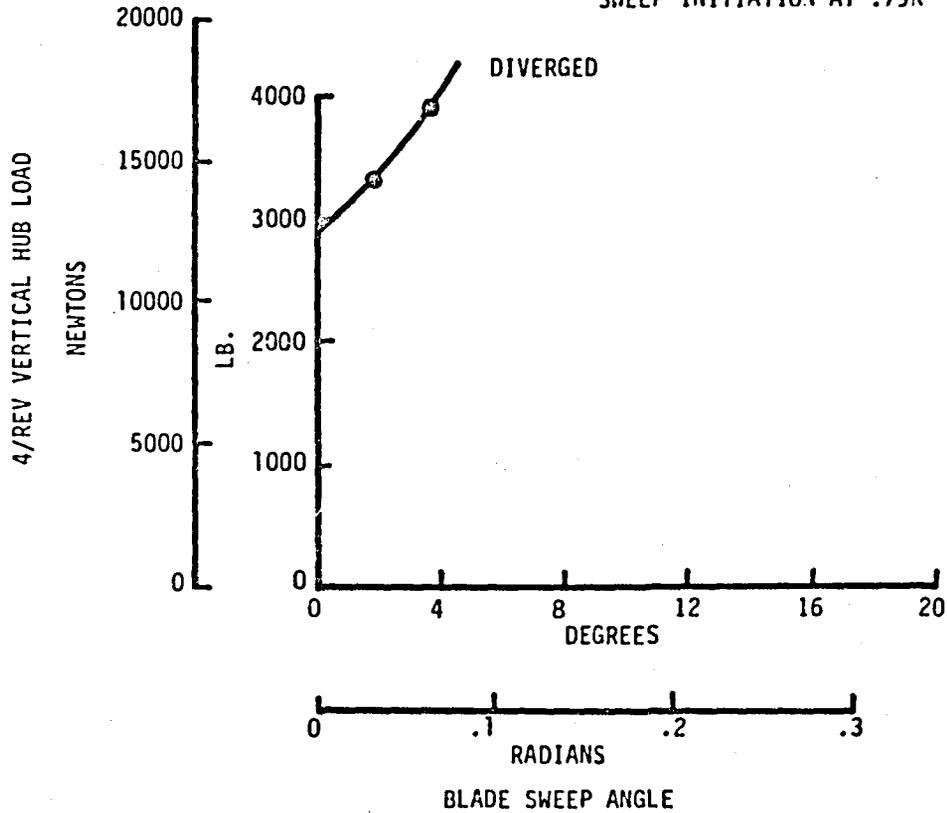
FIGURE 1.-2 4/REV VERTICAL HUB LOAD VS. BLADE SWEEP ANGLE, BLADE DESIGN B
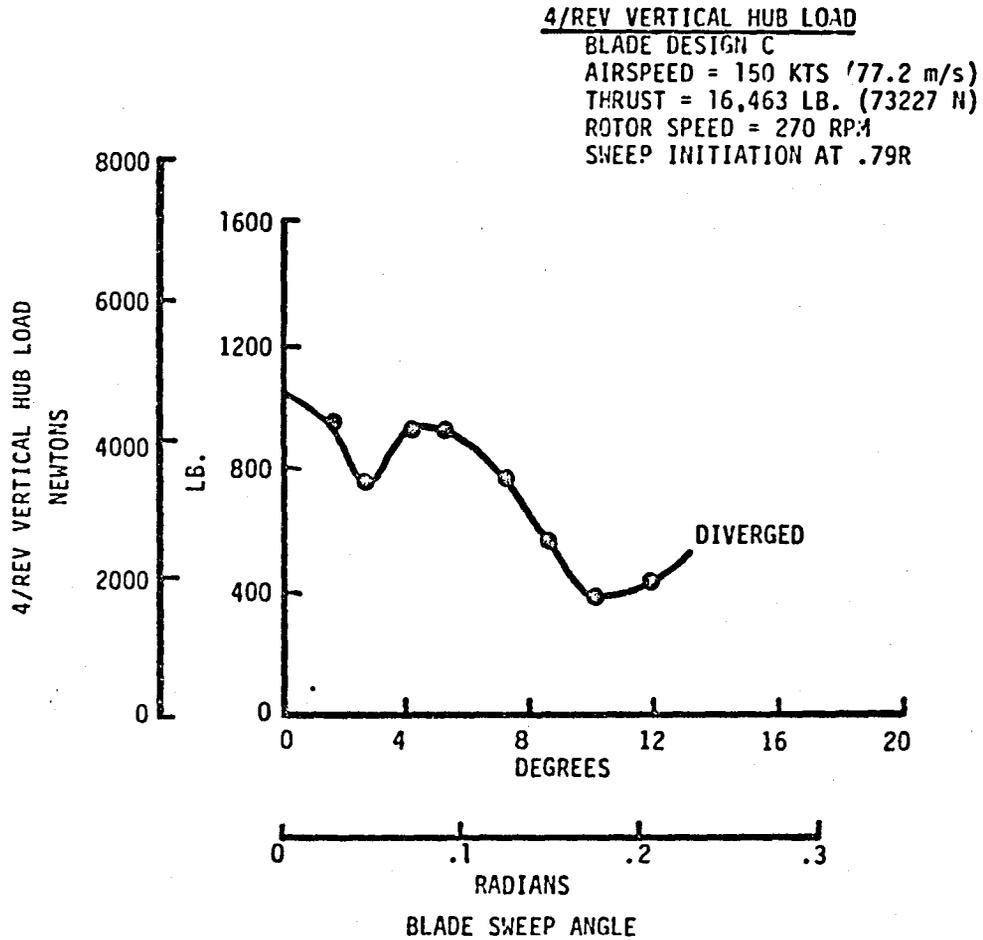
FIGURE 1.-3 4/REV VERTICAL HUB LOADS VS. BLADE SWEEP ANGLE, BLADE DESIGN C

72
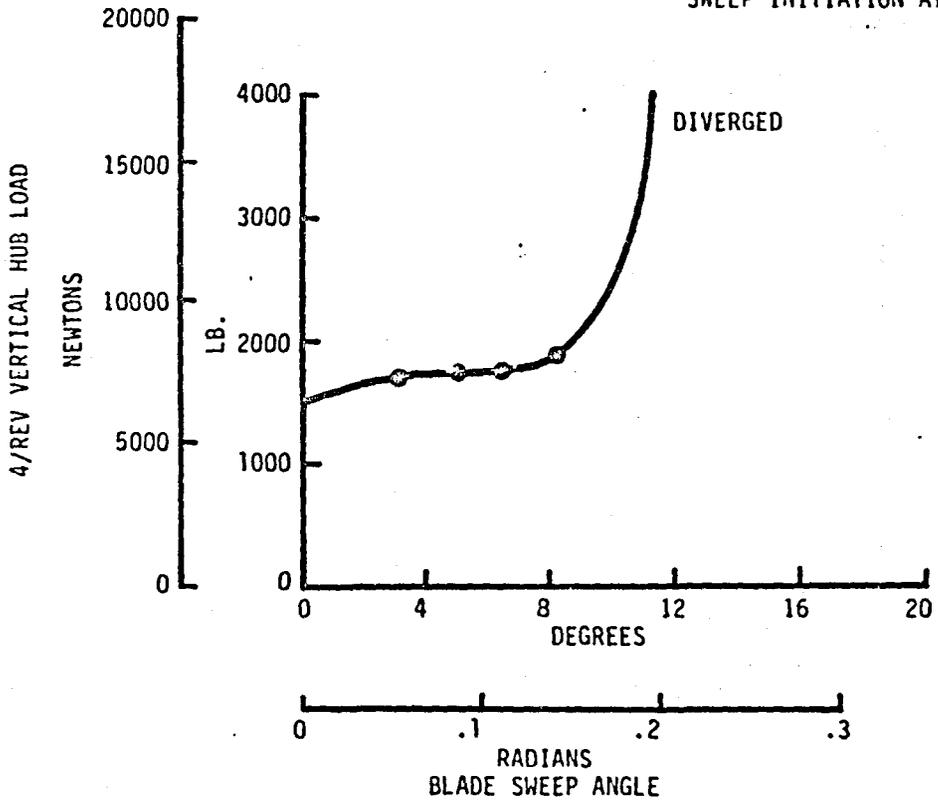
FIGURE 1.-4 4/REV VERTICAL HUB LOAD VS. BLADE SWEEP ANGLE, BLADE DESIGN D
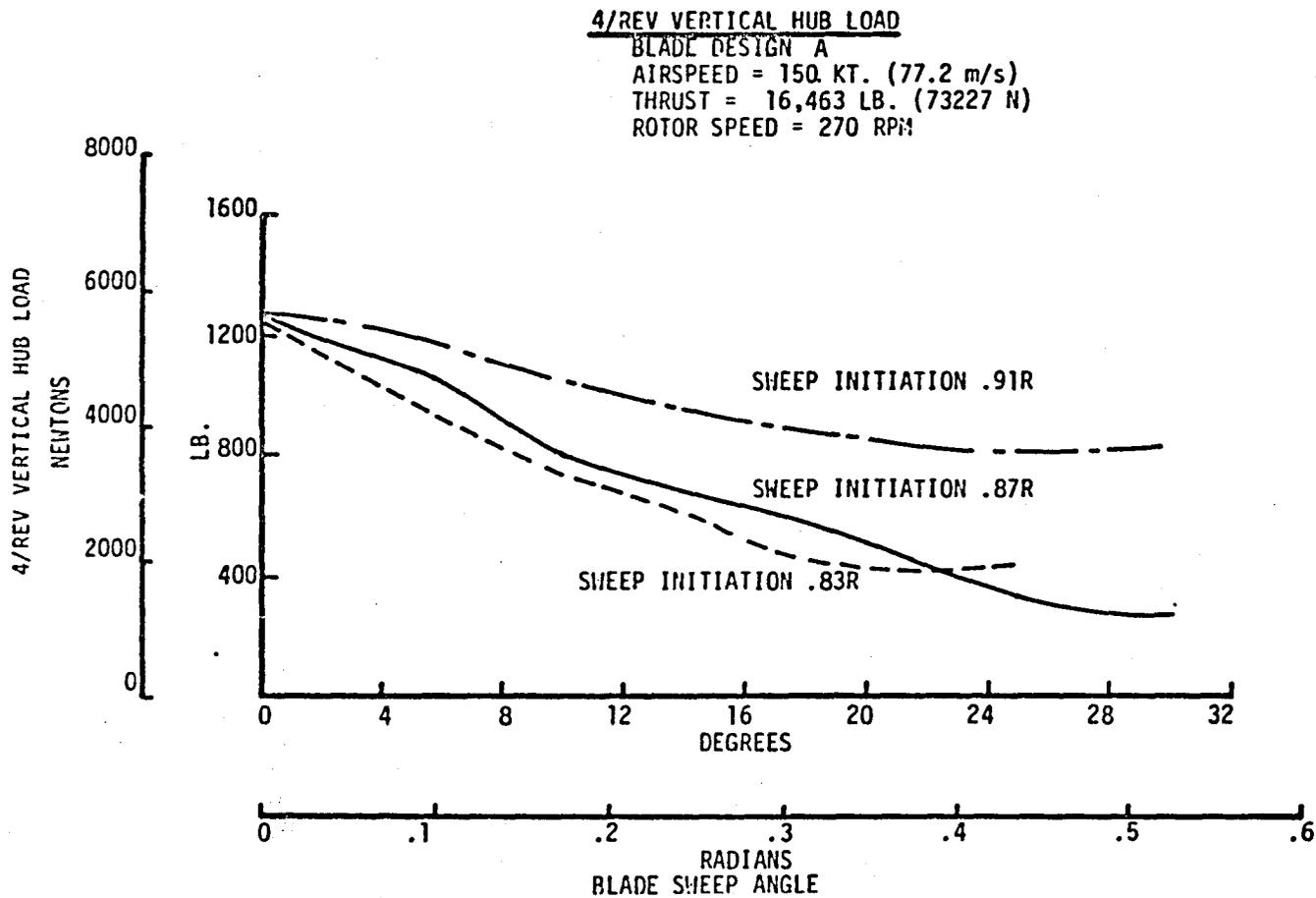
FIGURE 2.1-1   4/REV VERTICAL HUB LOAD VS. BLADE SWEEP ANGLE

FIGURE 2.2-1   VERTICAL ROOT SHEAR HARMONICS

FLAP BENDING MOMENT AT .165R HARMONICS
BLADE DESIGN A
AIRSPEED = 150 KT (77.2 m/s)
THRUST = 16463 LB. (73222 N)
ROTOR SPEED = 270 RPM

BASELINE UNSWEPT BLADE

20 DEG (.349 RAD)
SWEEP .87R

FLAP BENDING MOMENT
NEWTON METERS

INCH LB. x 10^{-3}

NEWTON METERS

INCH LB. x 10^{-3}

HARMONIC NUMBER
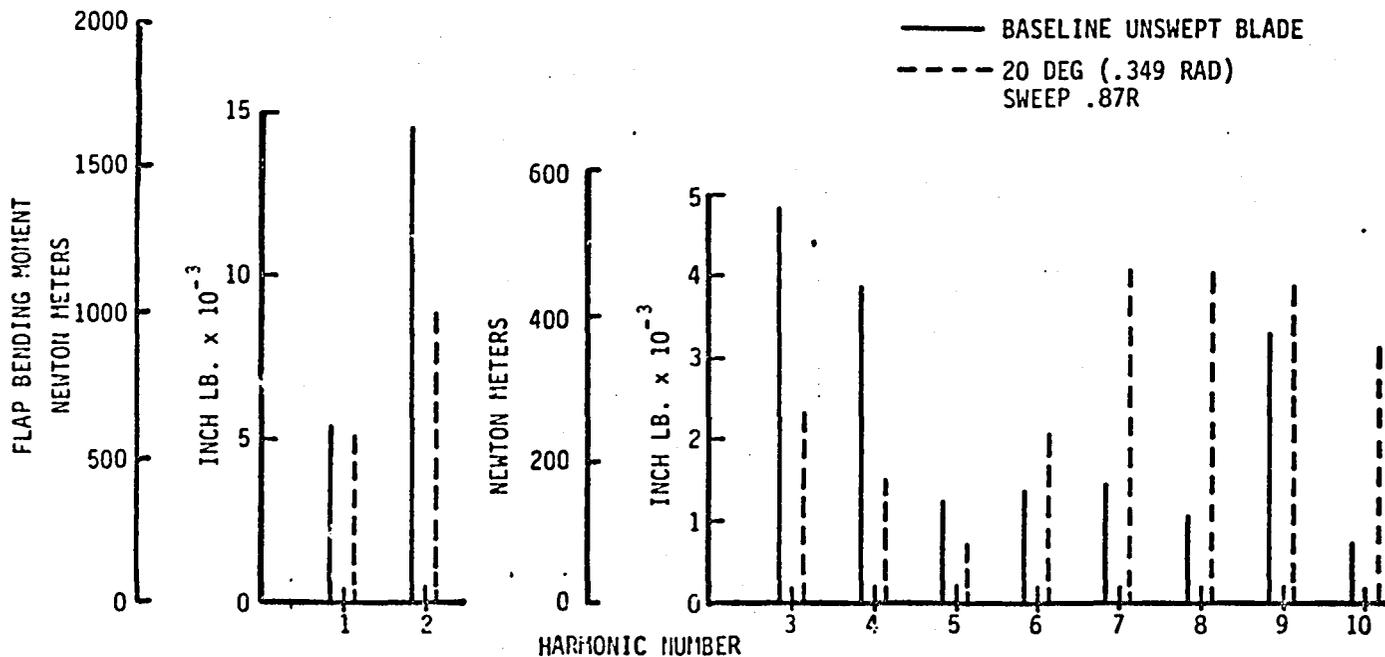
FIGURE 2.3-1   FLAP BENDING MOMENT AT .165R HARMONICS

PITCH LINK LOAD
BLADE DESIGN A
AIRSPEED = 150 KT. (77.2 m/s)
THRUST = 16,463 LB. (73227N)
ROTOR SPEED = 270 RPM

20 DEG. (.3490 RAD)
SWEEP .87R

BASELINE UNSWEPT BLADE

DEGREES

RADIANS
BLADE AZIMUTH POSITION
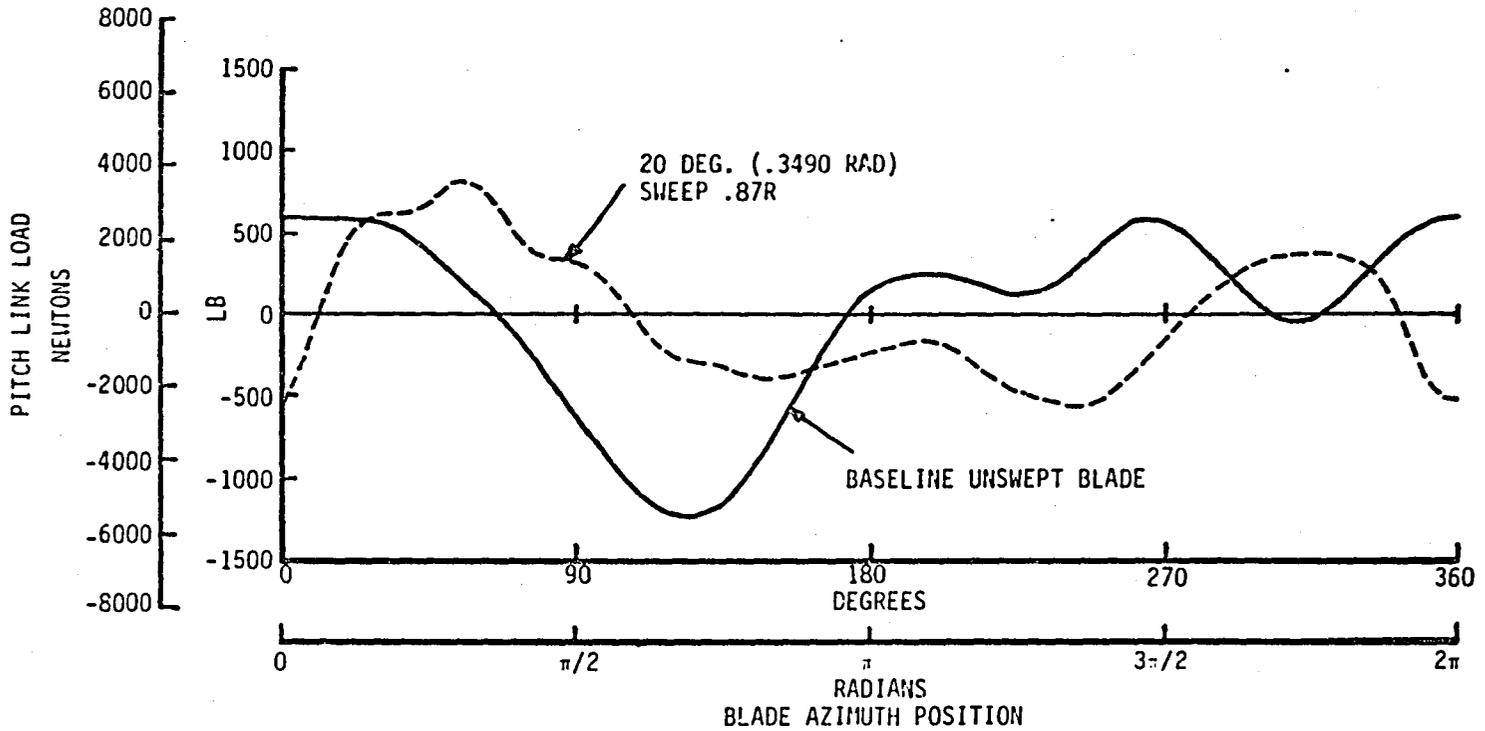
FIGURE 2.4-1   PITCH LINK LOAD VS. BLADE AZIMUTH POSITION

CHORD BENDING MOMENT AT .51R HARMONICS
BLADE DESIGN A
AIRSPEED = 150 KT. (77.2 m/s)
THRUST = 16463 LB. (73222 N)
ROTOR SPEED = 270 RPM
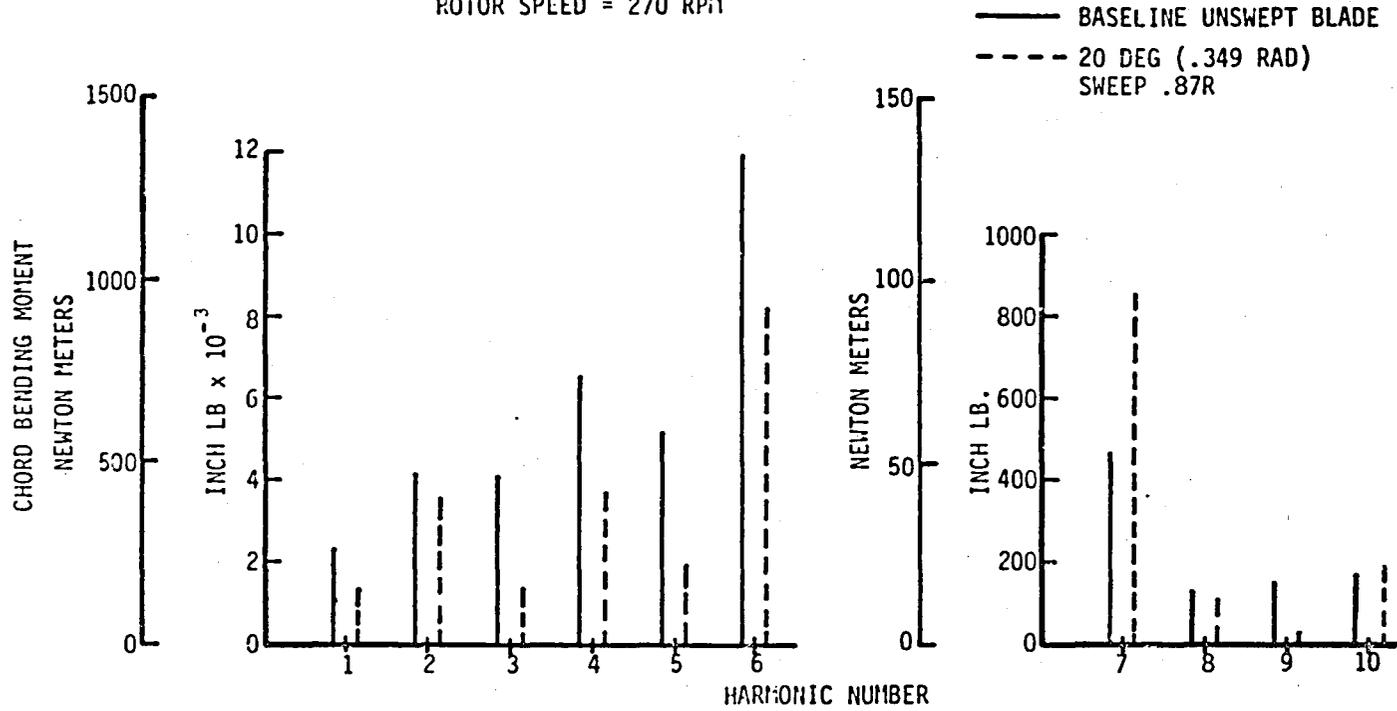
FIGURE 2.5-1 CHORD BENDING MOMENT AT .51R HARMONICS
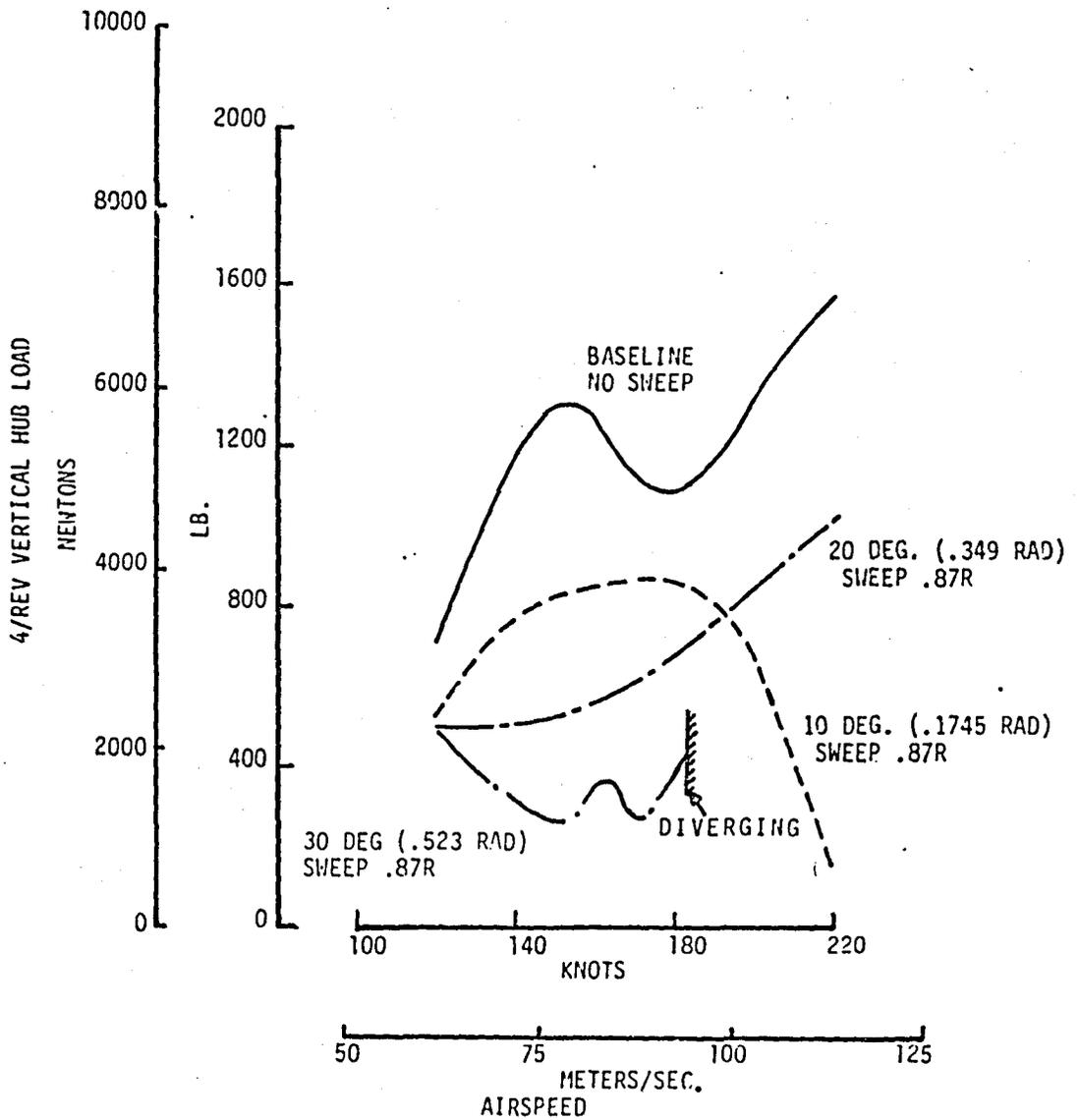
FIGURE 3.1-1   4/REV VERTICAL HUB LOAD VS. AIRSPEED
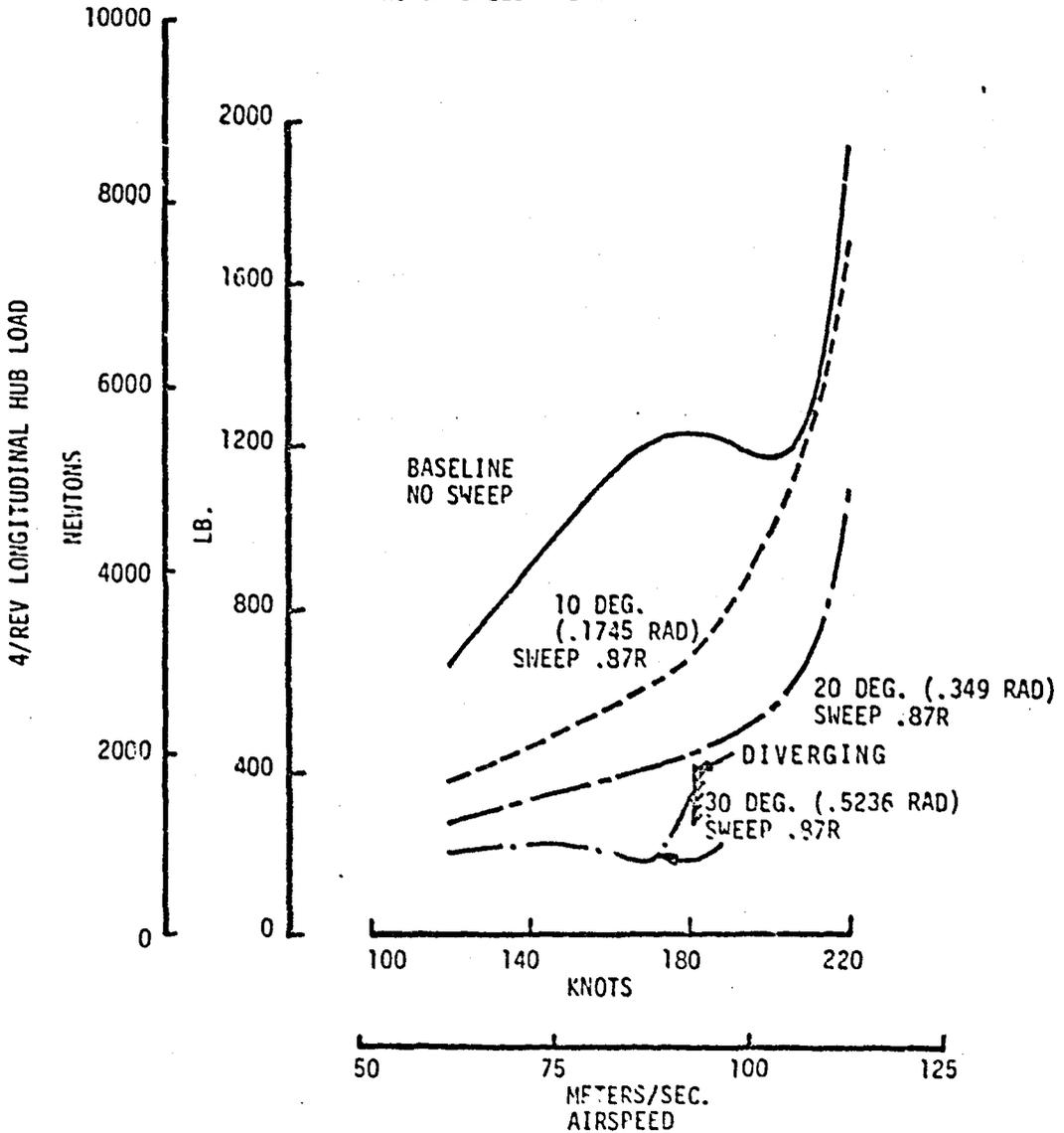
FIGURE 3.2-1   4/REV LONGITUDINAL HUB LOAD VS. AIRSPEED
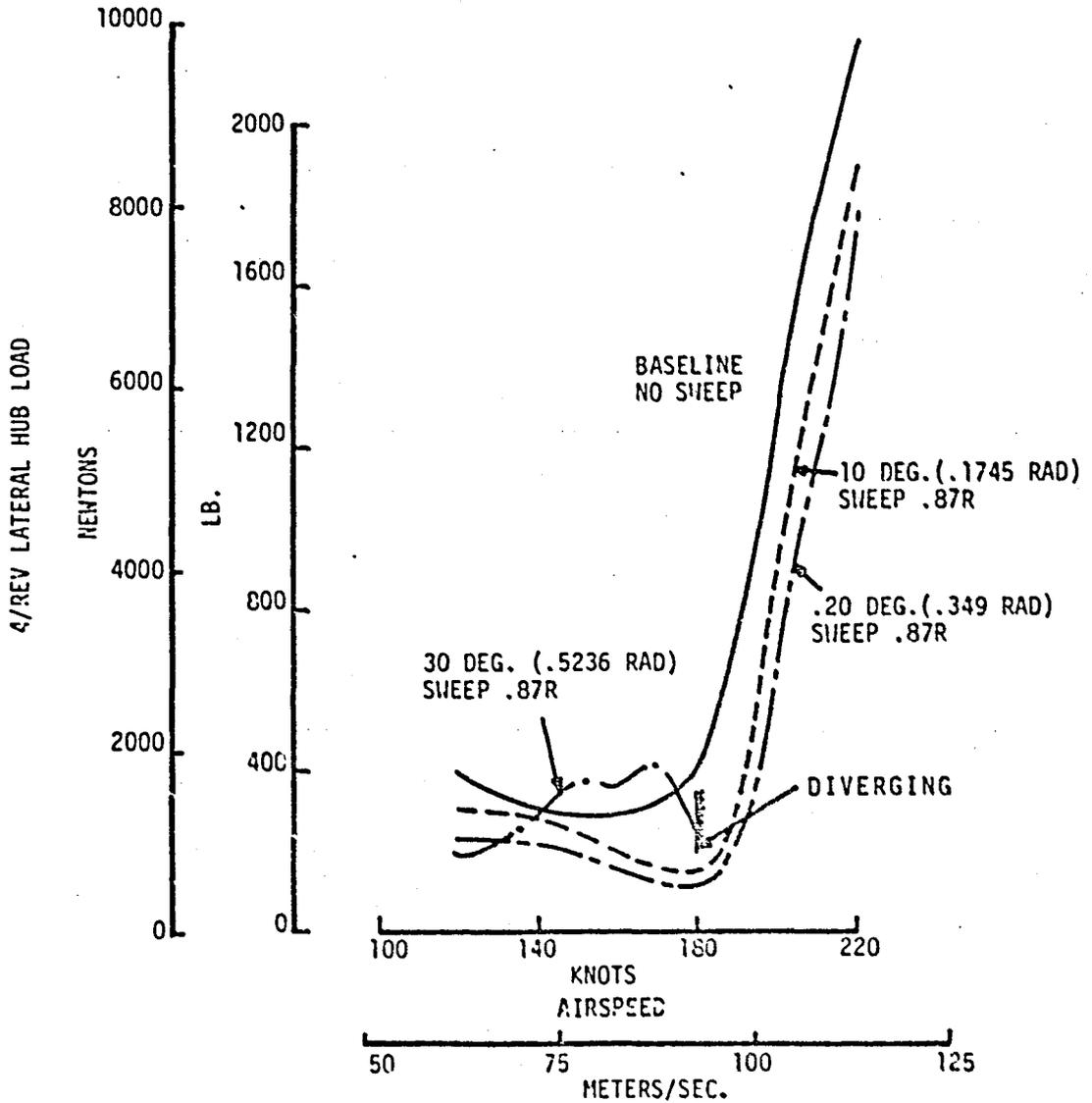
FIGURE 3.2-2   4/REV LATERAL HUB LOAD VS. AIRSPEED

81

4/REV ROLL HUB MOMENT
BLADE DESIGN A
THRUST = 16463 LB. (73227 N)
ROTOR SPEED = 270 RPM

BASELINE
NO SWEEP

30 DEG (.5236 RAD)
SWEEP .87R

10 DEG (.1745 RAD)
SWEEP .87R

DIVERGING

20 DEG (.349 RAD)
SWEEP .87R
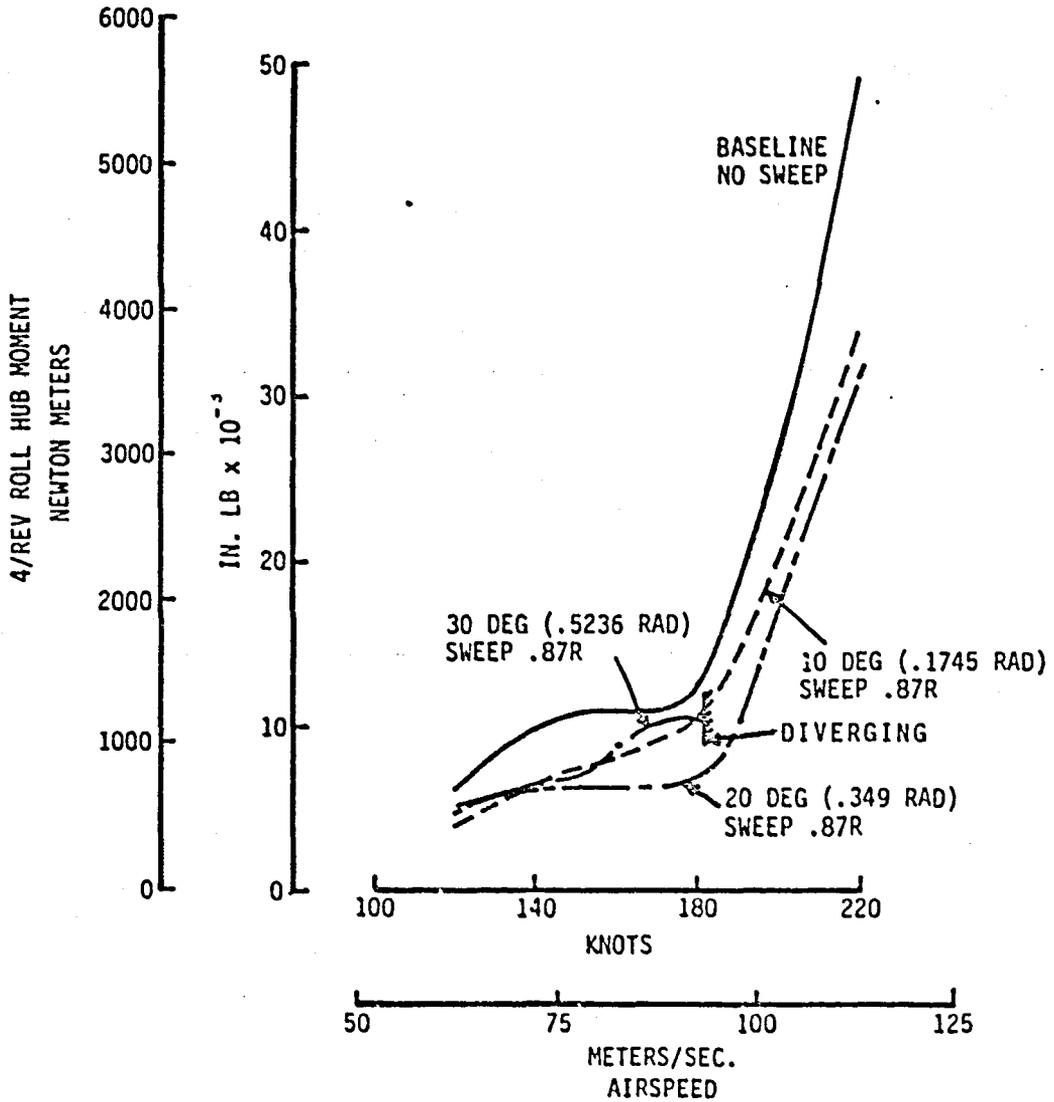
FIGURE 3.3-1   4/REV ROLL HUB MOMENT VS. AIRSPEED

82

4/REV PITCH HUB MOMENT
BLADE DESIGN A
THRUST = 16463 LB. (73227 N)
ROTOR SPEED = 270 RPM
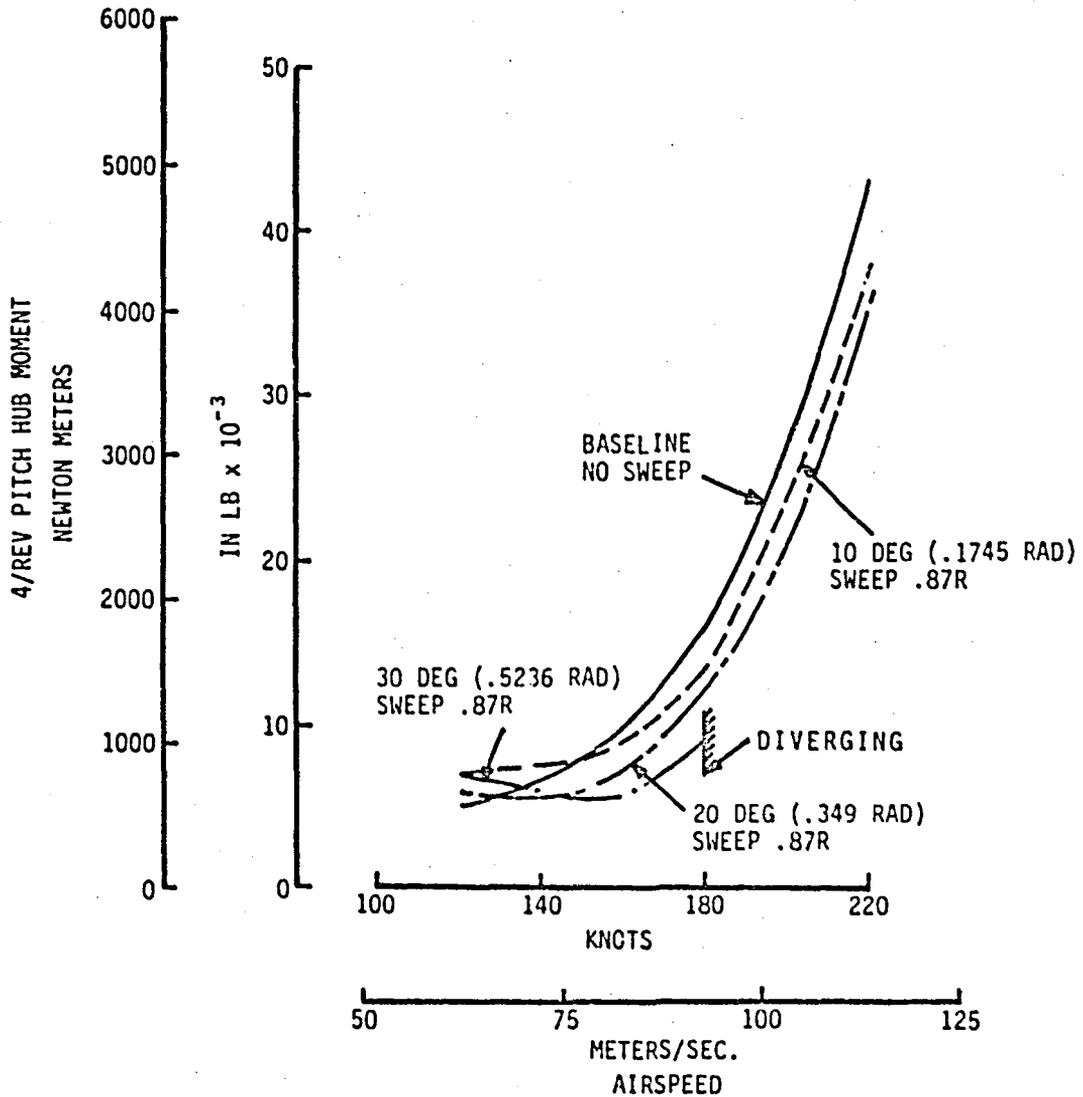
FIGURE 3.3-2   4/REV PITCH HUB MOMENT VS. AIRSPEED

83

3/REV VERTICAL ROOT SHEAR
BLADE DESIGN A
THRUST = 16463 LB. (73227 N)
ROTOR SPEED = 270 RPM
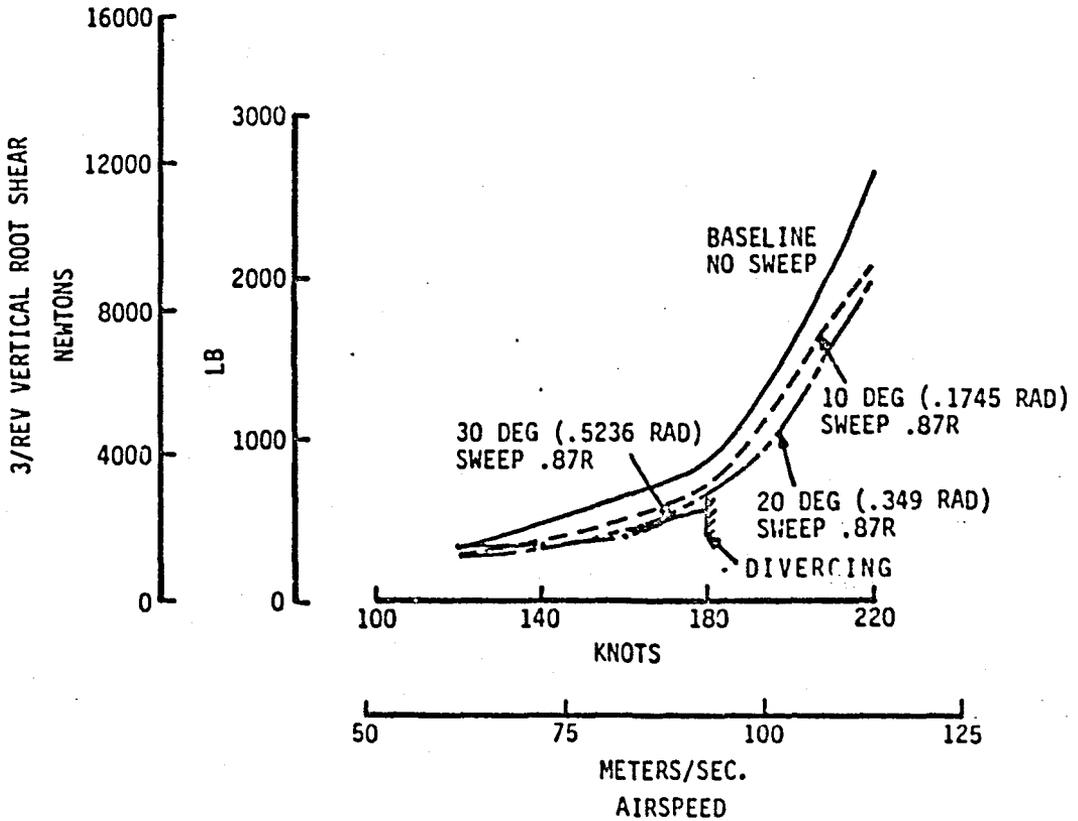
FIGURE 3.3-3   3/REV VERTICAL ROOT SHEAR VS. AIRSPEED

ROTOR HORSEPOWER
BLADE DESIGN A
THRUST = 16463 LB (73227 N)
ROTOR SPEED = 270 RPM
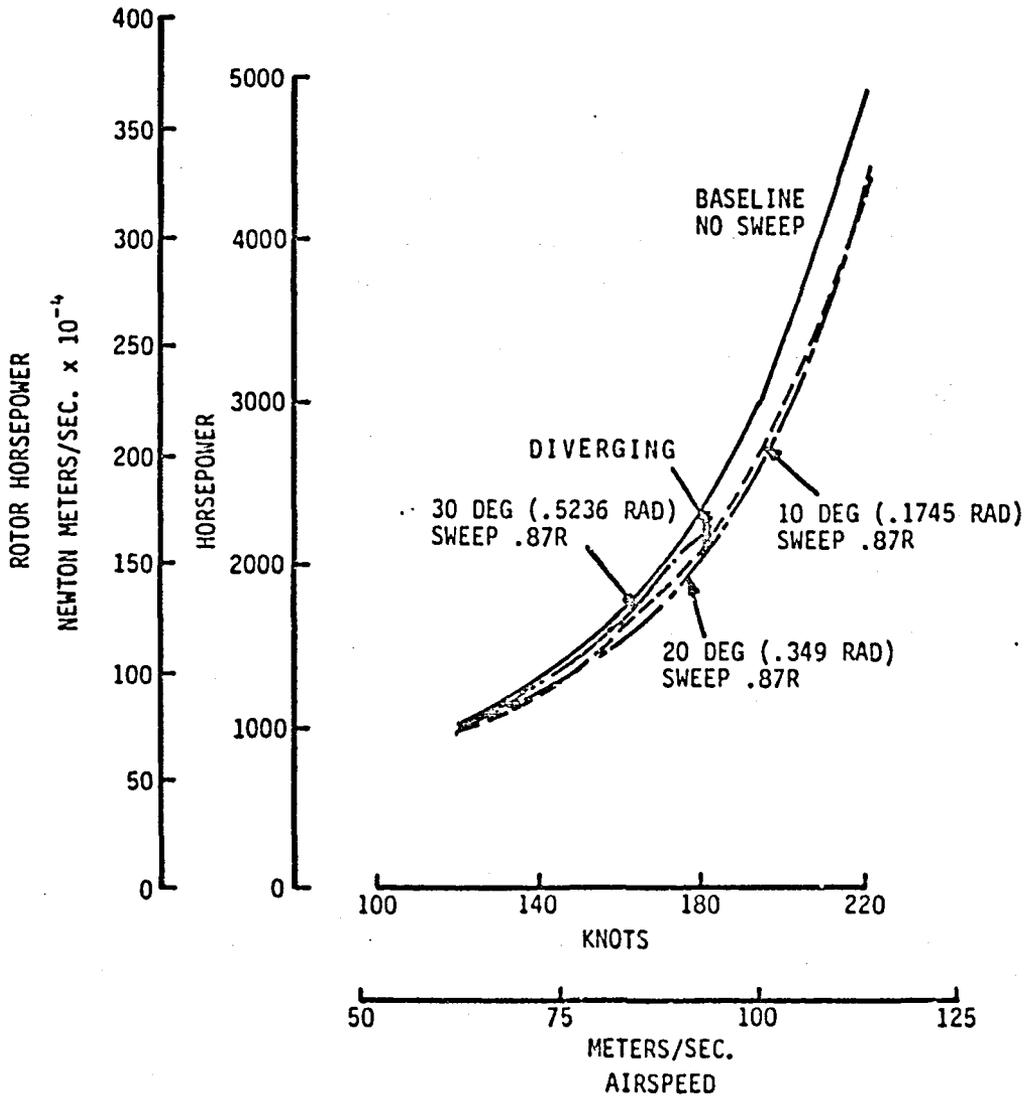
FIGURE 3.4-1   ROTOR HORSEPOWER VS. AIRSPEED

85

MAXIMUM ALTERNATING FLAP BENDING MOMENT
BLADE DESIGN A
THRUST = 16463 LB (73227 N)
ROTOR SPEED = 270 RPM
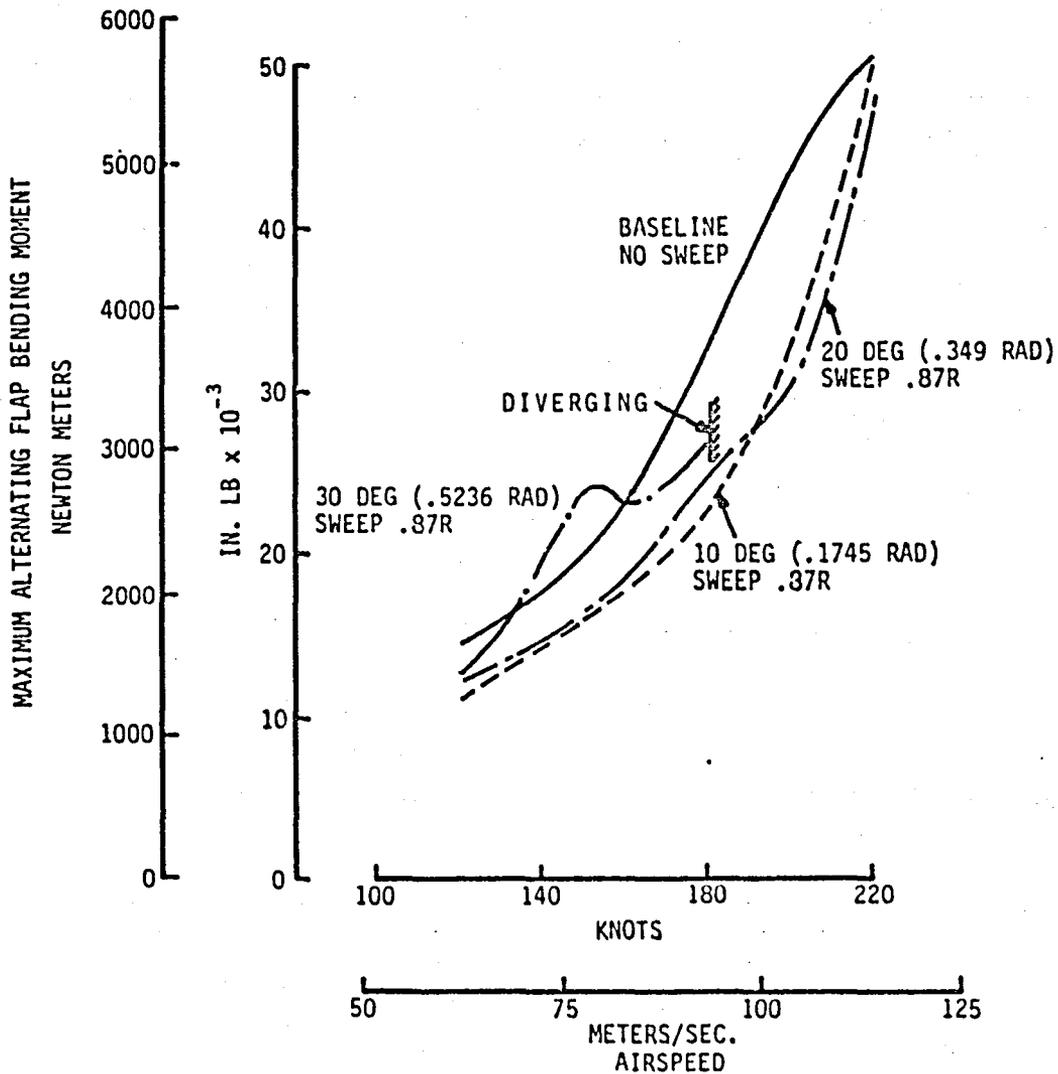
FIGURE 3.5-1   MAXIMUM ALTERNATING FLAP BENDING MOMENT VS. AIRSPEED

86

4/REV FLAP BENDING MOMENT
BLADE DESIGN A
AIRSPEED = 150 KT. (77.2 m/s)
THRUST = 16,463 LB. (73227N)
ROTOR SPEED = 270 RPM
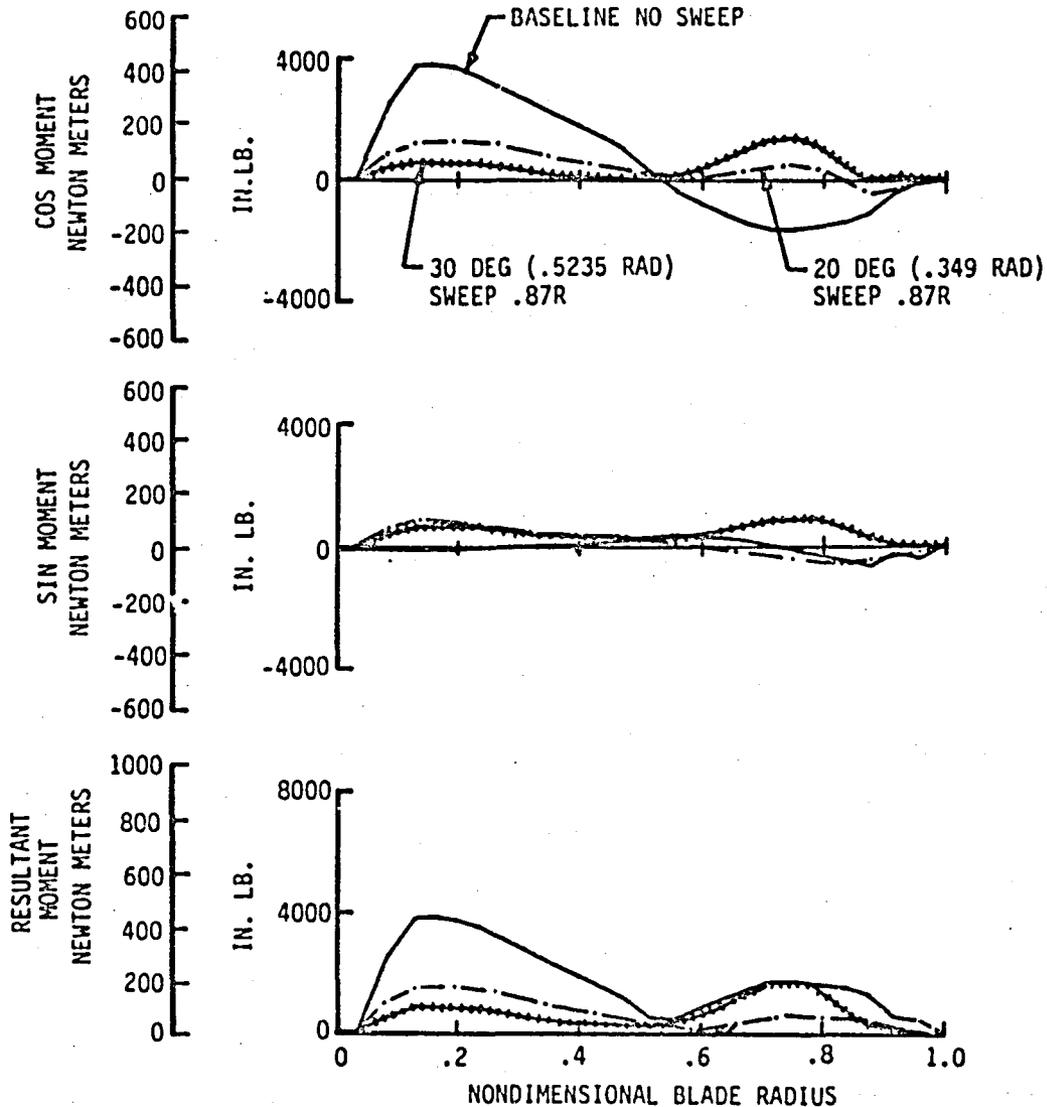
FIGURE 3.5-2   4/REV FLAP BENDING MOMENT VS. NONDIMENSIONAL
BLADE RADIUS

ALTERNATING PITCH LINK LOAD
BLADE DESIGN A
THRUST = 16463 LB. (73227 N)
ROTOR SPEED = 270 RPM
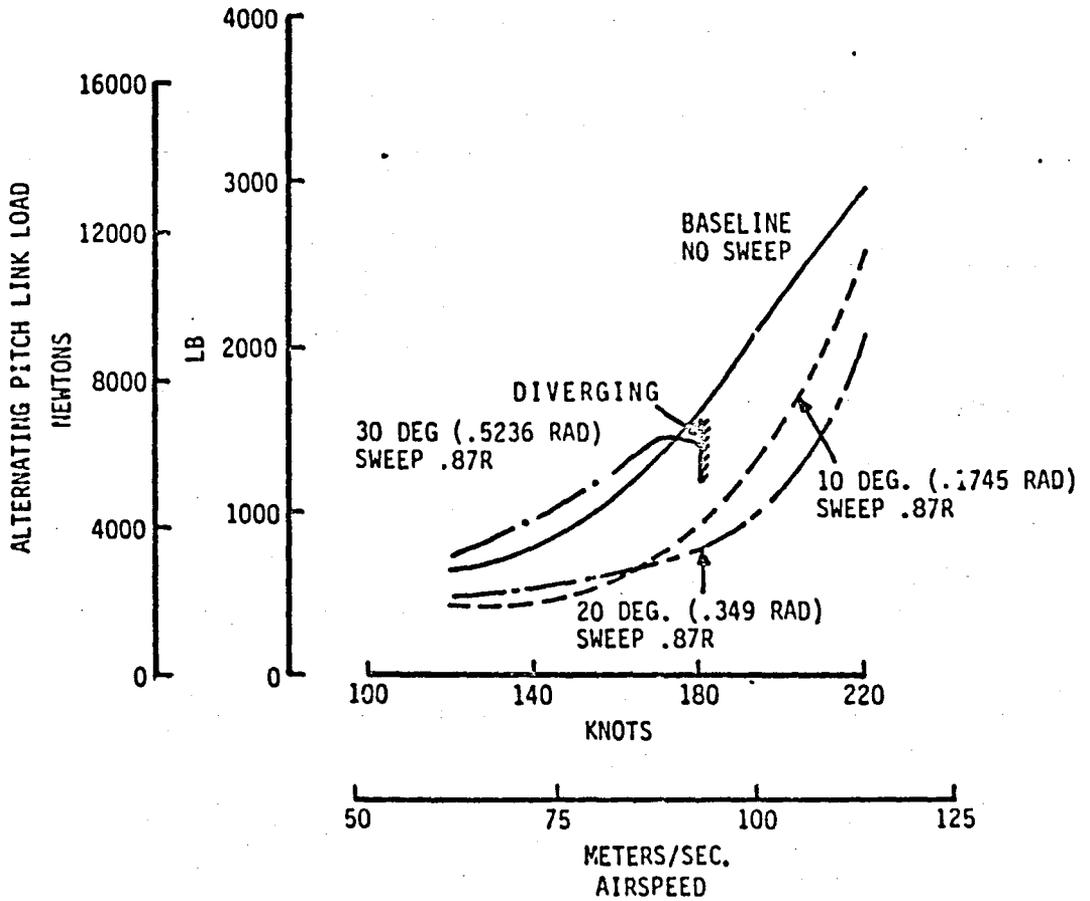
FIGURE 3.6-1   ALTERNATING PITCH LINK LOAD VS. AIRSPEED

BLADE DESIGN A NATURAL FREQUENCY SUMMARY

COUPLED FLAP/PITCH
NOMINAL ROTOR SPEED = 270 RPM
SWEEP INITIATION .87R

SWEEP ANGLE DEG. (RAD)	IN VACUUM		IN AIR WITHOUT DAMPING		IN AIR WITH DAMPING	
	MODE	FREQ PER REV	MODE	FREQ PER REV	MODE	FREQ PER REV
0	$\omega 1F$	1.05	$\omega 1F$	1.12	$\omega 1F$	.95
	$\omega 2F$	2.55	$\omega 2F$	2.65	$\omega 2F$	2.50
	$\omega 3F$	5.65	$\omega 3F$	5.65	$\omega 3F$	5.65
	ωT	4.34	ωT	4.20	ωT	3.95
10 (.1745)	$\omega 1F$	1.05	$\omega 1F$	1.08	$\omega 1F$	.95
	$\omega 2F$	2.55	$\omega 2F$	2.65	$\omega 2F$	2.55
	$\omega 3F$	5.68	$\omega 3F$	5.80	$\omega 3F$	5.75
	ωT	4.30	ωT	4.10	ωT	4.07
20 (.3490)	$\omega 1F$	1.05	$\omega 1F$	1.10	$\omega 1F$	1.0
	$\omega 2F$	2.55	$\omega 2F$	2.65	$\omega 2F$	2.74
	$\omega 3F$	5.80	$\omega 3F$	6.00	$\omega 3F$	5.85
	ωT	4.00	ωT	3.80	ωT	3.75
30 (.5235)	$\omega 1F$	1.05	$\omega 1F$	1.13	$\omega 1F$	1.0
	$\omega 2F$	2.55	$\omega 2F$	2.80	$\omega 2F$	2.55
	$\omega 3F$	5.85	$\omega 3F$	6.20	$\omega 3F$	5.90
	ωT	3.75	ωT	3.18	ωT	3.45
40 (.698)	$\omega 1F$	1.03	$\omega 1F$	1.19	$\omega 1F$	1.05
	$\omega 2F$	2.52	$\omega 2F$	-	$\omega 2F$	2.65
	$\omega 3F$	5.99	$\omega 3F$	6.22	$\omega 3F$	5.95
	ωT	3.49	ωT	-	ωT	3.35

FIGURE 4.-1   BLADE FREQUENCY SUMMARY, COUPLED FLAP/PITCH, NOMINAL ROTOR SPEED

FIGURE 4.-2 BLADE FREQUENCY SPECTRA, IN VACUUM

FIGURE 4.-3 BLADE FREQUENCY SPECTRA, IN AIR WITHOUT DAMPING

91
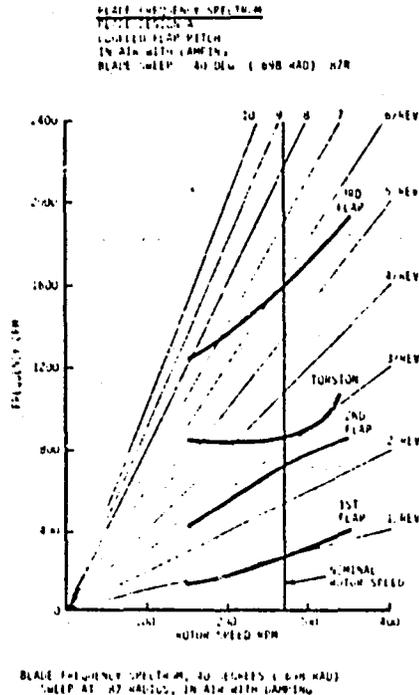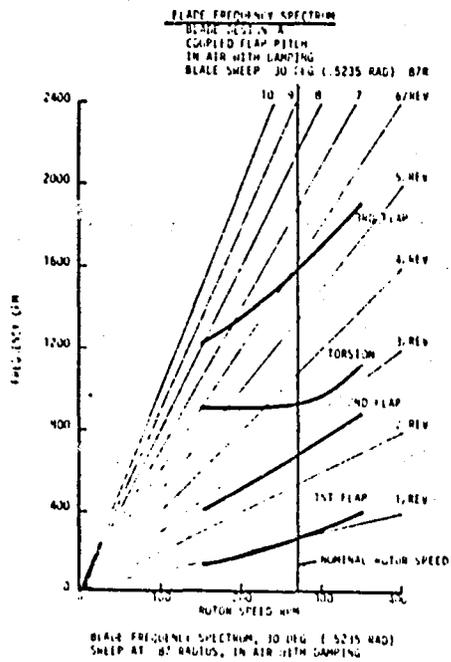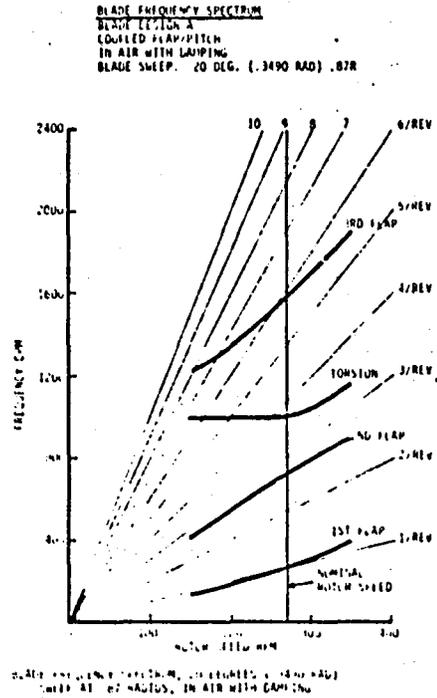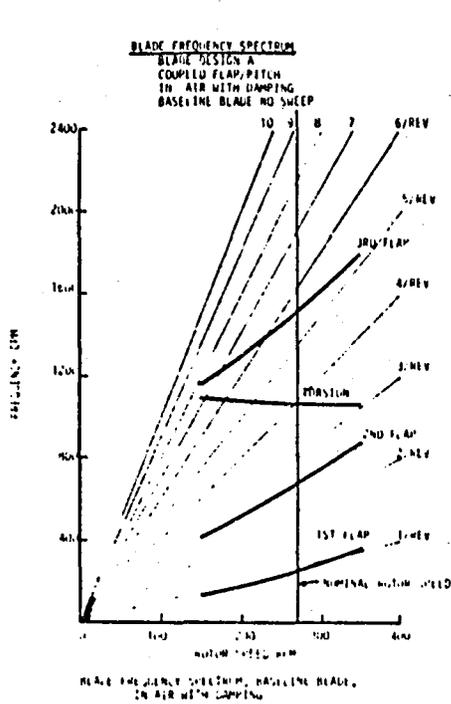
FIGURE 4.-4 BLADE FREQUENCY SPECTRA, IN AIR WITH DAMPING

BLADE NATURAL FREQUENCIES
BLADE DESIGN A
THRUST = 16463 LB (73227 N)
ROTOR SPEED = 270 RPM
COUPLED FLAP/PITCH
IN VACUUM
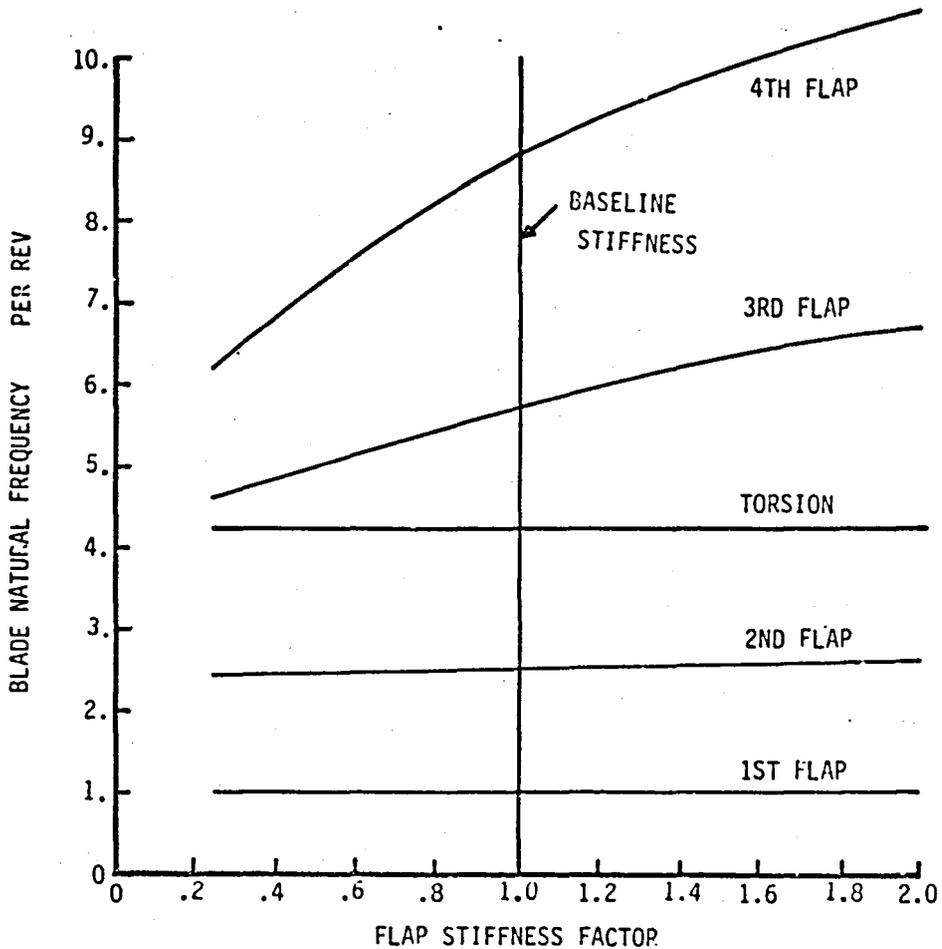
FIGURE 5.1.1 -1 BLADE FREQUENCY VS. FLAP STIFFNESS FACTOR
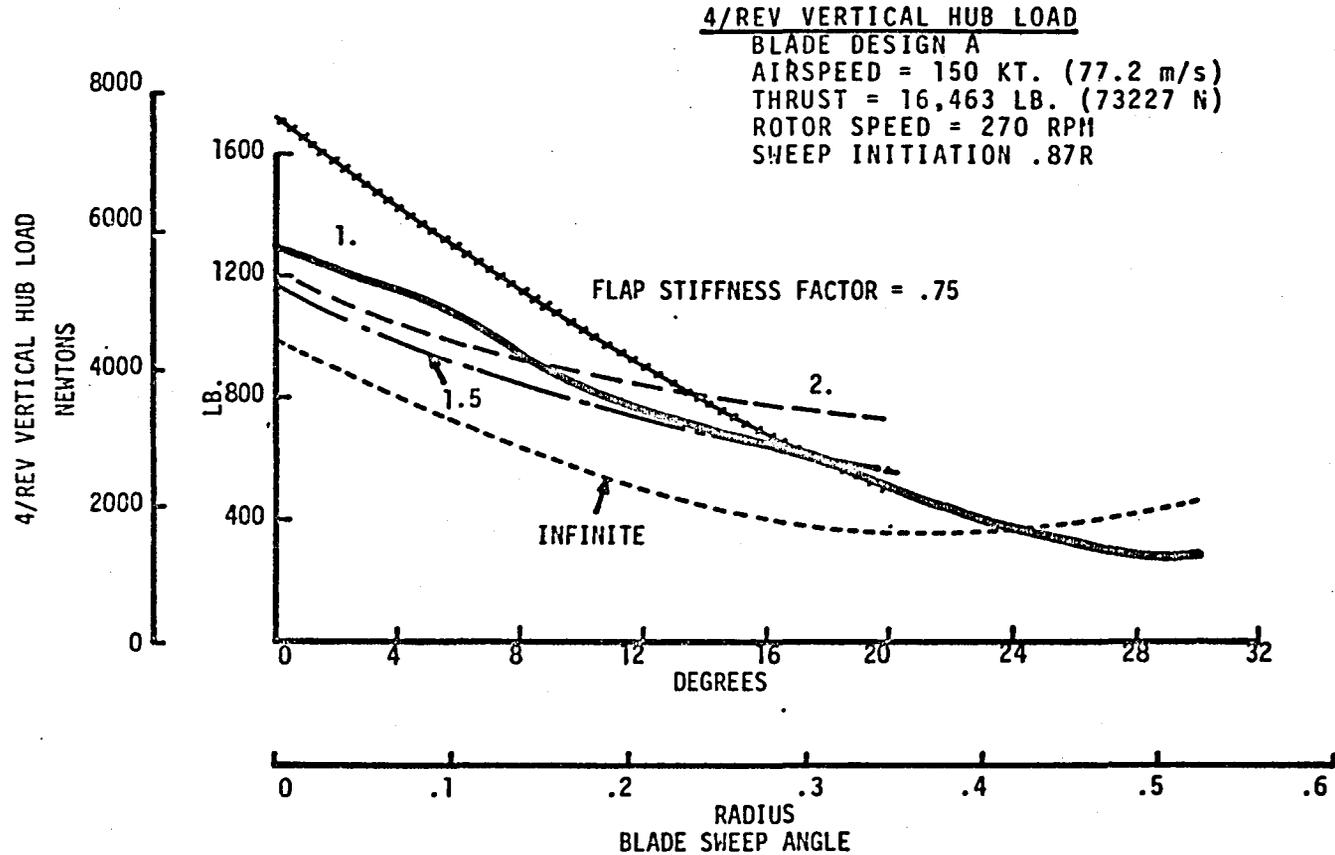
FIGURE 5.1.2-1   4/REV VERTICAL HUB LOAD VS. BLADE SWEEP ANGLE
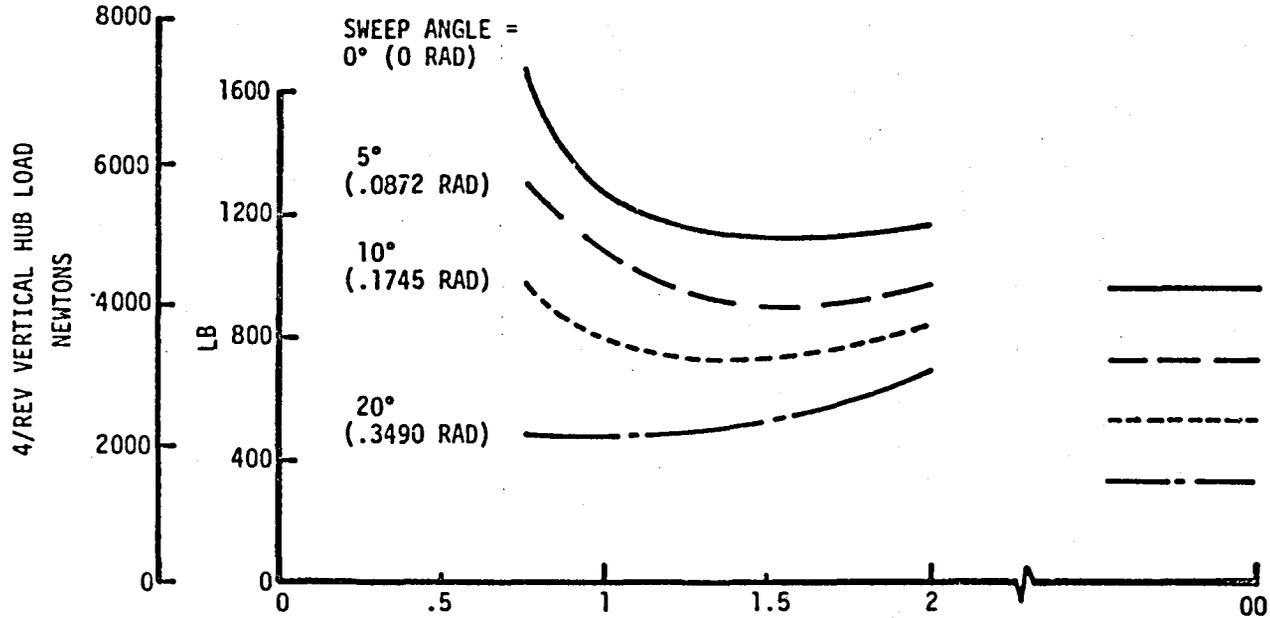
FIGURE 5.1.2-1A 4/REV VERTICAL HUB LOAD VS. FLAP STIFFNESS FACTOR

BLADE NATURAL FREQUENCIES
BLADE DESIGN A
THRUST = 16463 LB (73227 N)
ROTOR SPEED = 270 RPM
COUPLED FLAP/PITCH
IN VACUUM
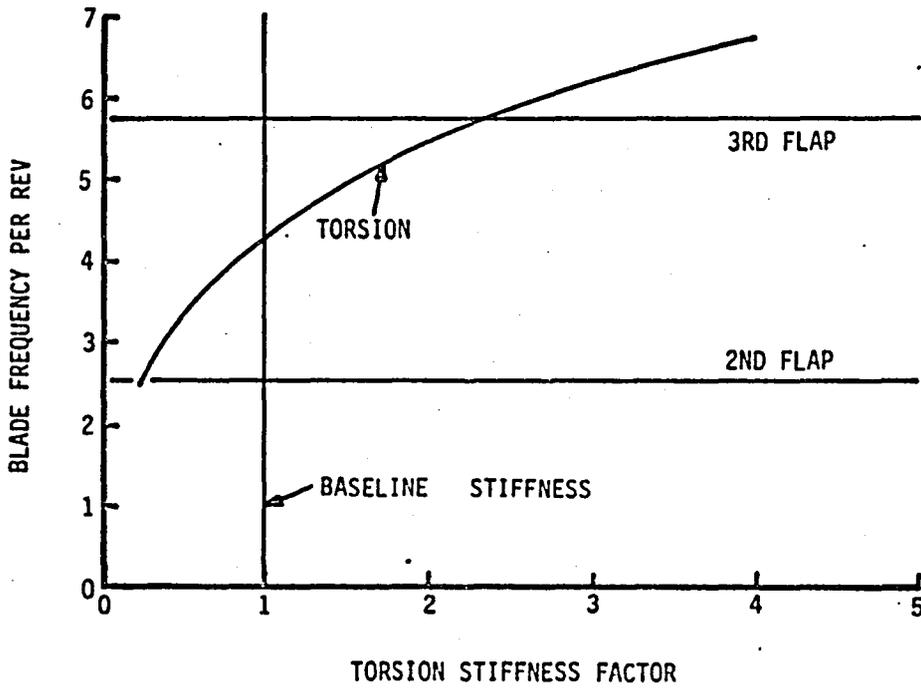
FIGURE 5.2.1-1   BLADE FREQUENCY VS. TORSION STIFFNESS FACTOR
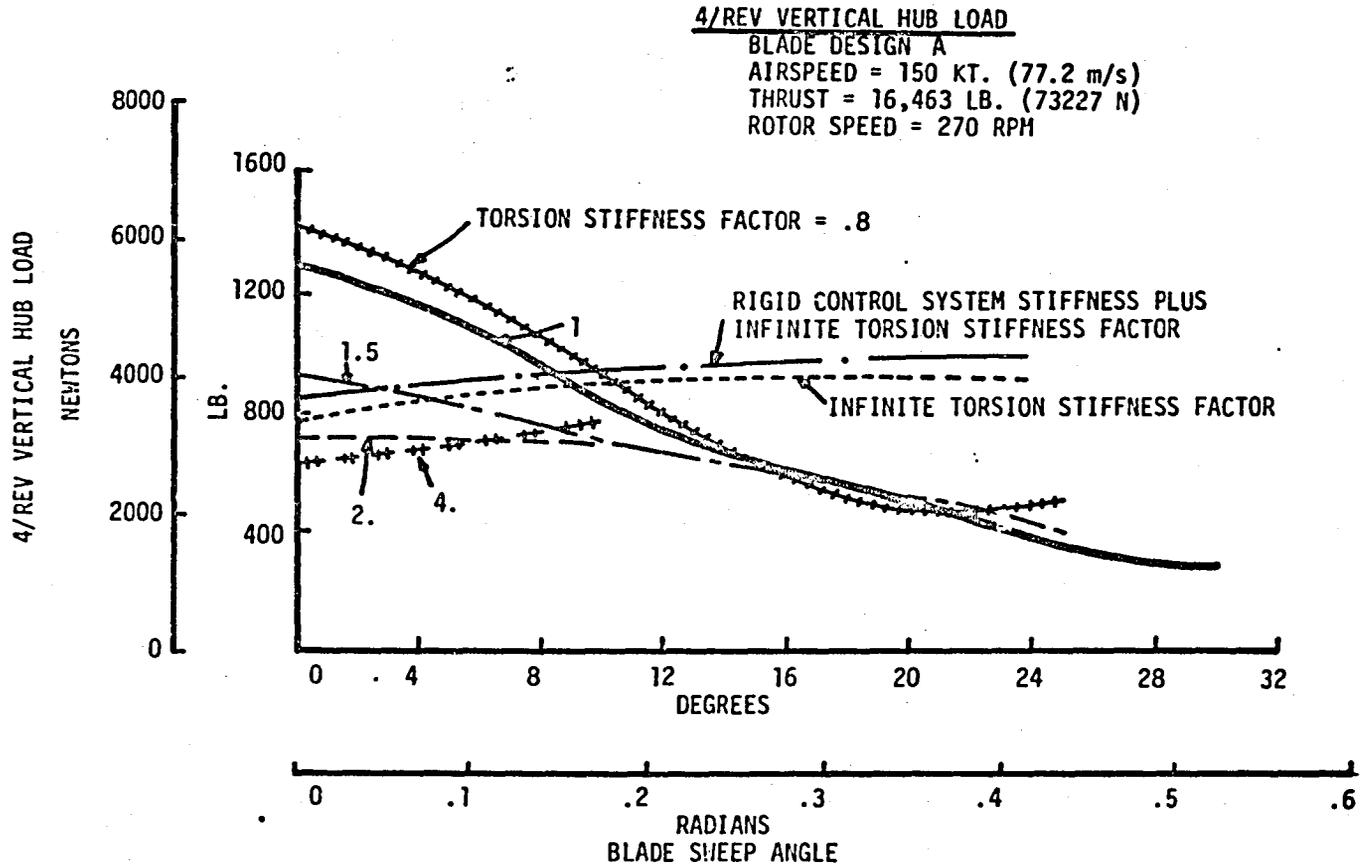
FIGURE 5.2.2-1   4/REV VERTICAL HUB LOAD VS. BLADE SWEEP ANGLE

97

4/REV VERTICAL HUB LOAD
BLADE DESIGN A
AIRSPEED = 150 KT. (77.2 m/s)
THRUST = 16,463 LB (73227 N)
ROTOR SPEED = 270 RPM

SWEEP ANGLE = 0° (0. RAD)

10°
(.1745 RAD)

20°
(.3490 RAD)

25° (.4362 RAD)

TORSIONAL STIFFNESS FACTOR

CONTROL
STIFFNESS
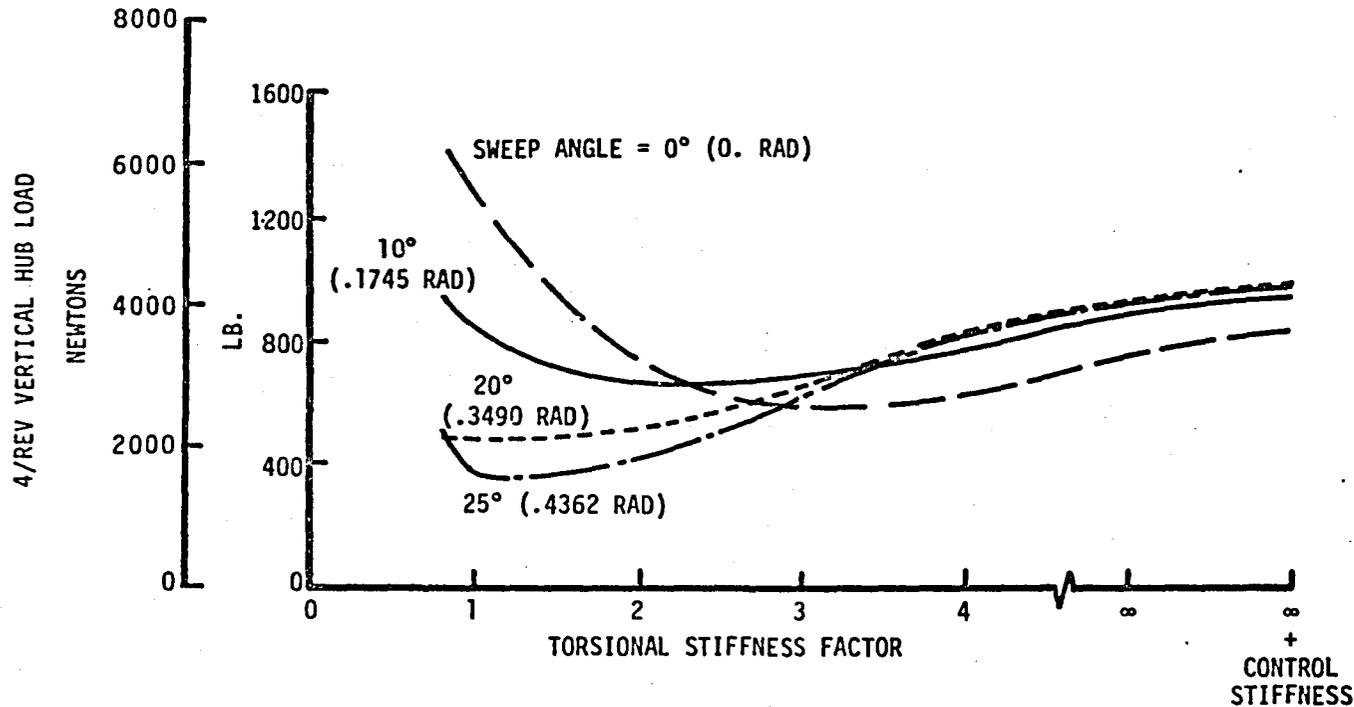
FIGURE 5.2.2-1A   4/REV VERTICAL HUB LOAD VS. TORSIONAL STIFFNESS FACTOR
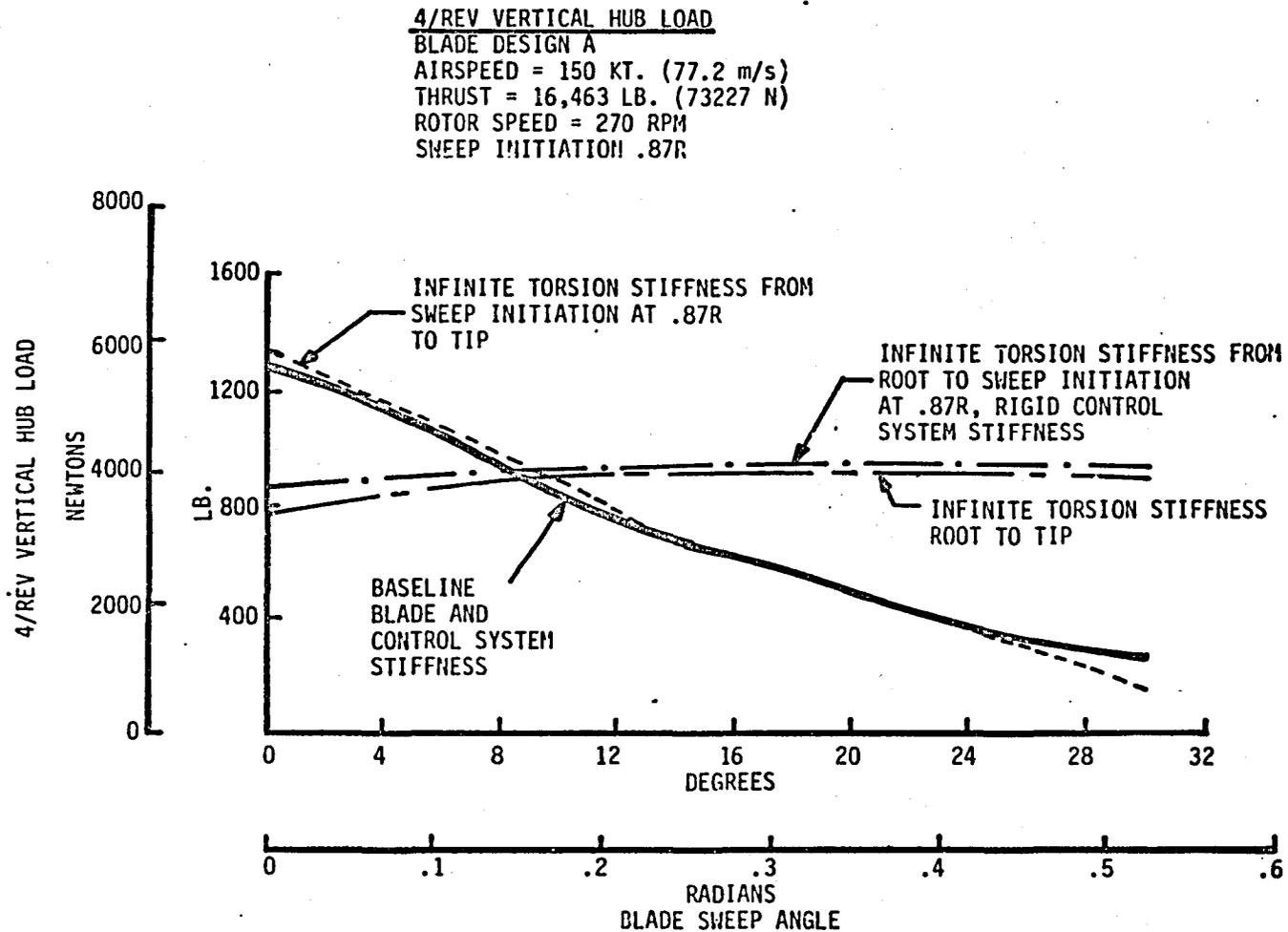
FIGURE 5.2.2-2 4/REV VERTICAL HUB LOAD VS. BLADE SWEEP ANGLE

VERTICAL ROOT SHEAR
BLADE DESIGN A
10 LB (44.5N) FORCE AT BLADE TIP
IN VACUUM
BASELINE BLADE NO SWEEP
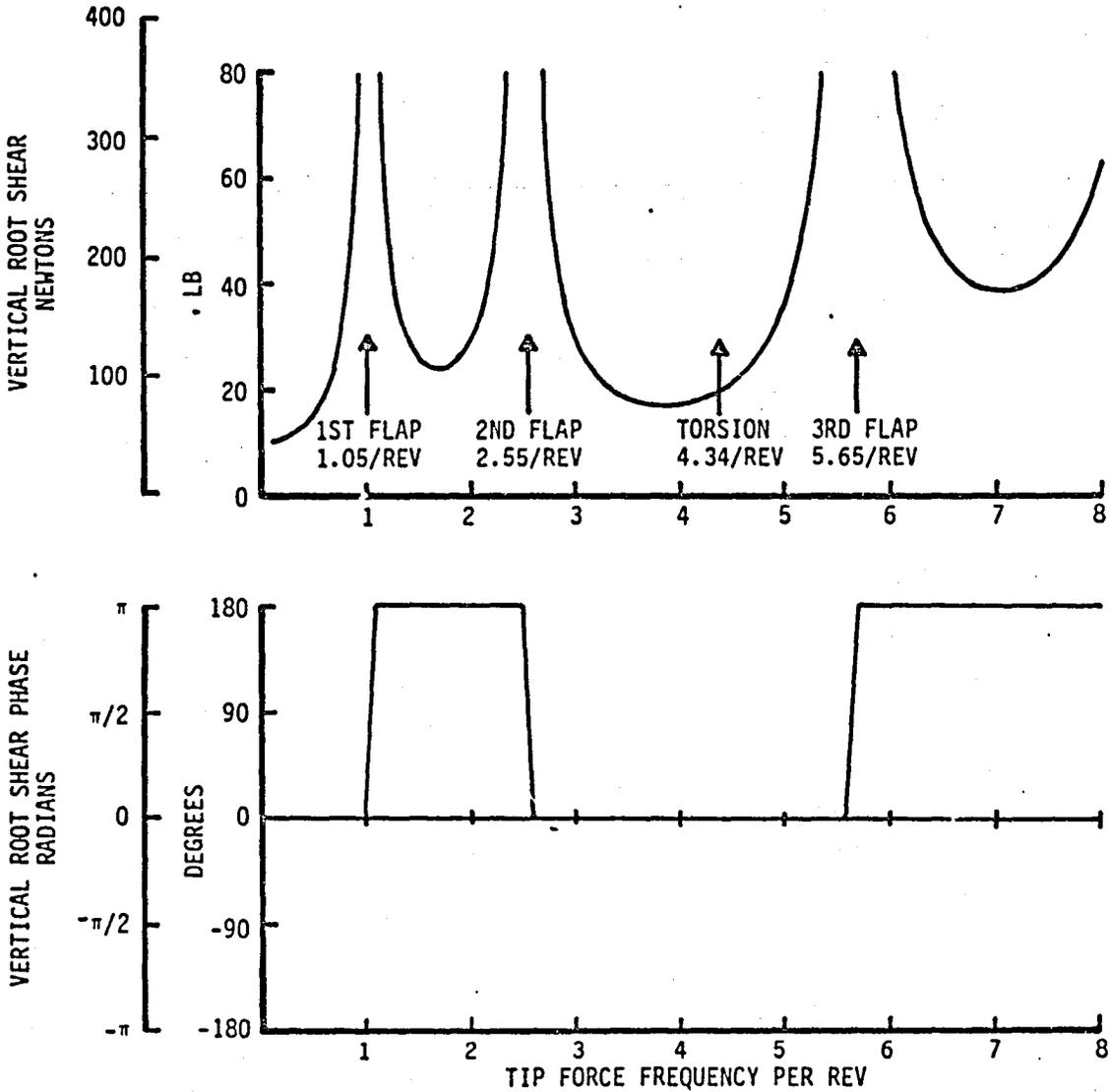
FIGURE 6.1-1   VERTICAL ROOT SHEAR AMPLITUDE AND PHASE VS.
TIP FORCE FREQUENCY, BASELINE BLADE, IN VACUUM

VERTICAL ROOT SHEAR
BLADE DESIGN A
10 LB. (44.5N) FORCE AT BLADE TIP
IN AIR WITHOUT DAMPING
BASELINE BLADE NO SWEEP
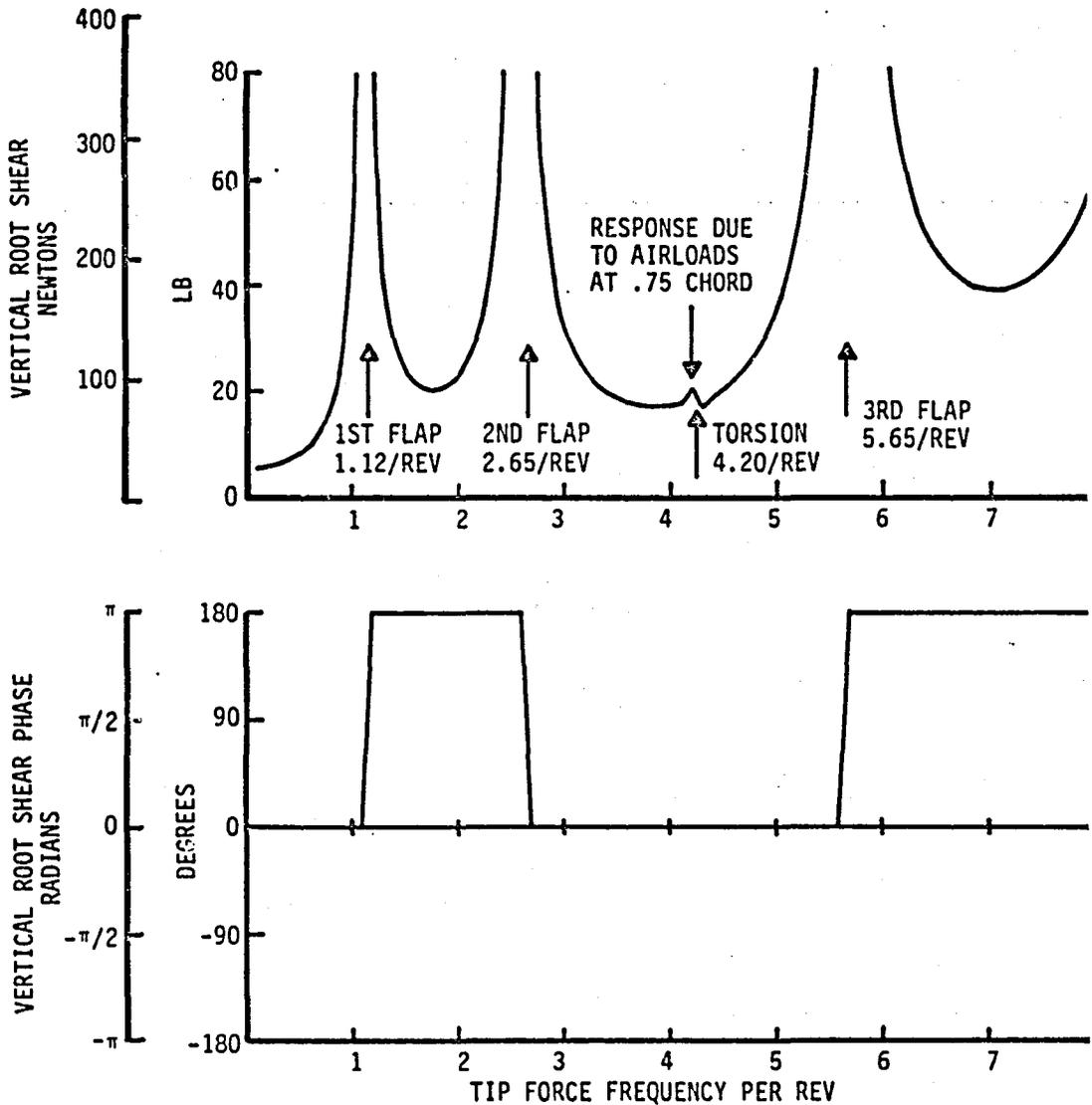
FIGURE 6.1-2   VERTICAL ROOT SHEAR AMPLITUDE AND PHASE VS.
TIP FORCE FREQUENCY, BASELINE BLADE, IN AIR WITHOUT DAMPING

101

VERTICAL ROOT SHEAR
BLADE DESIGN A
10 LB. (44.5N) FORCE AT BLADE TIP
IN AIR WITH DAMPING
BASELINE BLADE NO SWEEP

DAMPING ELIMINATES
RESPONSE DUE TO
AIRLOADS AT
.75 CHORD

1ST FLAP
.95/1 REV

2ND FLAP
2.50/REV

TORSION
3.95/REV

3RD FLAP
5.65/REV
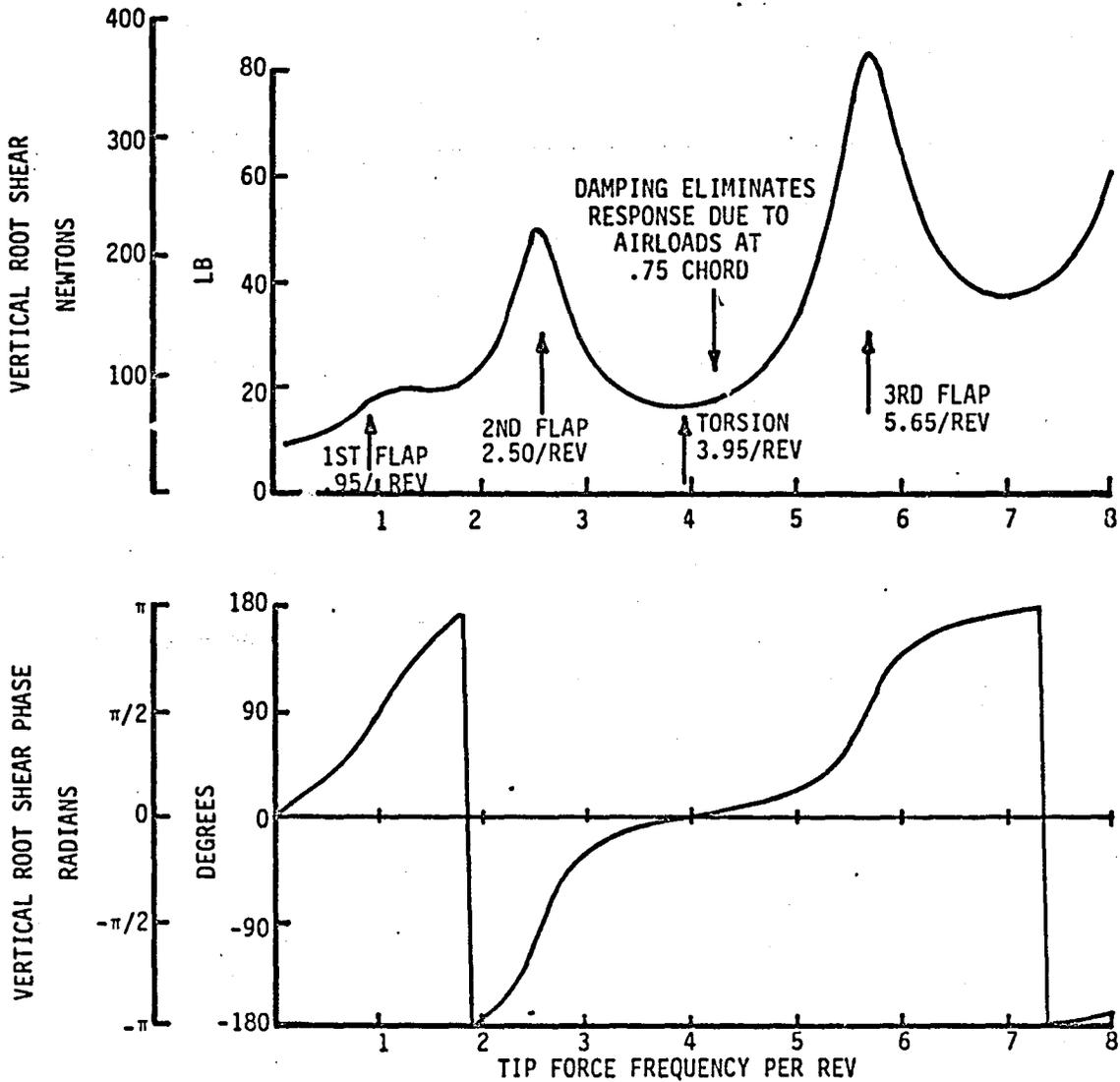
FIGURE 6.1-3   VERTICAL ROOT SHEAR AMPLITUDE AND PHASE VS.
TIP FORCE FREQUENCY, BASELINE BLADE, IN AIR WITH DAMPING

VERTICAL ROOT SHEAR
BLADE DESIGN A
10 LB. (44.5) FORCE AT BLADE TIP
IN VACUUM
BLADE SWEEP: 20 DEG (.349 RAD) .87R
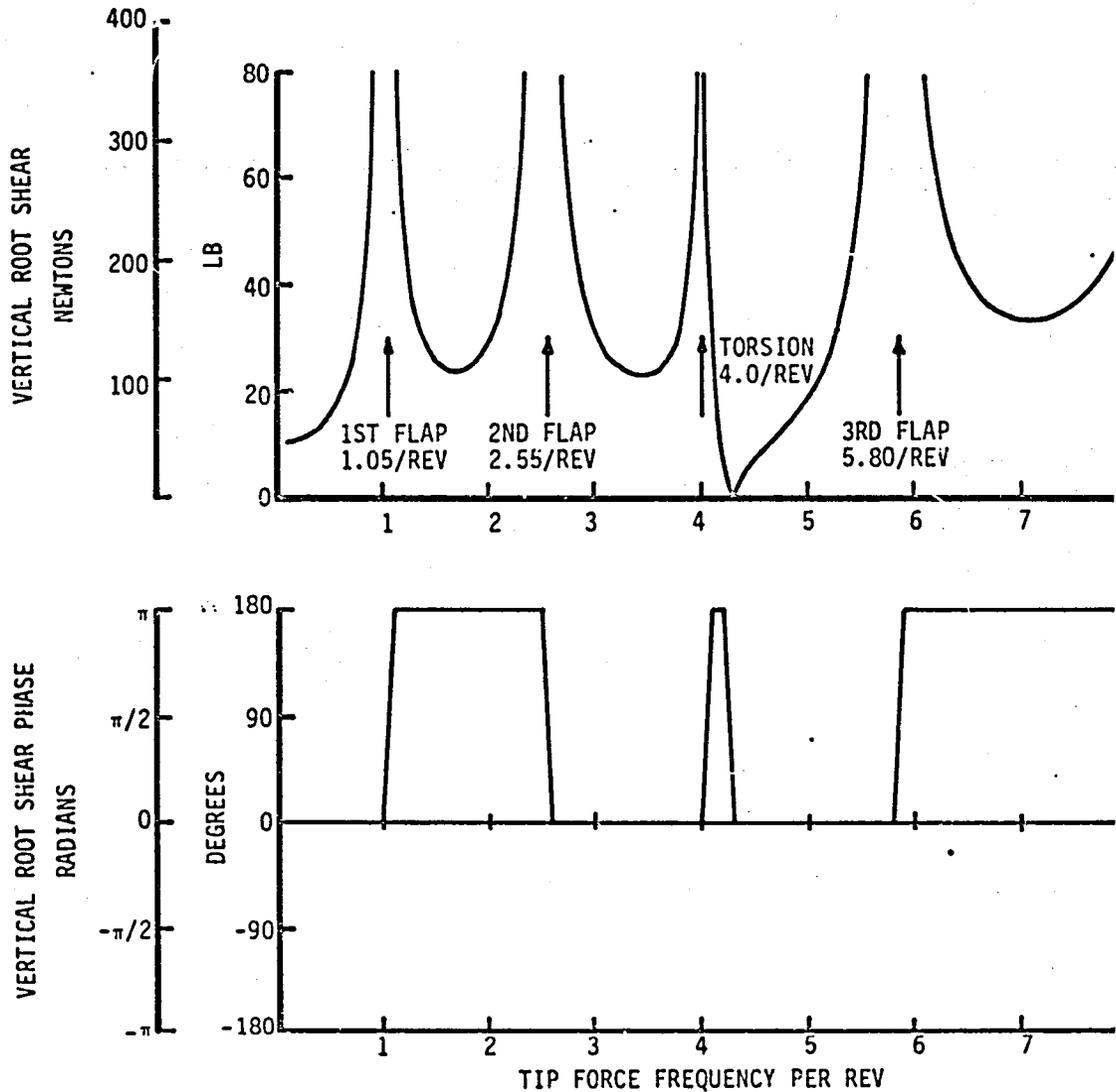
FIGURE 6.1-4   VERTICAL ROOT SHEAR AMPLITUDE AND PHASE VS.
TIP FORCE FREQUENCY, 20 DEGREES (.349 RAD) SWEEP, IN VACUUM

103

VERTICAL ROOT SHEAR
BLADE DESIGN A
10 LB (44.5N) FORCE AT BLADE TIP
IN AIR WITHOUT DAMPING
BLADE SWEEP: 20 DEG (.349 RAD) .87R
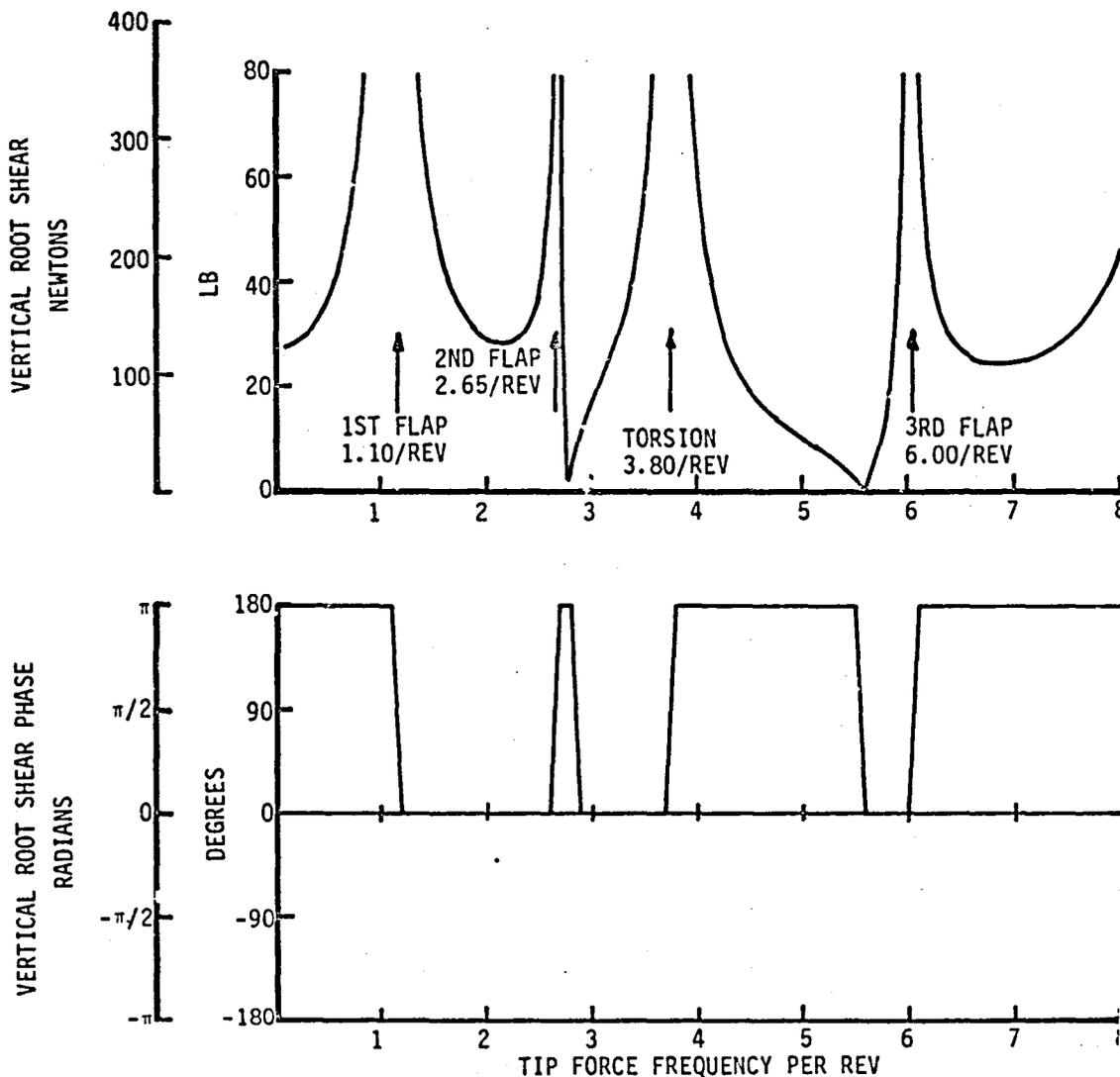
FIGURE 6.1-5   VERTICAL ROOT SHEAR AMPLITUDE AND PHASE VS.
TIP FORCE FREQUENCY, 20 DEGREES (.349 RAD) SWEEP, IN AIR WITHOUT DAMPING

104

VERTICAL ROOT SHEAR
BLADE DESIGN A
10 LB. (44.5N) FORCE AT BLADE TIP
IN AIR WITH DAMPING
BLADE SWEEP: 20 DEG (.349 RAD) 87R

2ND FLAP
2.70/REV

TORSION
3.75/REV

1ST FLAP
1.0/REV

3RD FLAP
5.85/REV
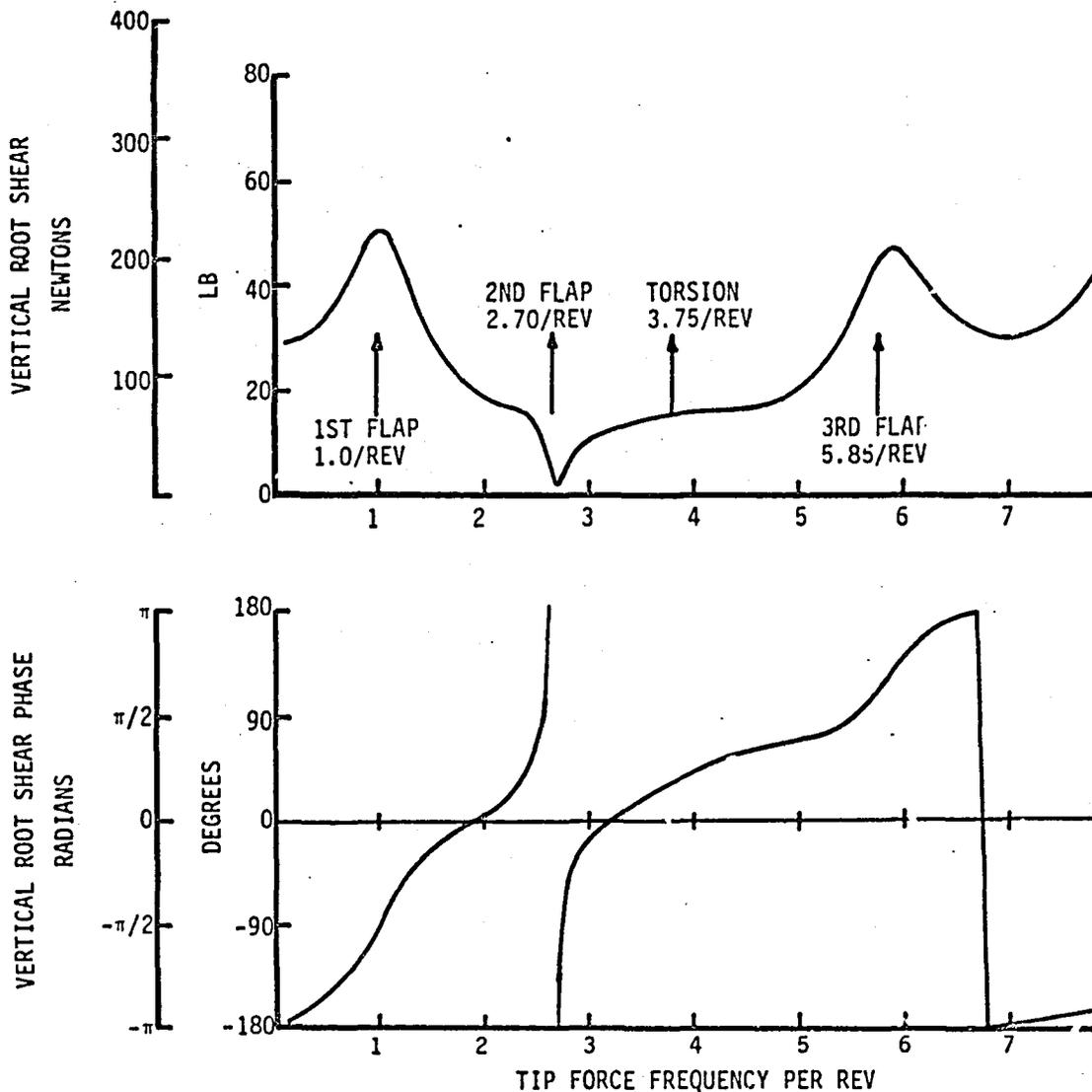
FIGURE 6.1-6 VERTICAL ROOT SHEAR AMPLITUDE AND PHASE VS.
TIP FORCE FREQUENCY, 20 DEGREES (.349 RAD) SWEEP, IN AIR WITH DAMPING

VERTICAL ROOT SHEAR
BLADE DESIGN A
10 LB. (44.5N) FORCE AT BLADE TIP
IN AIR WITH DAMPING
SWEEP INITIATION .87R
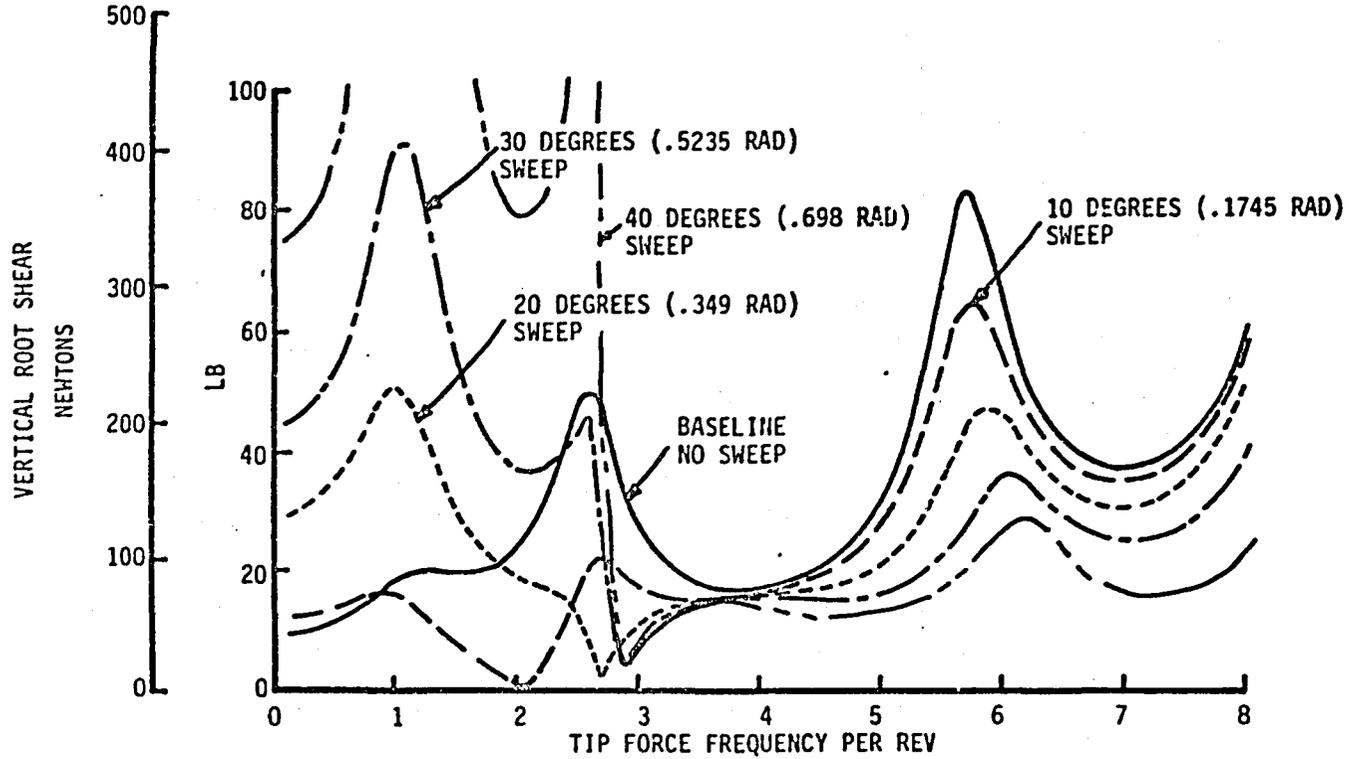
FIGURE 6.1-7   VERTICAL ROOT SHEAR VS. TIP FORCE FREQUENCY, IN AIR WITH DAMPING

FIGURE 6.2-1 4/REV INERTIAL AND THRUST FORCES VS.
NONDIMENSIONAL BLADE RADIUS, BASELINE BLADE NO SWEEP

107

4/REV INERTIAL AND THRUST FORCES
BLADE DESIGN A
AIRSPEED = 150 KT (77.16 m/s)
THRUST = 16463 LB (73227 N)
ROTOR SPEED = 270 RPM
BLADE SWEEP: 20 DEG (.3490 RAD) .87R
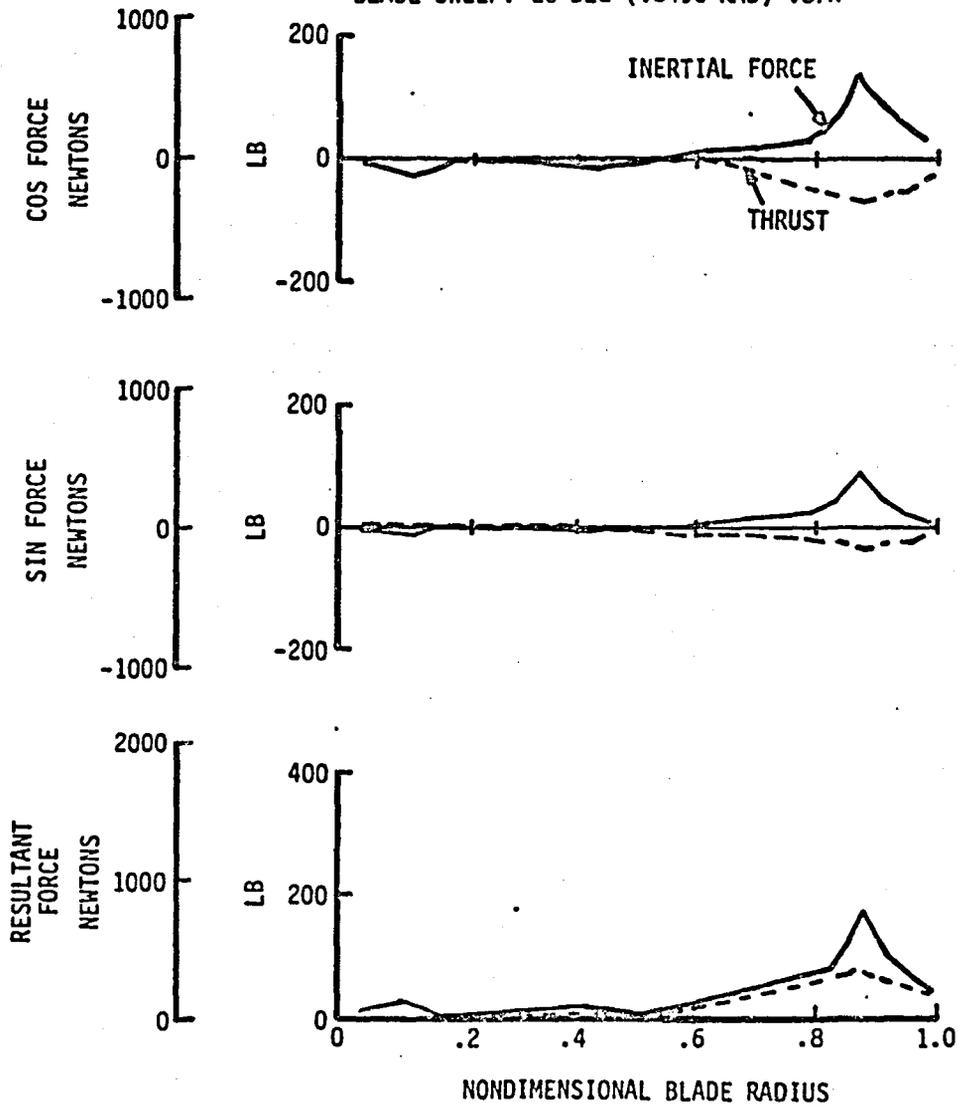
FIGURE 6.2-2 4/REV INERTIAL AND THRUST FORCES VS.
NONDIMENSIONAL BLADE RADIUS, 20 DEG (.3490 RAD) SWEEP .87R

108

BLADE LUMPED MASS DISTRIBUTION

Blade Design A
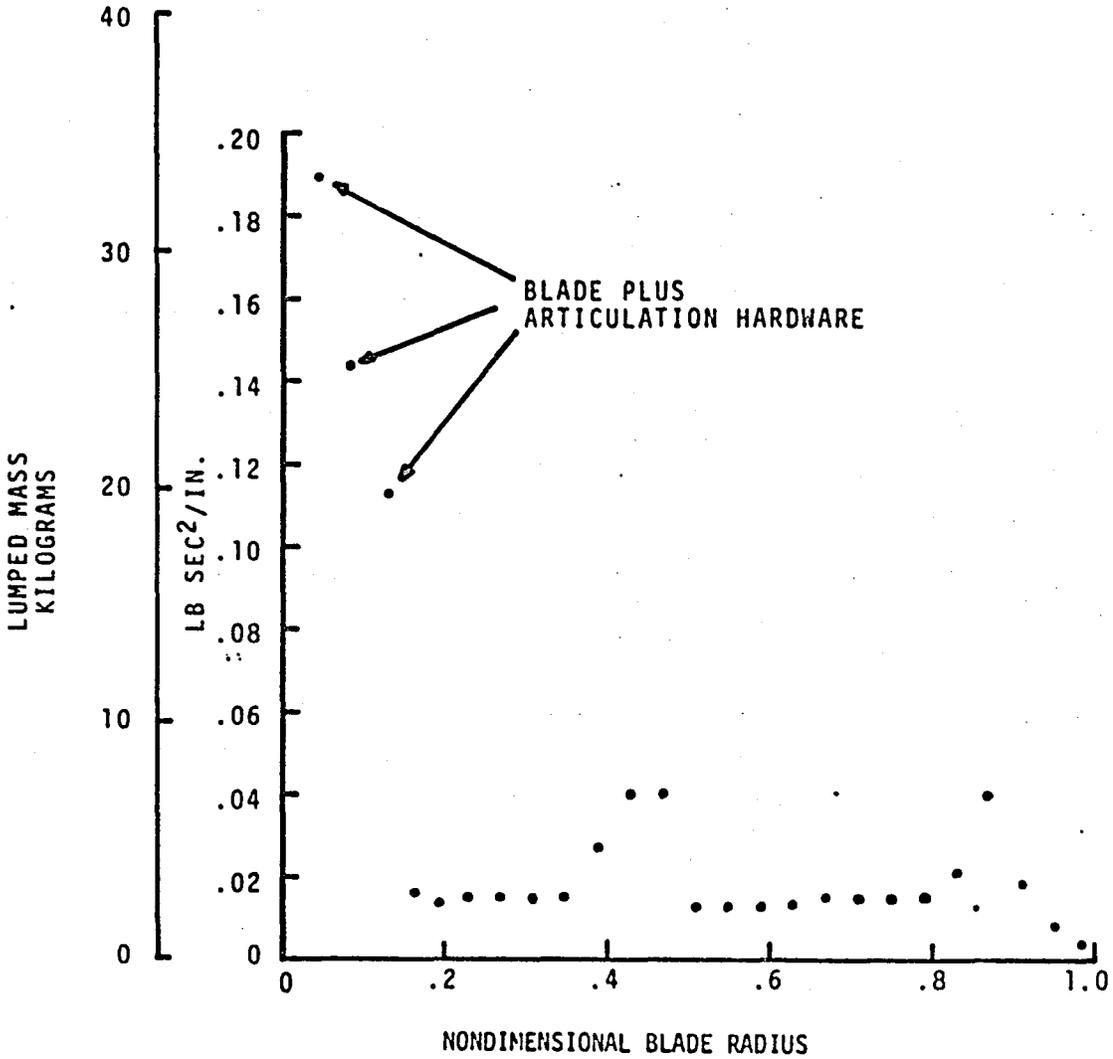
FIGURE 6.2-2A   BLADE DESIGN A LUMPED
MASS DISTRIBUTION

4/REV VERTICAL INCREMENTAL SHEAR
BLADE DESIGN A
AIRSPEED = 150 KT (77.16 m/s)
THRUST = 16463 LB (73227 N)
ROTOR SPEED = 270 RPM
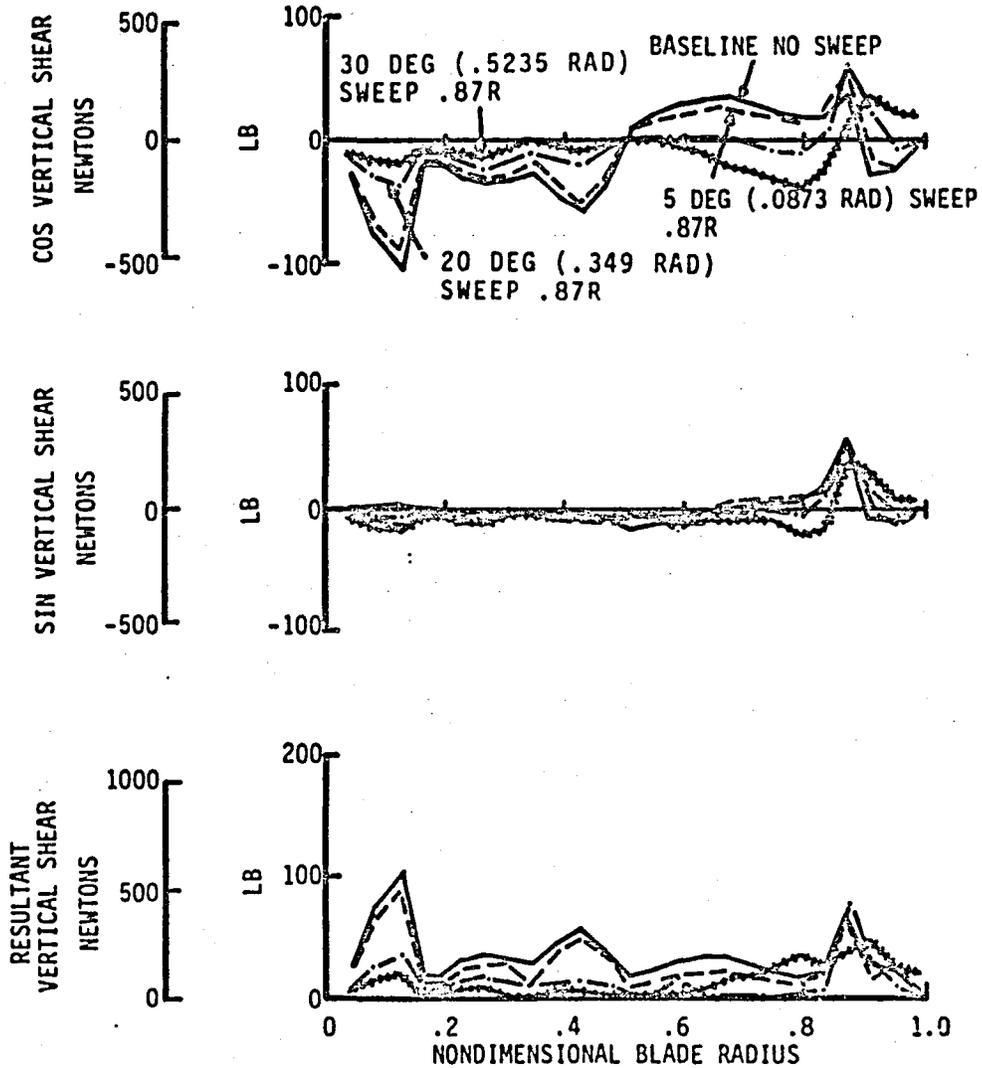
FIGURE 6.2-3 4/REV VERTICAL INCREMENTAL SHEAR VS. NONDIMENSIONAL BLADE RADIUS

4/REV VERTICAL SHEAR SUMMATION
BLADE DESIGN A
AIRSPEED = 150 KT (77.16 m/s)
THRUST = 16463 LB (73227 N)
ROTOR SPEED = 270 RPM
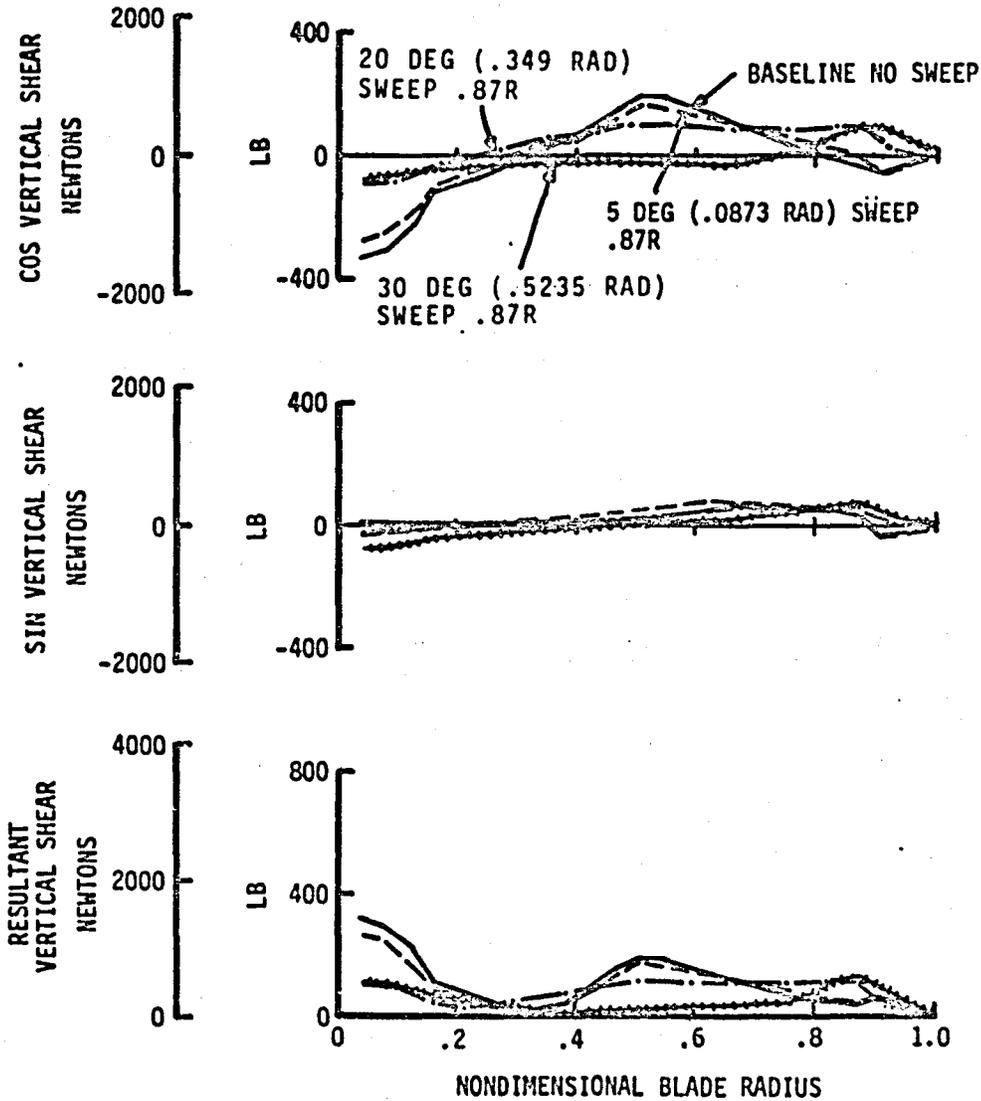
FIGURE 6.2-4   4/REV VERTICAL SHEAR SUMMATION VS. NONDIMENSIONAL BLADE RADIUS

4/REV VERTICAL ACCELERATION
BLADE DESIGN A
AIRSPEED = 150 KT. (77.2 m/s)
THRUST = 16463 LB. (73227 N)
ROTOR SPEED = 270 RPM
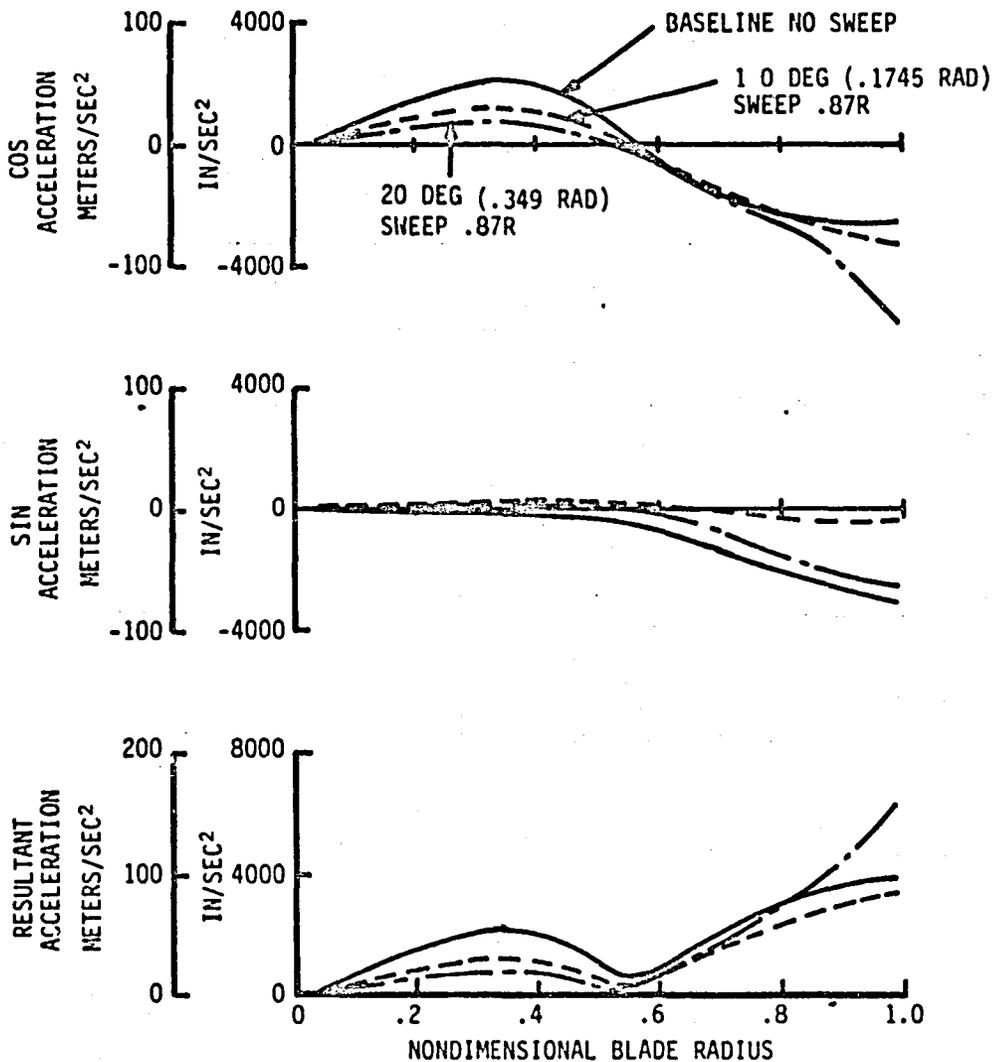
FIGURE 6.2-5 4/REV VERTICAL ACCELERATION VS. NONDIMENSIONAL BLADE RADIUS

4/REV PITCH ANGLE SUMMATION
BLADE DESIGN A
AIRSPEED = 150 KT. (77.2 m/s)
THRUST = 16463 LB. (73227 N)
ROTOR SPEED = 270 RPM
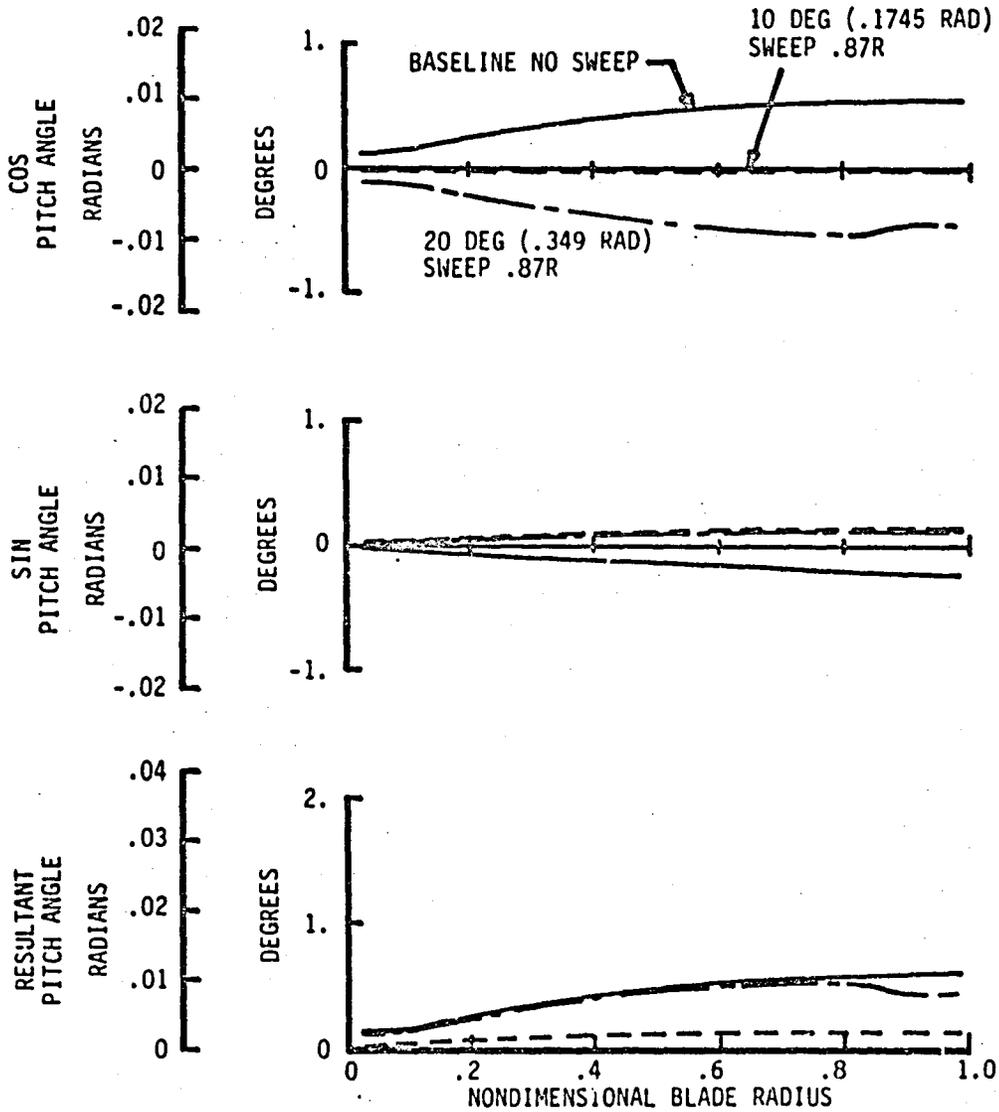
FIGURE 6.2-5 4/REV PITCH ANGLE SUMMATION VS. NONDIMENSIONAL BLADE RADIUS

113

BLADE ANGULAR MOTIONS

BLADE DESIGN A
AIRSPEED = 150 KT (77.16 m/s)
THRUST = 16463 LB (73237 N)
ROTOR SPEED = 270 RPM
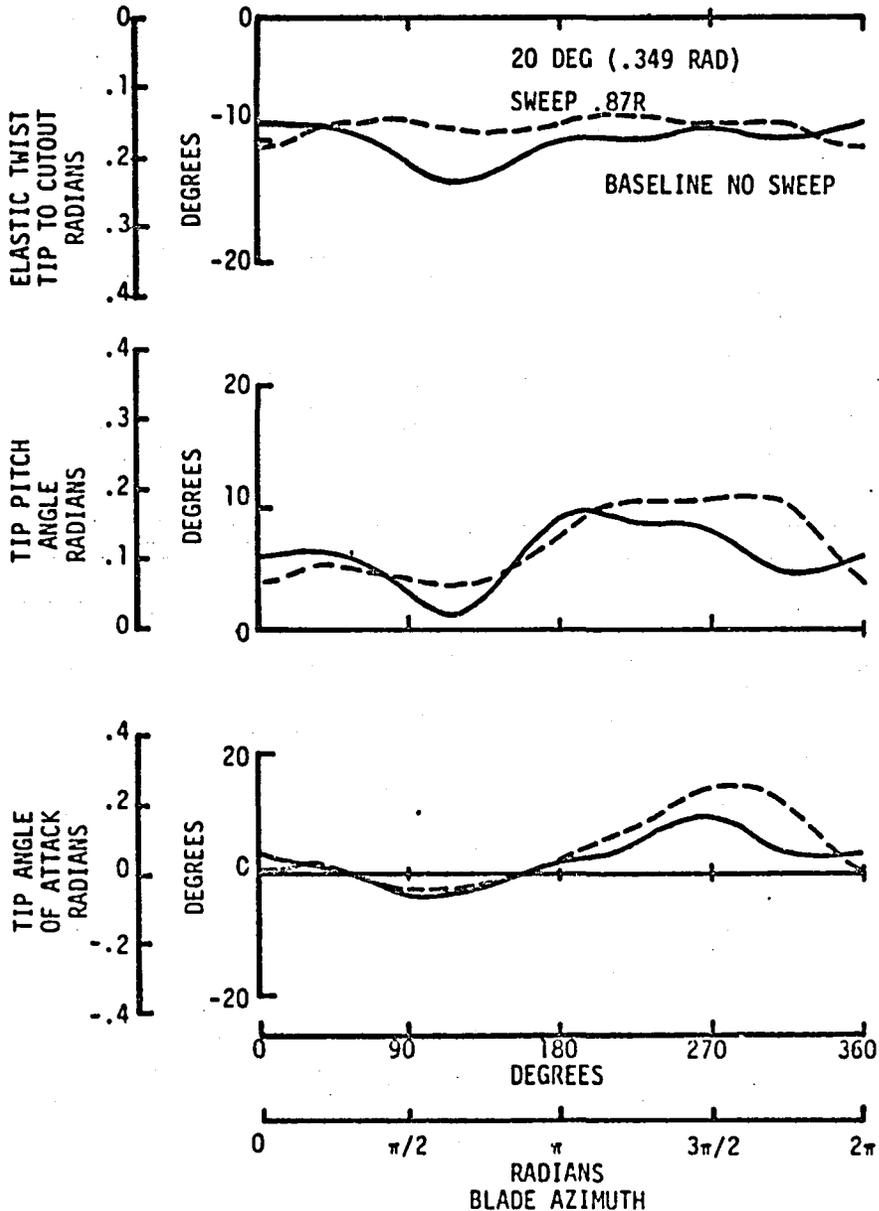
FIGURE 6.2-7 ELASTIC TWIST, PITCH ANGLE, AND ANGLE OF ATTACK,
BASELINE UNSWEPT AND 20 DEGREE (.349 RAD) .87R SWEEP
CONFIGURATIONS

114

4/REV VERTICAL HUB LOADS

BLADE DESIGN A
AIRSPEED = 150 KT. (77.2 m/s)
THRUST = 16,463 LB. (73227N)
ROTOR SPEED = 270 RPM
SWEEP INITIATION .87R

DATA FOR ACTUAL OR SIMULATED 5 DEG. (.0873 RAD) SWEEP.

4/REV VERT.HUB LOAD
1295 LB. (5760 N)
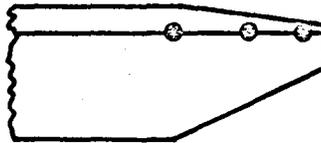
BASELINE
UNSWEPT BLADE

4/REV VERT. HUB LOAD
1121 LB. (4986 N)
(13.4% REDUCTION
FROM BASELINE)
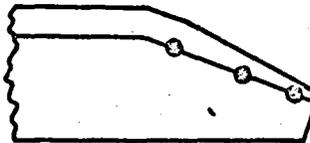
SWEPT BLADE

4/REV VERT. HUB LOAD
1057 LB. (4702 N)
(18.4% REDUCTION
FROM BASELINE)
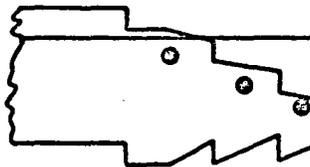
UNSWEPT BLADE

SIMULATED
AFT MASS SWEEP
AFT AERO SWEEP

FIGURE 6.3-1 4/REV VERTICAL HUB LOADS, ACTUAL AND SIMULATED SWEEP

BLADE ELASTIC TWIST
OUTBOARD OF SWEEP INITIATION
BLADE DESIGN A
AIRSPEED = 150 KT (77.2 m/s)
THRUST = 16463 LB (73227 N)
ROTOR SPEED = 270 RPM

SIMULATED 5 DEG (.0873 RAD)
SWEEP .87R

ACTUAL 5 DEG (.0873 RAD)
SWEEP .87R

BASELINE UNSWEPT
BLADE

ELASTIC TWIST

RADIANS

DEGREES

RADIANS

BLADE AZIMUTH

916
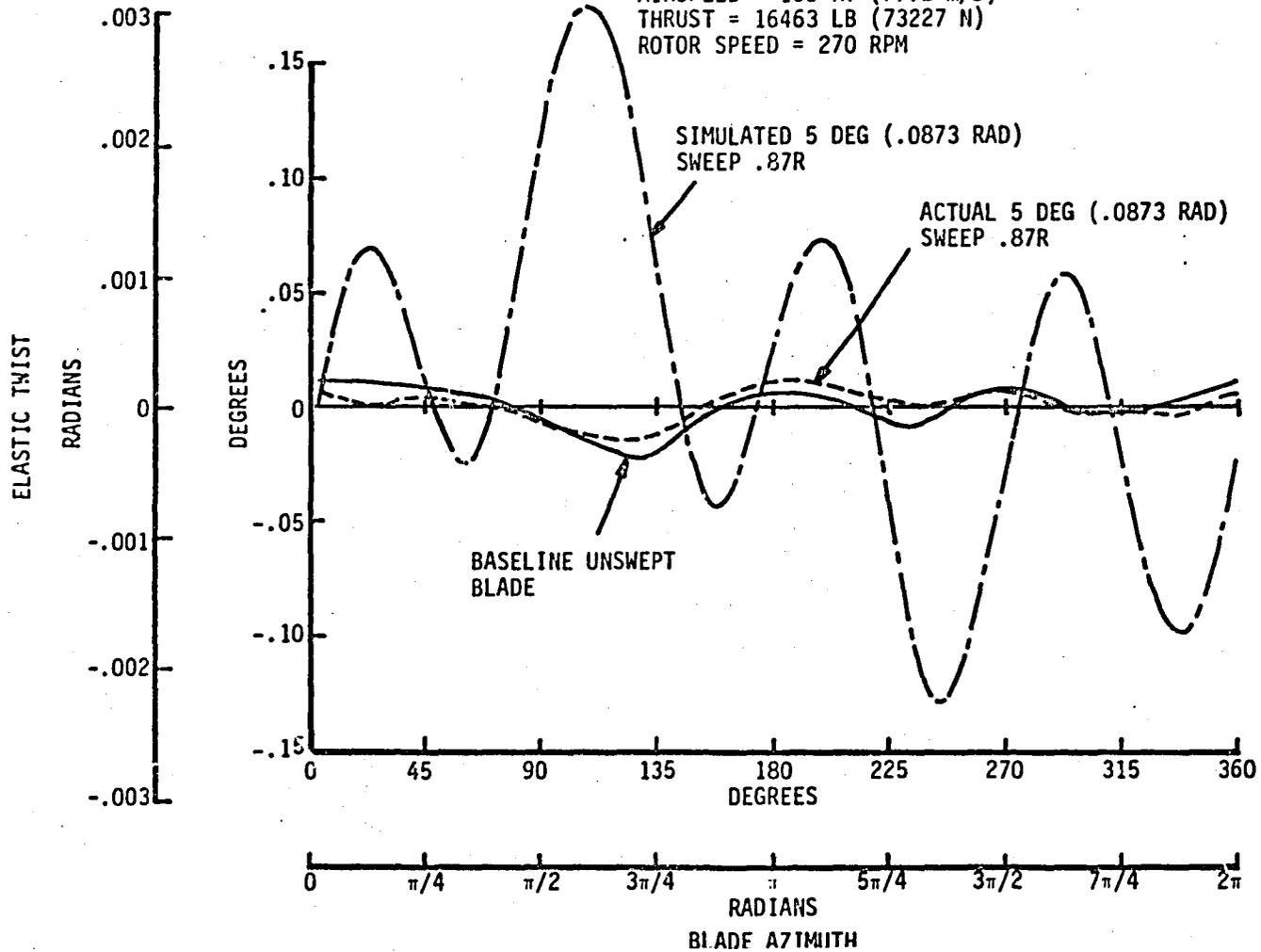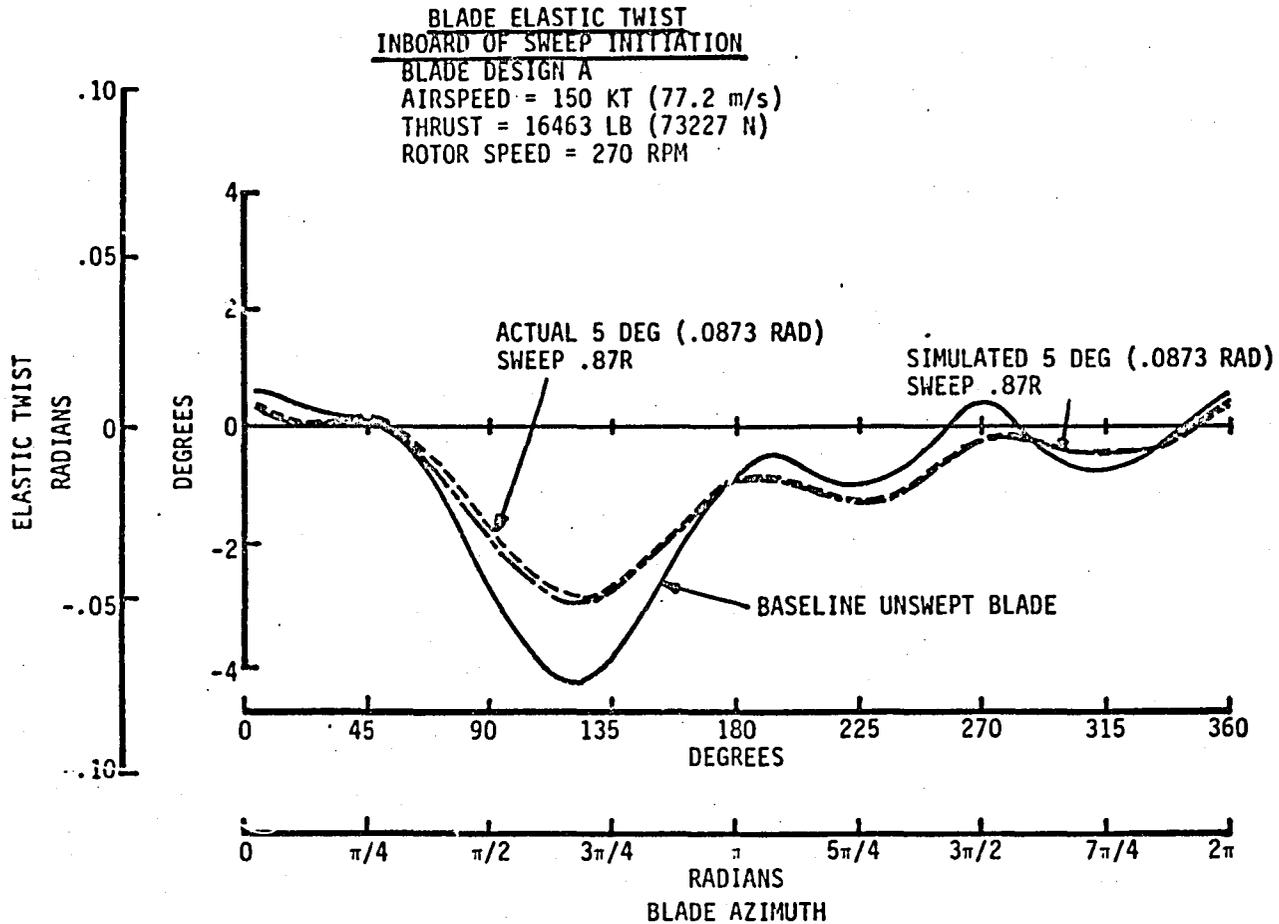
FIGURE 6.3-3 BLADE ELASTIC TWIST INBOARD OF SWEEP INITIATION VS. AZIMUTH

BLADE DESIGN A
AIRSPEED = 150 KT. (77.2 m/s)
THRUST = 16463 LB. (73227 N)

ROTOR SPEED = 270 RPM
SWEEP INITIATION .87R

DATA FOR ACTUAL OR SIMULATED 5 DEG. (.0873 RAD) SWEEP

4/REV VERT. HUB LOAD
675 LB. (3002 N)
(47.9% REDUCTION
FROM BASELINE)
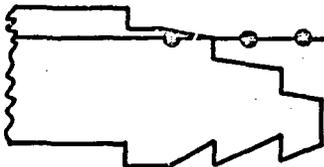
UNSWEPT BLADE
SIMULATED
AFT AERO SWEEP

4/REV VERT. HUB LOAD
1847 LB. (8215 N)
(42.6% INCREASE
FROM BASELINE)
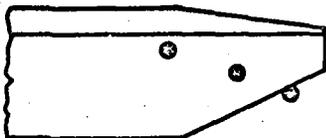
UNSWEPT BLADE
SIMULATED
AFT MASS SWEEP

4/REV VERT. HUB LOAD
854 LB. (3799 N)
(34.1% REDUCTION
FROM BASELINE)
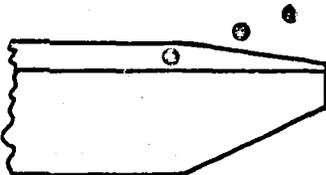
UNSWEPT BLADE
SIMULATED
FWD MASS SWEEP

4/REV VERT. HUB LOAD
577 LB. (2566 N)
(55.4% REDUCTION
FROM BASELINE)
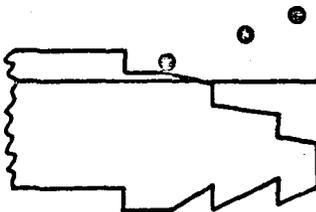
UNSWEPT BLADE
SIMULATED
FWD MASS SWEEP
AFT AERO SWEEP

FIGURE 6.3-4   4/REV VERTICAL HUB LOADS, ACTUAL AND SIMULATED SWEEP

4/REV VERTICAL HUB LOADS
BLADE DESIGN A
AIRSPEED = 150 KT (77.2 m/s)
THRUST = 16463 LB (73227 N)
ROTOR SPEED = 270 RPM
SWEEP INITIATION .87R

DATA FOR ACTUAL OR SIMULATED 5 DEG. (.0873 RAD) SWEEP

4/REV VERT HUB LOAD
726 LB (3229 N)
(43.9% REDUCTION
 FROM BASELINE)
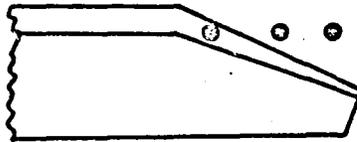
SWEPT BLADE
MASS TRANSLATED
TO UNSWEPT
PITCH AXIS

4/REV VERT HUB LOAD
1665 LB (7406 N)
(28.6% INCREASE
 FROM BASELINE)
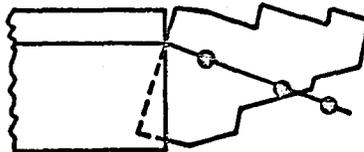
SWEPT BLADE
AERO BAYS TRANSLATED
TO UNSWEPT
PITCH AXIS

FIGURE 6.3-5 4/REV VERTICAL HUB LOADS, ACTUAL AND SIMULATED SWEEP

119
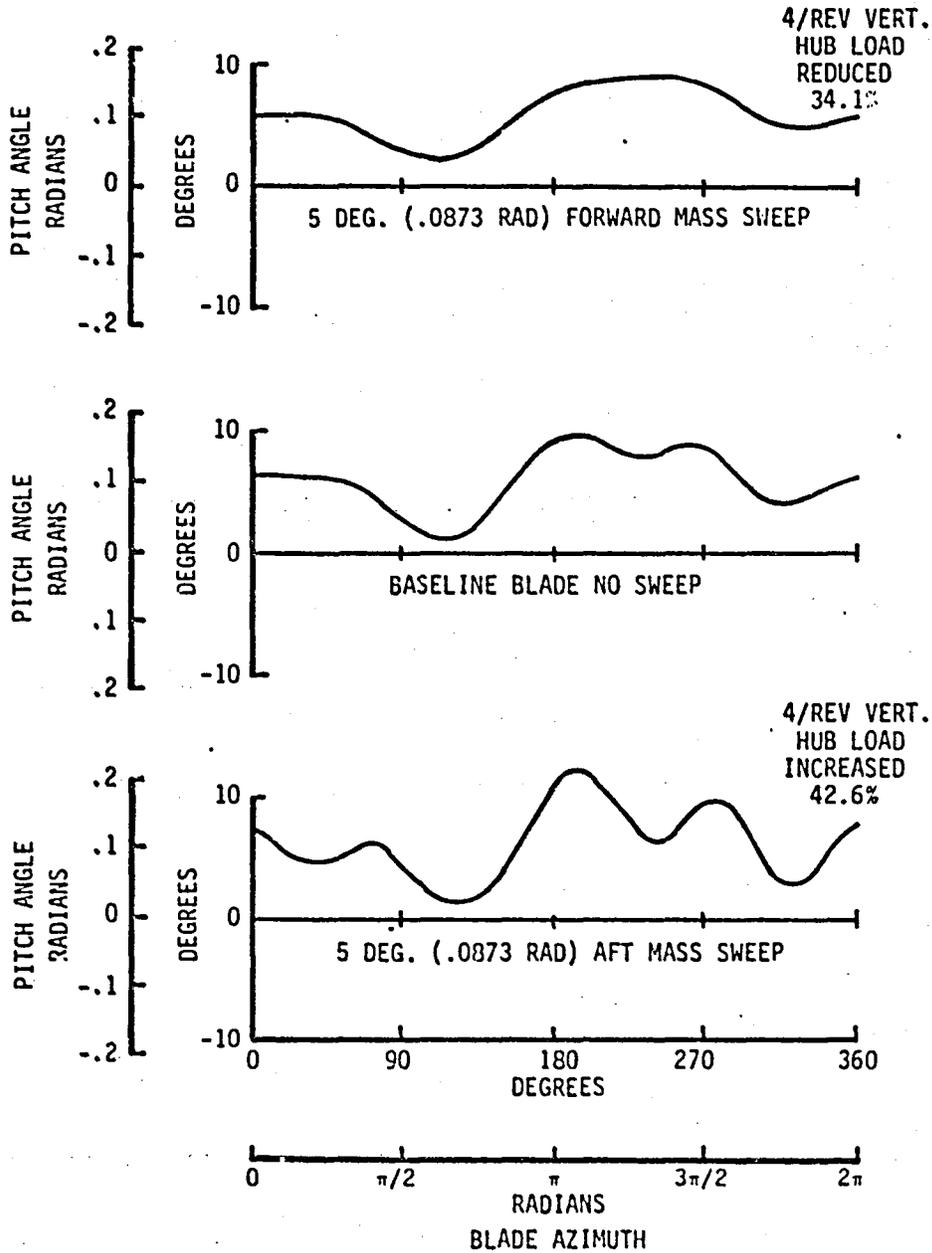
FIGURE 6.3-6 BLADE TIP PITCH ANGLE, SIMULATED MASS SWEEP

120
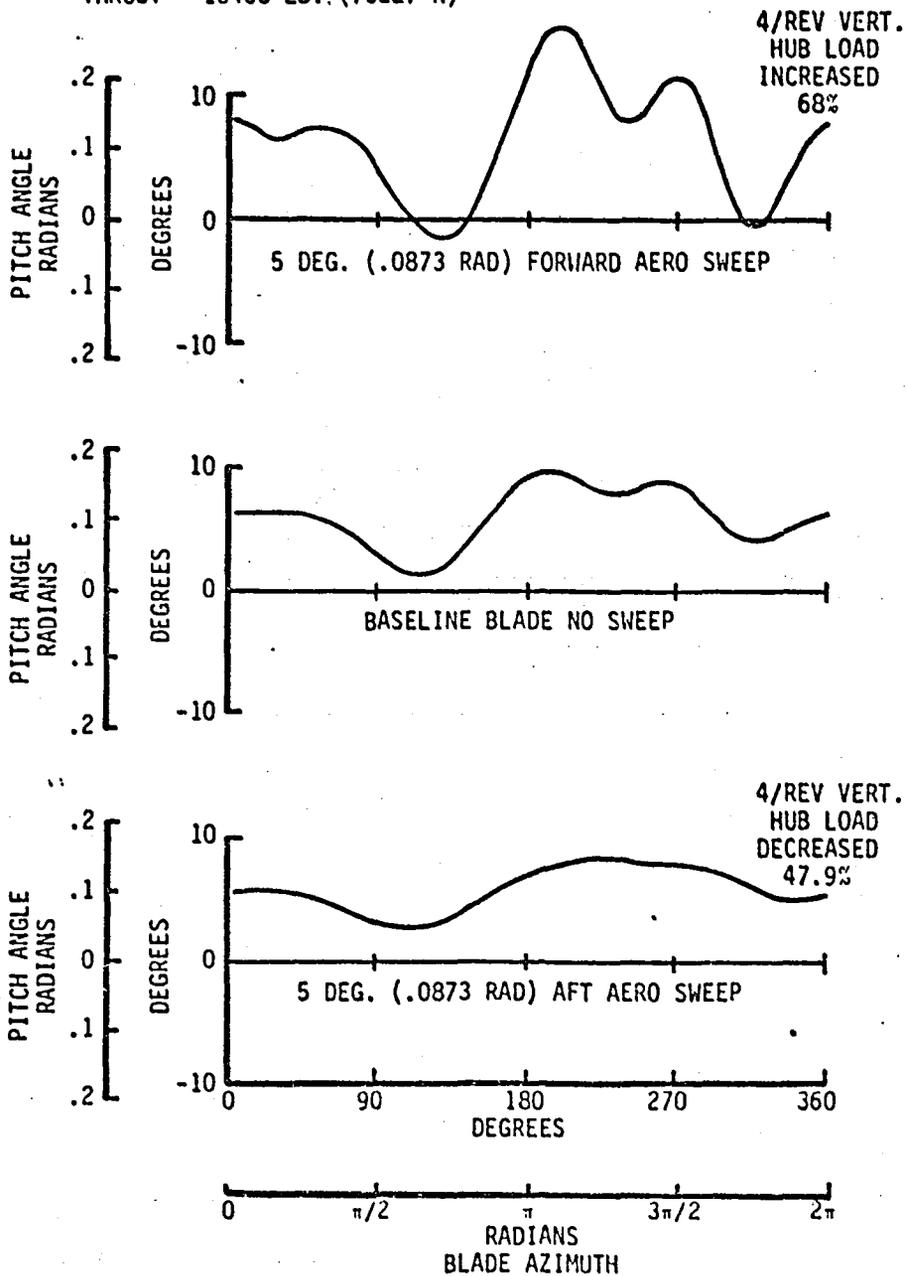
FIGURE 6.3-7   BLADE TIP PITCH ANGLE, SIMULATED AERODYNAMIC SWEEP

121

4/REV VERTICAL HUB LOAD
BLADE DESIGN A
AIRSPEED = 150 KT (77.2 m/s)
THRUST = 16463 LB (73227 N)
ROTOR SPEED = 270 RPM

SQUARE TIP

TAPERED TIP

DEGREES

RADIANS
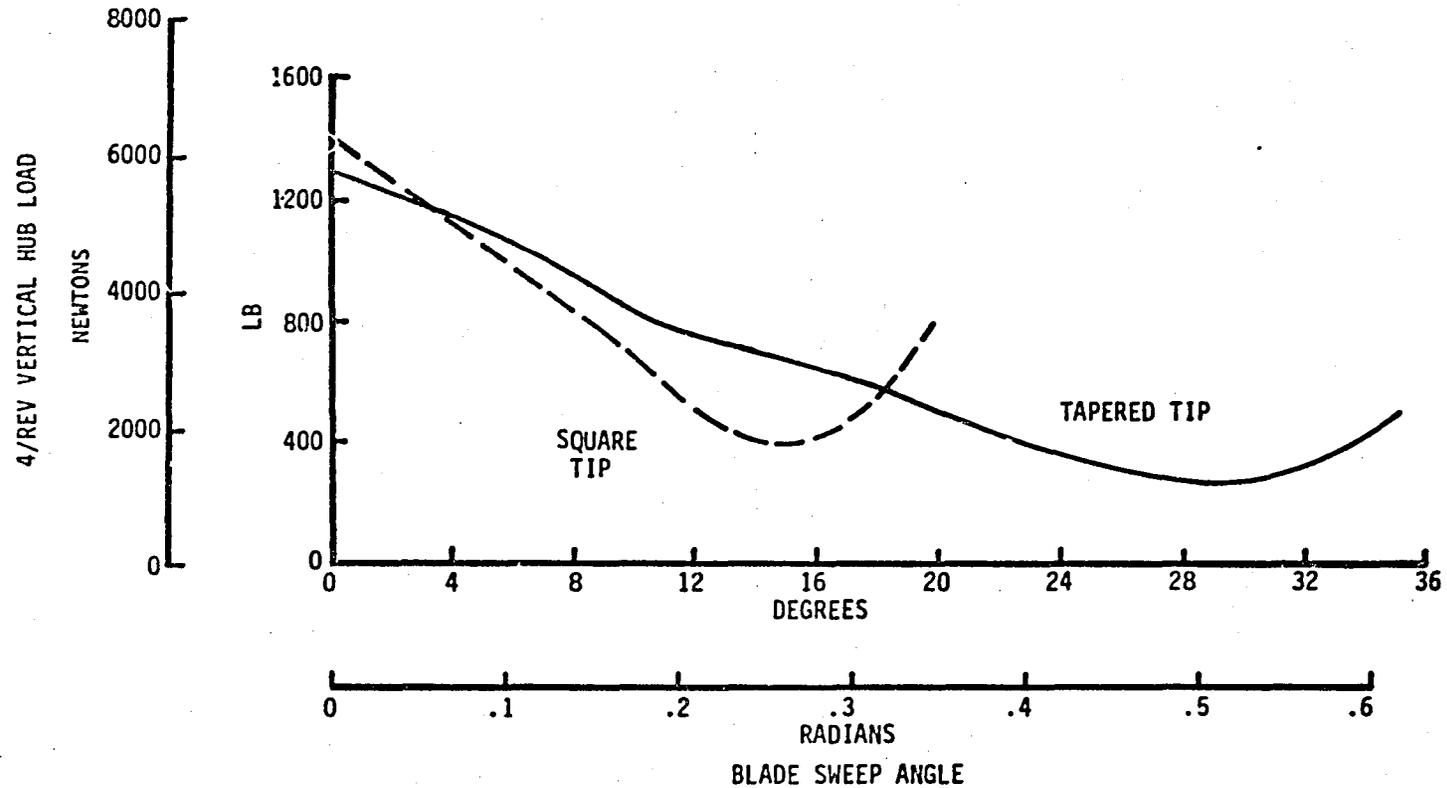
BLADE SWEEP ANGLE

FIGURE 6.4-1   4/REV VERTICAL HUB LOAD VS. BLADE SWEEP ANGLE,
SQUARE AND TAPERED TIPS

4/REV VERTICAL HUB LOAD
CH-47C METAL BLADE
THRUST = 16463 LB. (73227 N)
ROTOR SPEED = 235 RPM

10 DEG (.1745 RAD)
SWEEP .87R

BASELINE
NO SWEEP
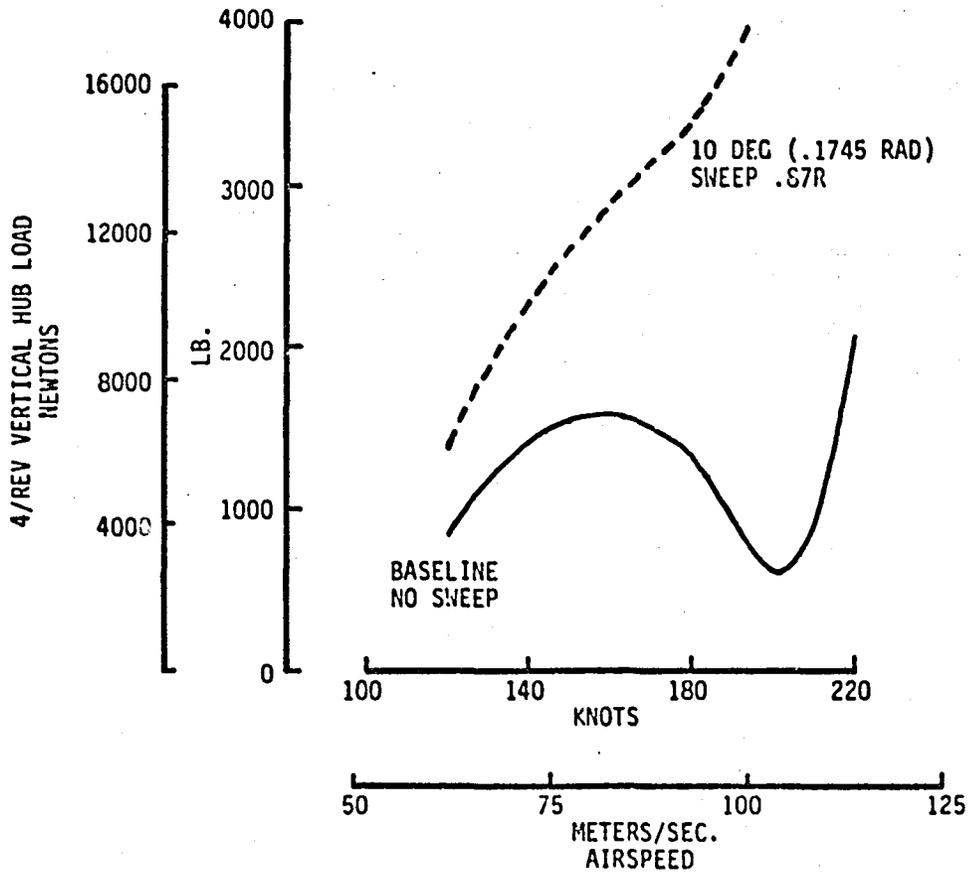
FIGURE 7.-1   4/REV VERTICAL HUB LOAD VS. AIRSPEED, CH-47C METAL BLADE

123

BLADE MASS AND PITCH AXIS LOCATIONS
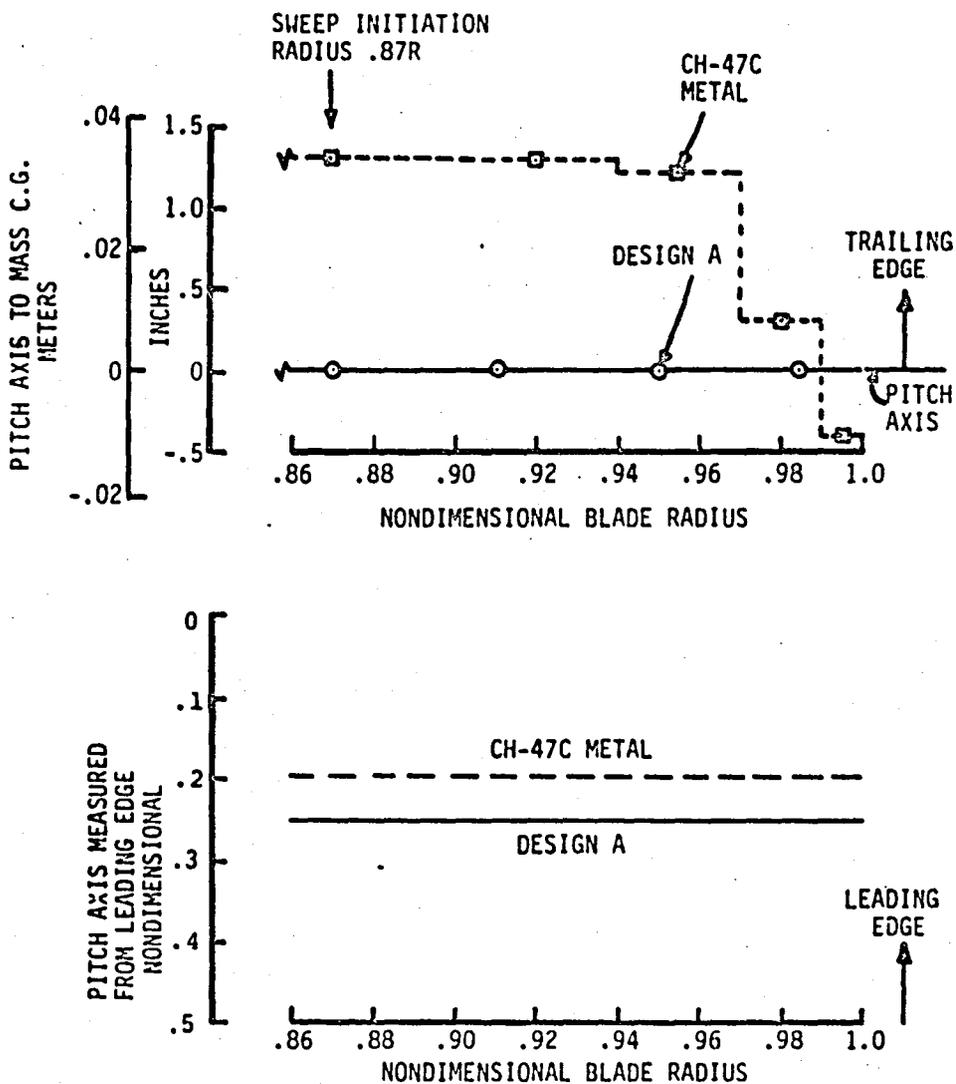
FIGURE 7.-2 BLADE MASS AND PITCH AXIS LOCATIONS, DESIGN A
AND CH-47C METAL BLADES

124

BLADE MASS AND PITCH AXIS LOCATIONS

CH-47C METAL

P.A.= 4.39 IN (.112M)
AFT OF L.E.
(.195C)

CHORD = 22.5 IN (.5715M)

DESIGN A

P.A.=5.5 IN (.140M)
AFT OF L.E.
(.25C)

CHORD = 22 IN (.5588M)
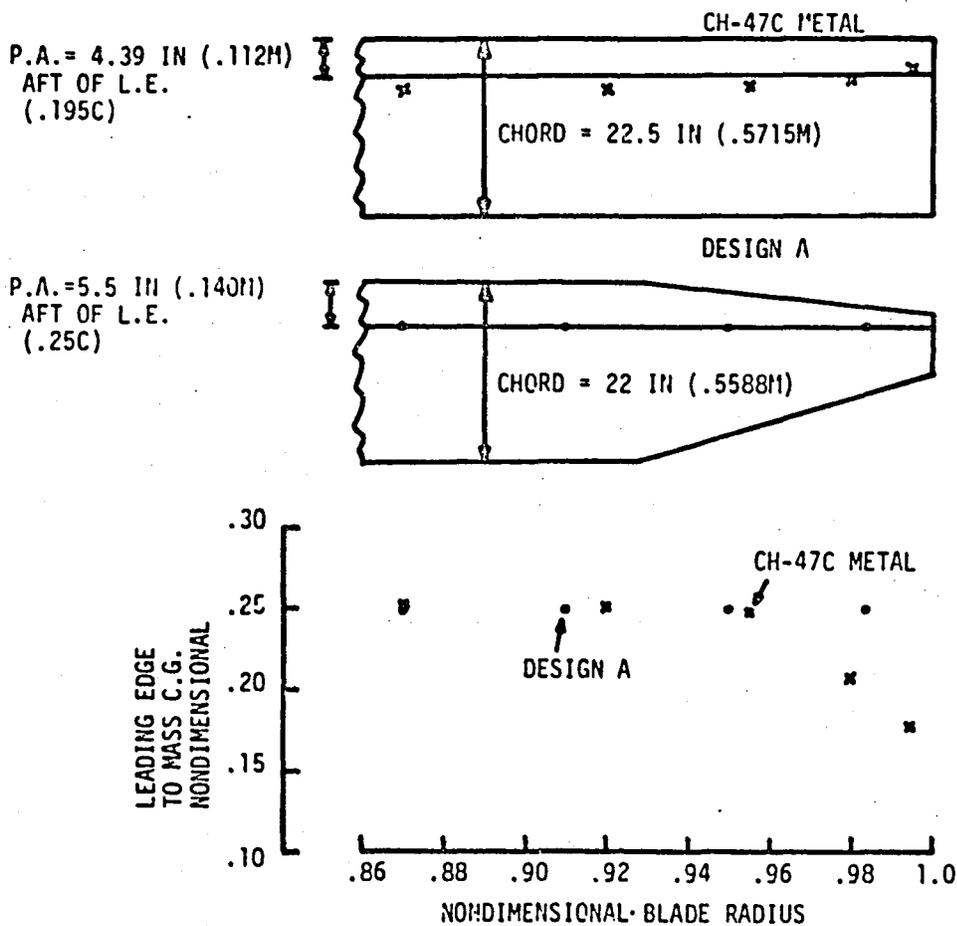

FIGURE 7.-3   BLADE MASS AND PITCH AXIS LOCATIONS,
DESIGN A AND CH-47C METAL BLADES

125

FIGURE 7.-4   BLADE MASS AND PITCH INERTIA, DESIGN A AND
CH-47C METAL BLADES

126

4/REV VERTICAL HUB LOAD
CH-47C METAL BLADE
AIRSPEED = 150 KT (77.2 m/s)
THRUST = 16463 LB. (73227 N)
ROTOR SPEED = 235 RPM
SWEEP INITIATION RADIUS .87R
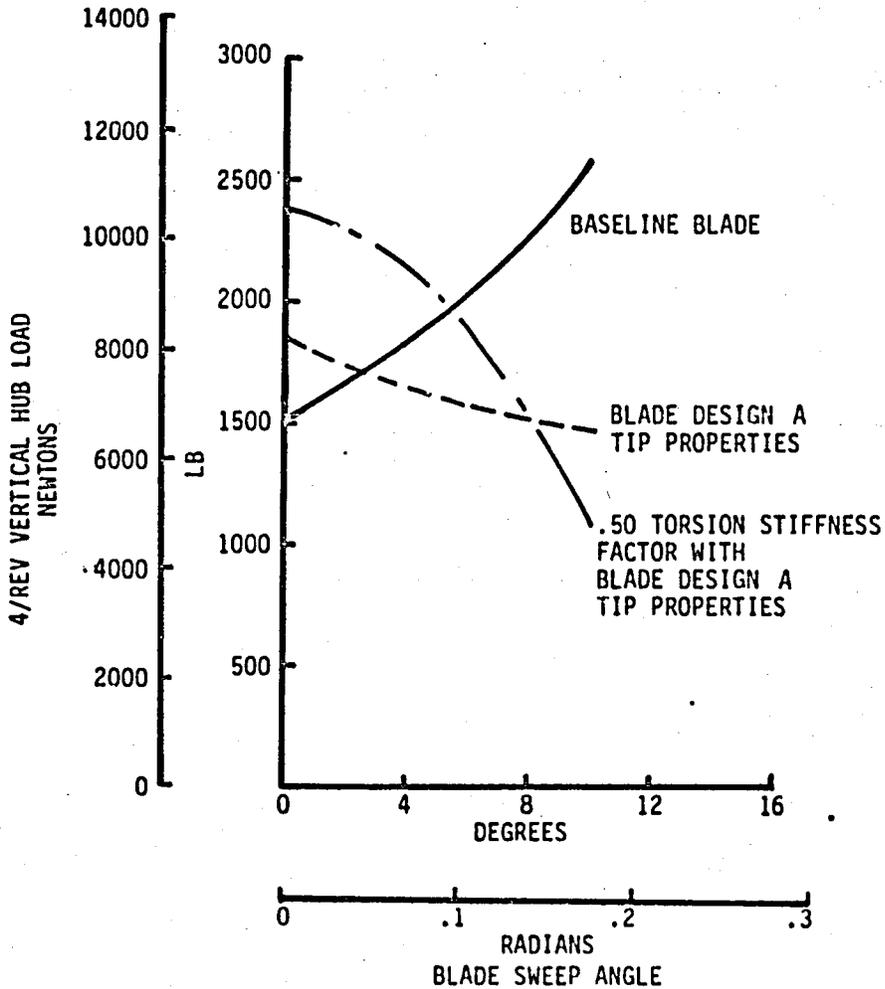
FIGURE 7.-5   4/REV VERTICAL HUB LOAD VS. BLADE SWEEP ANGLE, CH-47C METAL BLADE

127

FLAP STIFFNESS HAS ONLY A SMALL
INFLUENCE ON SWEEP EFFECTIVENESS

TORSIONAL STIFFNESS IN THE
SWEPT PORTION OF THE BLADE
HAS SMALL INFLUENCE

FLAP
HINGE

MINIMAL TORSIONAL STIFFNESS

IN THE UNSWEPT PORTION OF THE BLADE
IS REQUIRED TO OBTAIN THE NECESSARY
ELASTIC TWIST

CAN PROBABLY BE DISTRIBUTED BETWEEN
BLADE AND CONTROL SYSTEM STIFFNESS
IF DESIRED

REQUIRE CERTAIN PHYSICAL
PROPERTIES

IN THE SWEPT PORTION OF
THE BLADE TO GENERATE THE
REQUIRED AERO/INERTIAL
FORCE

MECHANISM: - AERO/INERTIAL FORCE OF THE SWEPT PORTION OF THE BLADE USED THE
              SWEEP ARM TO TWIST THE UNSWEPT PORTION OF THE BLADE.

          - IF THE PHASE AND AMPLITUDE OF THE SWEEP INDUCED ELASTIC TWIST
              REDUCES THE TIP DOWN TWIST ON THE ADVANCING BLADE AND REDUCES
              THE HIGHER HARMONIC TWIST FROM OTHER SOURCES, THE 4/REV VERTICAL
   HUB LOAD IS REDUCED.

FIGURE 7.-6   CURRENT UNDERSTANDING OF HUB LOAD REDUCTION MECHANISM

ANALYTICAL FEATURES OF PROGRAM C-60

- ### AERODYNAMICS

  - NON-LINEAR, COMPRESSIBLE, UNSTEADY LIFTING LINE THEORY WITH YAWED FLOW AND 3-DIMENSIONAL CORRECTIONS

  UNSTEADY STALL
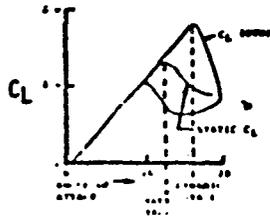
  YAWED FLOW

  ANGLE OF ATTACK
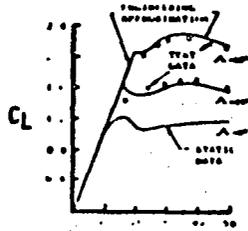
  YAW ANGLE

  - NON-UNIFORM DOWNWASH, INCLUDING SELF INDUCED AND ROTOR INTERFERENCE

  DOWNWASH CALCULATED FROM TRAILED VORTICES
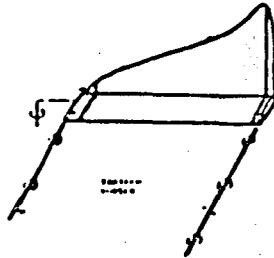
  ROTOR INTERFERENCE INCLUDED


- ### DYNAMICS

  - LUMPED PARAMETER IDEALIZATION WITH 25 BAYS

  - COUPLED FLAP-TORSION

  - UNCOUPLED LAG

  ACTUAL BLADE
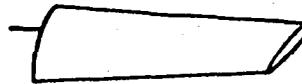
  SEGMENTED APPROXIMATION

 EQUIVALENT DYNAMIC SYSTEM
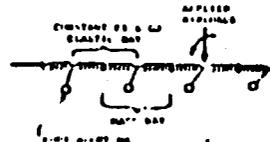
  INCLUDING A FLAP ABSORBER

 ABSORBER
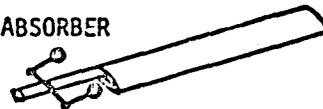
- ### SOLUTION

  - FREQUENCY DOMAIN SOLUTION (HARMONIC BALANCE)

  - ITERATIVE NON-LINEAR AEROELASTIC COUPLING
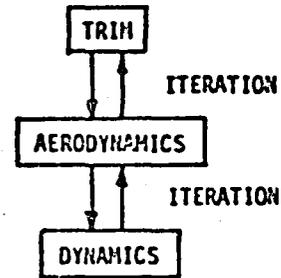
  - ITERATIVE TRIM MATCH (MATCHES TRIM PROGRAM ROTOR FORCES)
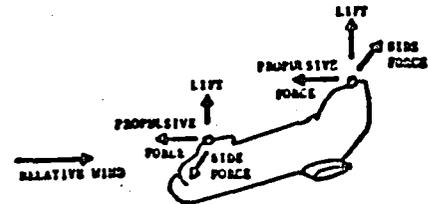
- ### PROGRAM CALCULATES:

  - ROTOR PERFORMANCE
  - BLADE LOADS
  - CONTROL LOADS

FIGURE A-1   ANALYTICAL FEATURES OF PROGRAM C-60

129

M	X/R	X	DISTRIBUTED STIFFNESS						LUMPED MASS AND INERTIA		
			GJ(N) LB-IN2	LOC.	EI FLAP LB-IN2	LOC.	EI LAG LB-IN2	LOC.	M(N) LB-SEC2/IN	LOC.	PITCH INERTIA LB-SEC2-IN (REF TO PA)
1	0.9850	293.7260	4.6400E+06		3.4300E+06		2.1000E+08		4.1200E-03		4.7900E-02
2	0.9500	283.2898	1.0500E+07		7.6400E+06		4.5300E+08		8.4400E-03		2.0200E-01
3	0.9100	271.3618	1.5900E+07		2.3200E+07		6.4500E+08		1.8680E-02		3.0700E-01
4	0.8780	259.4338	1.8900E+07		4.2800E+07		6.5300E+08		4.0200E-02		5.2800E-01
5	0.8300	247.5059	1.9400E+07		4.3500E+07		6.5300E+08		2.1500E-02		4.5800E-01
6	0.7900	235.5779	1.9490E+07		4.3500E+07		6.5300E+08		1.5200E-02		4.0800E-01
7	0.7500	223.6500	1.9500E+07		4.3500E+07		6.5300E+08		1.5200E-02		4.0000E-01
8	0.7100	211.7218	1.9500E+07		4.3500E+07		6.5300E+08		1.5200E-02		4.0000E-01
9	0.6700	199.7938	1.9600E+07		2.0300E+07		6.5300E+08		1.5200E-02		4.0800E-01
10	0.6300	187.8659	1.9600E+07		1.3200E+07		6.5300E+08		1.2700E-02		3.9800E-01
11	0.5900	175.9379	1.9780E+07		1.3200E+07		6.5300E+08		1.2700E-02		3.9000E-01
12	0.5500	164.0099	1.9700E+07		1.3200E+07		6.5300E+08		1.2700E-02		3.9300E-01
13	0.5100	152.0819	1.9800E+07		1.3200E+07		6.5300E+08		1.2700E-02		3.9300E-01
14	0.4700	140.1540	1.9800E+07		1.3200E+07		6.5300E+08		4.0100E-02		4.4700E-01
15	0.4300	128.2260	1.9900E+07		1.3200E+07		6.5300E+08		4.0100E-02		4.4700E-01
16	0.3900	116.2980	1.9900E+07		4.3500E+07		6.5300E+08		2.7600E-02		4.2800E-01
17	0.3500	104.3700	2.0000E+07		4.3500E+07		6.5300E+08		1.5200E-02		4.0000E-01
18	0.3100	92.4420	2.0000E+07		4.3500E+07		6.5300E+08		1.5200E-02		4.0000E-01
19	0.2700	80.5140	2.0000E+07		7.5700E+07		5.5000E+08		1.5200E-02		4.4900E-01
20	0.2300	68.5860	1.9000E+07		2.1200E+08		4.0400E+08		1.5400E-02		8.1700E-01
21	0.1950	58.1490	1.6300E+07		4.5200E+08		4.0000E+08		1.3800E-02		6.9400E-01
22	0.1650	49.2030	1.3500E+07		6.5000E+08		4.0000E+08		1.6300E-02		4.0430E-01
23	0.1300	38.7660	1.9400E+07		1.5300E+08		1.5300E+08		1.1300E-01		3.3300E-01
24	0.0850	25.3470	3.6800E+07		3.4100E+08		2.5500E+08		1.4400E-01		2.7000E-01
25	0.0438	13.0761	4.8300E+07		7.1000E+08		2.5500E+08		1.9000E-01		1.7400E-01

FIGURE C-1   PHYSICAL PROPERTIES FOR BLADE DESIGN A

.276R

.134R   .224R

.928R

BASELINE BLADE NO SWEEP

BLADE
SWEEP
ANGLE

SWEPT BLADE

SWEEP INITIATION
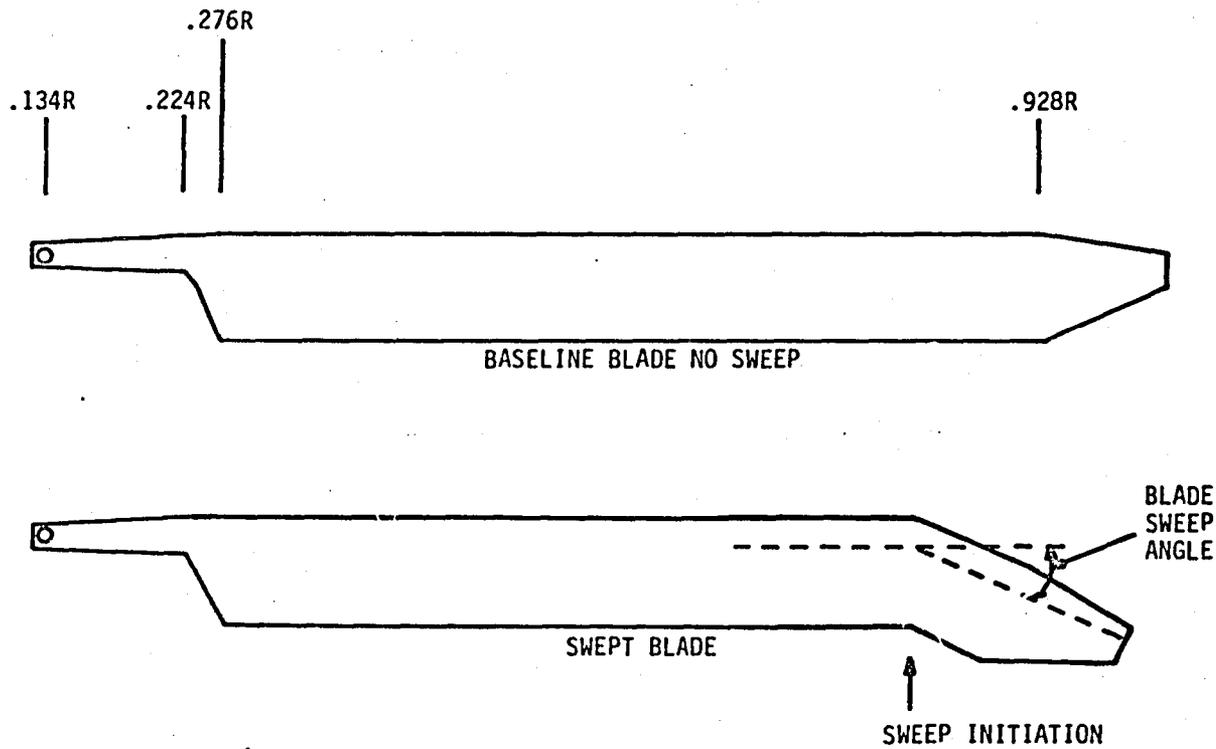
FIGURE C-2   BLADE GEOMETRY

End of Document